UNIVERSITA' DEGLI STUDI DI MILANO

FACOLTA' DI MEDICINA VETERINARIA

Ph.D. Course in Veterinary and Animal Science

Class XXX

Preclinical and proteomic evaluation of a *Staphylococcus epidermidis* clinical isolate in orthopedic biofilm-related infections.

Ph.D. Candidate: Marta Bottagisio

R11008

Tutor: Professor Luigi Bonizzi

Supervisor: Dott.ssa Arianna Lovati

Academic Year 2015-2016

To Rosetta and Roberto

Always in my thoughts

Table of contents

Sintesi

Il termine pseudoartrosi è riferito a un tipo di frattura caratterizzata dall'impossibilità di una fisiologica guarigione. Le pseudoartrosi sono tra le complicazioni ortopediche più complesse non solo a livello clinico, ma anche a livello socio-economico incidendo drasticamente sia sulla qualità di vita dei pazienti colpiti, sia sulle casse dei Sistema Sanitario Nazionale.

Si stima che il 5-10% dei casi di frattura vada incontro allo sviluppo di pseudoartrosi e generalmente le ossa maggiormente interessate a questo fenomeno sono le ossa lunghe, tra le quali tibia, femore, omero, radio e ulna. Lo sviluppo di pseudoartrosi può conseguire la perdita di sostanza ossea, ad esempio a seguito di traumi o alla resezione di tumori, ma non solo, può anche derivare da una frattura che non riesce a consolidarsi. I fattori che possono maggiormente influenzare la corretta guarigione del tessuto osseo sono molteplici e spesso correlati allo stato di salute del paziente: la presenza di malattie metaboliche, l'età, le abitudini alimentare e il fumo incidono drasticamente sul processo di guarigione della frattura. Un'ulteriore causa dello sviluppo di pseudoartrosi è l'insorgere di infezioni date da contaminazioni che possono susseguire fratture esposte o che possono avere luogo in sede operatoria. In questi casi si parla di pseudoartrosi settiche.

È stato stimato che circa i due terzi dei casi clinici di pseudoartrosi settiche sono dovuti alla presenza di stafilococchi e più specificatamente alla presenza di *Staphylococcus aureus* and *Staphylococcus epidermidis*. In particolare, *S. epidermidis* è stato recentemente riconosciuto come un importante patogeno opportunista coinvolto nell'aumento di infezioni nosocomiali, essendo comunemente presente sulla cute umana. *S. epidermidis* è un microrganismo commensale presenta fisiologicamente nella flora di pelle e mucose. A causa della sua presenza ubiquitaria è spesso difficile distinguere se un isolato clinico di *S. epidermidis* rappresenta l'agente causale di un'infezione o un contaminante non specifico della coltura. A differenza di *S. aureus*, *S. epidermidis* non esprime molteplici fattori di virulenza; è contraddistinto come patogeno dalla abilità di formare biofilm sulla superficie di impianti o device introdotti all'interno del nostro corpo (ad esempio protesi, pacemakers, cateteri ecc.).

Il biofilm è una spessa matrice extracellulare secreta da batteri sessili irreversibilmente attaccati ad un substrato. All'interno del biofilm i microrganismi creano comunità organizzate in cui, a seconda delle influenze ambientali, la comunicazione tra cellula e cellula regola l'espressione di geni coinvolti in meccanismi di sopravvivenza. Pertanto il biofilm costituisce una nicchia protettiva, un luogo in cui proliferare e sfuggire alle difese immunitarie dell'ospite e ai trattamenti antibiotici, portando allo sviluppo di antibiotico resistenze.

Un mezzo fondamentale e necessario per lo studio della patogenesi delle pseudoartrosi settiche sono i modelli preclinici, grazie ai quali è possibile indagare come i batteri interagiscano con l'impianto e formino biofilm su di esso. In letteratura, ad oggi, non sono presenti modelli di pseudoartrosi

settica causata da *S. epidermidis* e pertanto nella prima fase del progetto di dottorato è stato quindi generato un modello di pseudoartrosi settica in grado di mimare un'infezione nosocomiale caratterizzata dalla presenza di un impianto metallico, al fine ultimo di indagare nuove strategie preventive e terapeutiche. Con l'obiettivo di identificare la carica batterica minima in grado di portare allo sviluppo di pseudoartrosi settiche, i ratti sono stati sottoposti a una frattura femorale in cui, a seconda del gruppo sperimentale, sono state inoculate diverse concentrazioni di *S. epidermidis* meticillino-resistente (MRSE). Grazie a questo modello siamo stati in grado di definire tre differenti modelli preclinici. È stato infatti possibile dimostrare come un basso inoculo batterico (10^3 CFU/inoculo) è in grado di determinare un modello subclinico di pseudoartrosi settica, caratterizzata dalla sporadica presenza di pochi segni clinici di infezione. Abbiamo inoltre descritto come un inoculo intermedio (10^5 CFU/inoculo) sia in grado di determinare segni acuti di infezione e come un inoculo alto (10^8 CFU/inoculo) sia capace di portare ad una rapida formazione di biofilm sull'impianto e quindi allo sviluppo di pseudoartrosi in tutti gli animali trattati. I successi ottenuti in questa prima fase del progetto hanno reso possibile la realizzazione della successiva fase sperimentale in cui, grazie al modello di infezione acuta, abbiamo potuto testare l'efficacia di nuove strategie preventive.

In letteratura sono descritti diversi approcci terapeutici per il trattamento di pseudoartrosi settiche e tante nuove ricerche stanno cercando di ottimizzare un trattamento che ancora ad oggi non è presente. L'ingegneria tissutale, ad esempio, da anni studia l'utilizzo di scaffold biologici o sintetici con proprietà osteoinduttive e antibatteriche per scagionare l'instaurazione di infezioni favorendo allo stesso momento la rigenerazione del tessuto osseo. Tuttavia la maggior parte delle proposte sviluppate possiede delle limitazioni, legate, ad esempio, alla non biodegradabilità del materiale che potrebbe in alcuni casi addirittura favorire l'adesione batterica o legate al tipo sostanze antibiotiche caricabili nel materiale. In questo senso gli hydrogel rappresentano un giusto compromesso, poiché in grado di fornire localmente antibiotici, fattori di crescita o cellule, sfavorendo lo sviluppo di infezioni batteriche associate a impianti.

È stato recentemente sviluppato un nuovo hydrogel a base di acido ialuronico e polilattico. Test *in vitro* e *in vivo* di questo rivestimento riassorbibile hanno dimostrato come esso sia in grado di prevenire la formazione di infezioni quando associato alla presenza di antibatterico. Tuttavia, non sono ancora note le proprietà osteoinduttive/osteoconduttive che si presume abbia questo innovativo hydrogel.

Altri importanti traguardi dell'ingegneria tissutale sono stati raggiunti grazie all'utilizzo di terapie cellulari, dove il trapianto di cellule progenitrice ha portato a impressionanti risultati nella rigenerazione di organi e tessuti, nonché nel trattamento di pseudoartrosi. Questo approccio mira a fornire cellule progenitrici sane in grado di produrre nuova matrice extracellulare all'interno del tessuto danneggiato per ripristinare la perdita di funzione del tessuto danneggiato. Le cellule staminali mesenchimali (mesenchymal stem cells, MSCs) hanno attirato l'attenzione dei ricercatori

di questo settore come fonte facilmente accessibile di cellule autologhe in grado di differenziarsi *in vitro* in diversi tessuti di origine mesenchimale (ad esempio osseo, cartilagineo, adiposo). Inoltre, alcuni studi hanno descritto le proprietà immunomodulatorie e antimicrobiche di queste cellule, dimostrando come le MSCs possano limitare la crescita batterica *in vivo* e come possano attivamente modulare la risposta infiammatoria nel sito dell'infezione. Tuttavia, il meccanismo d'azione delle MSCs nella modulazione del processo infiammatorio non è ancora chiaro. Un'altra importante caratteristica di queste cellule è la loro mancanza del complesso maggiore di istocompatibilità II che le rende quindi candidate ideali per il trapianto allogenico.

L'obiettivo della seconda fase sperimentale di questo progetto è quello di valutare l'efficacia di un innovativo hydrogel arricchito di vancomicina, nel prevenire lo sviluppo di una pseudoartrosi settica e allo stesso momento favorire la rigenerazione del tessuto osseo. L'utilizzo locale dell'hydrogel è stato comparato all'uso di vancomicina per via sistemica, essendo un trattamento standard in clinica in caso di infezione da batteri meticillino-resistenti.

Parallelamente all'interno dello stesso disegno sperimentale, abbiamo valutato l'efficacia dell'utilizzo di BMSCs, cellule mesenchimale da midollo osseo, per il controllo della risposta infiammatoria e della diffusione della crescita batterica *in vivo*. In particolare, ratti immunocompetenti sono stati sottoposti a una frattura femorale infettata con MRSE e, successivamente, inoculati con BMSCs per via sistemica o locale a seconda del gruppo di appartenenza degli animali. Scopo dello studio non solo è stato quello di analizzare gli effetti immunomodulatori delle BMSCs attraverso la valutazione dei livelli di espressione di citochine infiammatorie, ma anche valutare le proprietà osteoinduttive delle BMSCs in grado di produrre matrice extracellulare nel tessuto danneggiato. Anche in questo caso l'uso sistemico di cellule è stato paragonato a quello locale con il fine di stabilire una via di somministrazione sicura.

Per tutta la prima fase del progetto di dottorato si è ricercata una strategia in grado di impedire la colonizzazione batterica dell'impianto. Tuttavia, il nostro modello animale non è stato in grado di fornirci informazioni su come l'infezione sia stata debellata dall'organismo e quali sono stati i meccanismi attivati che hanno permesso l'eradicazione dell'infezione e della guarigione della frattura. Perché i batteri non sono stati più in grado di formare biofilm in presenza dei trattamenti? Pertanto, per rispondere a questa domanda sperimentale, nell'ultima fase del progetto di dottorato l'attenzione si è spostata sull'analisi del proteoma di *S. epidermidis* per capire i meccanismi molecolari che i batteri attivano quando formano e stabiliscono biofilm *in vitro* su inserti di titanio. Il percorso che regola la formazione del biofilm *in vivo* non è ancora completamente noto, ma è stato ampiamente studiato e descritto; diversamente troviamo in letteratura poche informazioni sul biofilm maturo. Pertanto, con lo scopo di individuare la chiave della stabilità del biofilm maturo, le proteine espresse da due ceppi di *S. epidermidis* coltivati sia in forma planctonica sia in forma sessile sono state studiate. In particolare, abbiamo concentrato la nostra attenzione sul ceppo clinico GOI1153754-03-14 e comparato la sua espressione di proteine con quelle espresse da *S.*

epidermidis ATCC 35984, considerato il ceppo standard e cui sequenza genomica è già stata studiata e depositata in banca dati. Infatti, punto cruciale dell'analisi del proteoma dei batteri è la conoscenza del loro genoma. Perciò, per prima cosa, l'intera genoma di *S. epidermidis* GOI1153754-03-14 è stato sequenziato e successivamente depositato in banca dati. La presenza dell'intera sequenza genomica di un isolato clinico è cruciale sia per le nostre successive analisi, ma permetterà anche di avere una maggiora conoscenza dei ceppi clinici coinvolti in infezioni ortopediche.

A seguito di questa fase preliminare necessaria, *S. epidermidis* GOI1153754-03-14 e ATCC 35984 sono stati staticamente coltivati in forma planctonica e in biofilm formante per 72 ore. La coltura sessile è stata condotta su dischetti di titanio sabbiato per permettere l'adesione dei batteri e la formazione di biofilm; al contrario la coltura planctonica è stata realizzata in agitazione per prevenire l'aggregazione delle cellule. I batteri poi sono stati prelevati e dopo vari lavaggi, mirati a eliminare i residui del brodo di coltura, sono stati lisati per poter estrarre le proteine. Dopo la quantificazione, le proteine sono state prima divise secondo punto isoelettrico e poi secondo peso molecolare per ottenere mappe bidimensionali contenenti singoli spot associati a una singola proteina. Gli spot statisticamente differenti sono stati poi staccati e le proteine identificate per mezzo di analisi di spettrometria di massa. Le analisi hanno rivelato l'incremento di espressione di geni legati allo stress cellulare in batteri coltivati in forma planctonica. La coltura a 72 ore ha reso possibile la formazione di biofilm sulla superficie del dischetto di titanio, ma allo stesso modo ha pregiudicato la crescita degli stessi in forma planctonica. La scelta del time point sperimentale in questo studio rappresenta la maggiore limitazione, ma allo stesso tempo un punto di partenza per valutare il proteoma di *S. epidermidis* a diversi tempi per lo studio dell'attivazione/repressione di geni coinvolti nella formazione e maturazione della matrice. Lo scopo principale di quest'ultima fase del progetto di dottorato e di futuri studi è quello di definire potenziali bersagli molecolari di innovative terapie o di definire nuovi biomarcatori diagnostici, tramite l'analisi delle proteine espresse dai batteri in determinate condizioni di crescita.

Abstract

Non-union fractures, as a severe failure of bone healing, are among the most difficult and challenging orthopedic complications. Non-unions represent a clinical burden, as well as a socio-economic encumbrance that decreases the quality of patients' lives and requires surgical treatment and long recovery times which increases the burden on the National Health Service. The percentage of fractures leading to non-union is between 5 and 10% and generally occurs in long bones like tibia, femur, humerus, radius, and ulna. Non-unions are strictly related to local bone loss caused, for example, by trauma or tumors; they may depend on patient health status (e.g. age, metabolic disease, comorbidities). In addition, they are frequently caused by bacterial infections established during surgical procedures (e.g. osteosynthesis, open fractures) and are referred to septic or infected non-unions.

The most common bacteria involved in infected non-unions are *Staphylococcus aureus* and *Staphylococcus epidermidis* and bacterial contamination accounts for the two-thirds of the clinical cases. In particular, *S. epidermidis* is of utmost importance, being one of the most significant bacteria related to hospital-acquired infections. *S. epidermidis* is an inhabitant of healthy human skin and mucosal flora and it is a commensal bacterium characterized by a low pathogenic potential. However, this pathogen has emerged as a common cause of numerous nosocomial infections associated with medical devices (e.g. catheters, pacemaker, metal implants, etc.), because of its capability to create a protective niche on the surface of implanted orthopedic devices, called biofilm. Biofilm is a thick matrix of extracellular polymeric substances derived from sessile bacteria irreversibly attached to a substratum. Within the biofilm, microorganisms establish organized hierarchies similar to that of multicellular organisms; cell-to-cell signaling regulates the expression of genes involved in survival mechanisms, depending on environmental influences. Thus, biofilm confers a protective niche to pathogens in which they can grow and evade host immune defenses and antimicrobial treatments, leading to the development of antimicrobial-resistant strains, such as methicillin-resistant *S. epidermidis* (MRSE).

Moreover, because of the ubiquitous prevalence of *S. epidermidis* as a commensal bacterium on human skin, it is often difficult to discern whether a clinical isolate represents the causative agent of an infection or an unspecific culture contaminant.

In order to study *S. epidermidis*-associated infections in orthopedic implants, animal models are extremely useful to investigate the pathogenesis of biofilm-related non-union, with particular regard to subclinical infections.

For the aforementioned reason and to fulfill the lack of knowledge in the literature, we established a preclinical model of methicillin-resistant *S. epidermidis* non-union in order to assess the role of subclinical infections in orthopedic and trauma surgery. Indeed, an animal model of infected non-

union able to resemble the features of a nosocomial implant-associated infection was generated, in order to investigate new preventive or therapeutic options. Thus, we evaluated the incidence of infected non-unions caused by dose-dependent concentrations of methicillin-resistant *S. epidermidis* (MRSE) in rats subjected to femoral fracture osteosynthesis with metal implants. At the end of the first experimental phase, we identified the lowest bacterial load of MRSE able to induce a clinical infected non-union. In particular, we determined that a low grade bacterial injection determines a subclinical infection, whereas the intermediate grade inoculum determines a clear acute clinical infection and the highest bacterial inoculum is able to form a visible biofilm upon the implant surface, impeding fracture healing in all the treated animals.

The development of a valid animal model is crucial for the subsequent experimental phases, allowing us to study the complex physiopathology of non-unions caused by microorganisms in order to optimize therapeutic strategies.

To treat non-unions, several therapeutic approaches are described in the literature, such as surgical debridement or local or systemic antibiotic therapies. Recently, also bone tissue engineers are developing biological or synthetic scaffolds with osteoinductive and antibacterial proprieties. However, most of these innovative materials used as drug delivery may have some drawbacks, including non-biodegradability, possible microbial adhesion and biofilm formation on their surfaces, restricted range of loadable antibiotics and long-lasting release with a potential increase of antibiotic resistance. Because of these limitations, hydrogels represent promising and potential alternative materials able to deliver antibiotics, growth factors or cells locally, while inducing osteogenesis and regulating bacterial bone infections associated with orthopedic devices. Recently, an innovative hydrogel composed of two biocompatible polymers (hyaluronic acid and poly-lactic acid) was tested i*n vitro* and subsequently validated *in vivo*, as a bio-resorbable barrier against infections. However, it is not known yet if this hydrogel also possesses osteoinductive and/or osteoconductive properties. Moreover, in the last few years, bone tissue engineering and cell-based therapies reported some impressive results in the regeneration of organs or tissues, as well as in the treatment of non-septic non-unions. The cell therapy approach aims to deliver healthy cells able to produce new calcified matrix within the damaged tissue in order to fix the loss of function. Mesenchymal stromal cells (MSCs) have prompted significant interest in biomedical research and cell-based therapies due to their ability to self-renew, differentiate *in vitro* into mesenchymal tissues, such as bone, cartilage, or fat and as an easily accessible source of autologous cells. Furthermore, some recent studies demonstrated the immunomodulatory and antimicrobial features of MSCs.

Finally, recent studies demonstrated that MSCs can limit bacterial growth *in vivo* thanks to the aforementioned proprieties able to modulate the inflammatory response and macrophage activation at the site of infection. Nevertheless, the mechanism of action of MSCs in the modulation of the inflammatory process is still unclear.

Finally, the lack of the major histocompatibility complex II (MHC II) in MSCs could permit the allogeneic transplant of these cells.

Aiming at testing innovative preventive and/or therapeutic strategies through our model of septic non-unions, the goal of the second experimental phase was to evaluate the efficacy of an innovative hydrogel, with presumed osteoinductive and antibacterial proprieties, to prevent and control the progression of bacterial biofilm formation in infected non-unions. Along with this goal, we investigated the feasibility and the efficacy of MSCs-based therapy to control both the inflammatory response and bacterial growth/spread *in vivo*. Specifically, immunocompetent rats, already exposed to a femoral fracture infected with MRSE, were inoculated with allogeneic mesenchymal stem cells isolated from the bone marrow (BMSCs) through two different administration routes - systemic (circulatory system) and local injection (fracture site). Through this study, we evaluated both the immunoregulatory effects of BMSCs, but also the osteoinductive proprieties of these cells able to produce calcified matrix in the damaged tissue. Similarly, we assessed the ability of an enriched hydrogel to prevent/treat infected non-unions by inhibiting biofilm formation and stimulating bone deposition due to its antibacterial and osteoinductive proprieties.

The overall and anticipated goal of this first part of the project was to establish new therapeutic strategies for the prevention and the treatment of infected non-unions, which result in morbidity and, sometimes, limb loss in critical patients. These results may have an important impact on the treatment of the infected non-union in orthopedics. Moreover, these tested therapeutic strategies may also be used synergically to locally deliver cells due to the engineered hydrogel to optimize physiological pathways of fracture healing and to control the progress of local inflammations/infections. Another potential use of the therapies from this study would be the use of animal models affected with comorbidities (e.g. type I and II diabetes) instead of healthy animals, in order to translate the findings on complex infections that may occur in orthopedics.

In the first experimental phase, all efforts were made to discourage bacterial attachment on the surface of metallic implants impairing the bacterial “race to the surface” while favoring the eradication of the infection and the fracture healing process. However, our animal model of septic non-union was unable to elucidate how the infection was suppressed and why bacteria were not able to form biofilm in the presence of the hydrogel or BMSCs. Thus, in order to decipher the genetic basis of biofilm formation, the second phase of this project focused on the *in vitro* analysis of the proteome of *S. epidermidis* when growing in planktonic or in sessile forms on sandblasted titanium.

Staphylococcus epidermidis does not encode many pathogenicity islands, and its principal virulent property is the ability to establish organized communities which regulate the expression of genes involved in the survival mechanisms and biofilm formation on implants. Indeed, biofilm provides bacteria the means to evade the host immune defense. However, the complete pathway that regulates biofilm *in vivo* is not well understood.

Thus, aiming at defining markers expressed by mature staphylococcal biofilm on metallic implants, in the last experimental phase, we analyzed the proteome of two different strains of *S. epidermidis* in both planktonic and sessile forms. In particular, we compared the whole proteomic profile of two different *S. epidermidis* strains, when growing in their planktonic and sessile forms, in a static culture system. We focused our attention on *S. epidermidis* ATCC 35984, a commercially-available bacterial species isolated from catheter sepsis and which the genome is already deposited in GeneBank, and on methicillin-resistant *S. epidermidis* GOI1153754-03-14 used in our previous studies.

First, the entire genome of *S. epidermidis* GOI1153754-03-14 was sequenced using Next Generation Sequencing not only to obtain the genome but also to analyze the protein profile. Indeed, the whole genome sequence of the clinical isolate was crucial for proteomic analysis in order to highlight the functional mechanisms of biofilm formation.

Then, ATCC 35984 and the clinical isolate GOI1153754-03-14 were statically cultured in their planktonic and sessile forms for 72 hours to establish a mature biofilm. The sessile culture was carried out on sandblasted titanium disks on which bacteria adhered and formed the biofilm; conversely, the planktonic culture was incubated under agitation to prevent cell clustering. Bacteria were then recovered, collected and lysed to extract and separate the proteins by pH and molecular weight. Differences in the two-dimensional gels were evaluated and the variably expressed spots were identified through mass spectrometry analysis. However, data obtained in our study revealed that many changes in the protein expression in both *S. epidermidis* strains occurred when planktonically cultured. In particular, the analysis of the proteins expressed by planktonic bacteria rafter 72 hours revealed results linked to a bacterial stress condition due to the culture condition.

A limitation of this experimental setup was the variation of the proteomic profile associated with the static culture system. The chosen experimental time point represents a limit of this study, but also an important clue for future analyses in which the same proteomic analysis may be carried out at different time points in order to overcome the limitation due to the cell density while allowing the comparison of their proteome at the same experimental time point.

The primary purpose of this final part of the research was to define how protein expression varies between two different bacterial strains belonging to the same species and how culture conditions can modulate these differences. Comparative proteomic analyses may allow the scientific community to understand the molecular pathways associated with biofilm formation on implants, thus identifying potential therapeutic targets or diagnostic biomarkers.

Introduction

Bone fracture and healing

Bone fractures are common non-lethal consequences of injuries related to vehicle and sports accidents, falls or trauma and their rates are doomed to rise with the increase in life expectancy. Long bone fractures are notorious for being slow to heal, often requiring months until the consolidation is completed [1, 2]. Fracture healing is a complex dynamic process characterized by the balance of mechanical and physiological stimuli; the biological environment is influenced by the fixation technique used to stabilize the fracture that will determine the outcome of the healing process [3]. The biological course of bone fracture healing is characterized by different steps, represented in Figure 1 along with the histological pattern depicted in Figure 2.

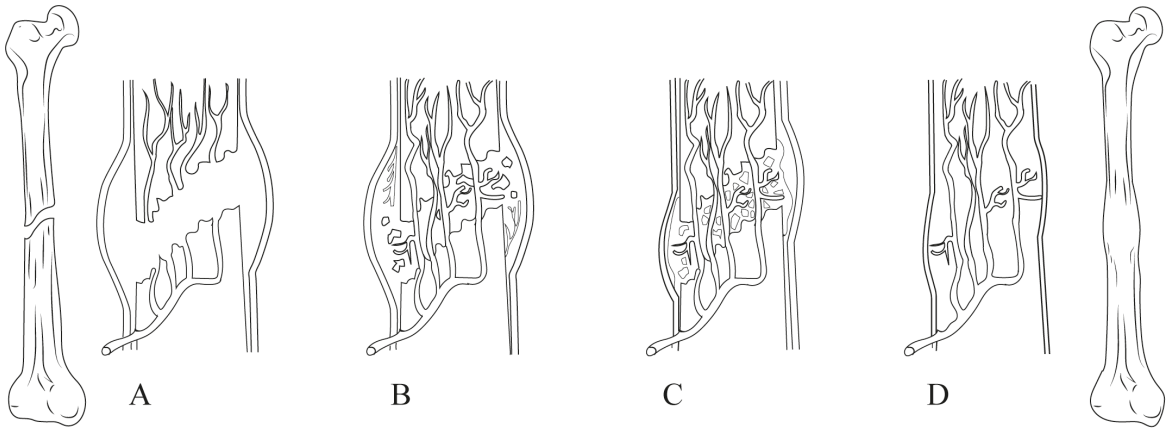

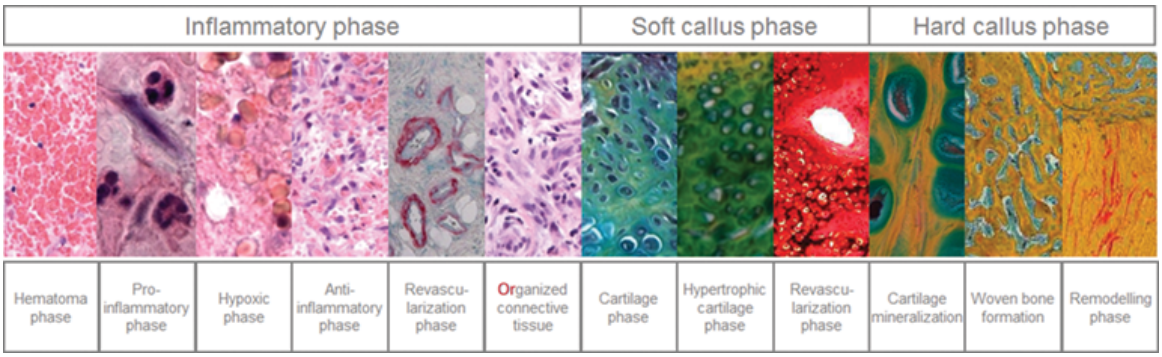

Figure 1. The bone healing process. (**A**) Hematoma formation around the fracture site; (**B**) Soft callus formation; (**C**) Hard callus formation; (**D**) Bone remodeling phase: [Adapted from http://philschatz.com/anatomy-book/contents/m46342.html]

Figure 2. Histological pattern of the bone healing process. The different phases of inflammatory process are illustrated through Hematoxylin and Eosin (H&E) staining except for the revascularization phase which was evaluated through an immunohistochemistry for alpha smooth muscle; The soft callus phase is represented by slides of the bone tissue stained with Movat pentachrome staining, while the revascularization phase by Saphranine/Von Kossa staining; Finally, the cartilage and woven bone formation in the hard callus phase are stained with Movat pentachrome staining [Bucher et al., 2016. DOI: 10.5772/62476].

The first, immediate response to fracture is the formation of a hematoma, as the result of blood vessel disruption and bone marrow effusion. As soon as the hematoma forms, the inflammatory cells reach the fracture site.

The acute inflammatory response is the first crucial step in the fracture healing process, activating the upregulation of angiogenic factors, thus supporting the vascularization of the injured site. Just 24 hours after the injury, the pro-inflammatory response is counterbalanced by the release of anti-inflammatory cytokines involved in the recruitment of cells enrolled in the healing of the injured tissue [4]. If the acute inflammatory response remains unresolved (e.g. due to a bacterial infection at the injury site or to chronic inflammatory diseases), the healing of the fracture can be inhibited or, even worse, it may fail [5].

The second stage of the fracture healing process is characterized by the progressive evolution of the hematoma into granulation tissue, followed by the gradual replacement of the latter in a soft callus composed of fibrous tissue and cartilage.

This anabolic phase is characterized by an increase in tissue volume due to the *de novo* recruitment of mesenchymal progenitor cells [6]. Subsequently, these cells differentiate into chondrocytes or osteoblasts producing the extracellular matrix and cartilage, while slowly replacing the hematoma and filling the fracture gap [4]. Even if soft callus formation confers to fractures an initial stability, the bone healing process is not yet completed.

Progressively, the soft callus is replaced through a process known as endochondral ossification, becoming more robust and mechanically rigid: the cartilaginous callus undergoes a process starting with mineralization, then resorption and finally replacement by woven bone [7].

Once the fracture site is restored, the woven bone is then slowly substituted by lamellar bone, concluding the process with the last stage: the remodeling phase. The remodeling process is carried out by the balance of hard callus resorption by osteoclasts and lamellar bone deposition by osteoblasts [7]. This stage finally concludes the process by restoring the mechanical and biological function of the bone.

Bone healing impairment and non-union development

A crucial step in the treatment of diaphyseal bone fractures is the reduction and stabilization of the fracture gap. Since the capability of bone to bridge a gap is known to be limited, the stumps must be positioned and fixed - the larger the fracture gap the more delayed the healing process [8].

Despite the impressive regenerative capability of skeletal tissue, the bone healing process may fail leading to a delay of tissue recovery or even worse to the development of non-unions.

Non-unions, a severe failure of bone healing, are among the most difficult and challenging orthopedic complications. Physiologically, the fracture healing process is completed after three months, while a delayed healing occurs if the recovery exceeds three months, and a non-union if healing is not achieved by nine months [9].

Non-unions can be classified as hypertrophic or atrophic depending on the imbalance between biological and mechanical factors (Figure 3).

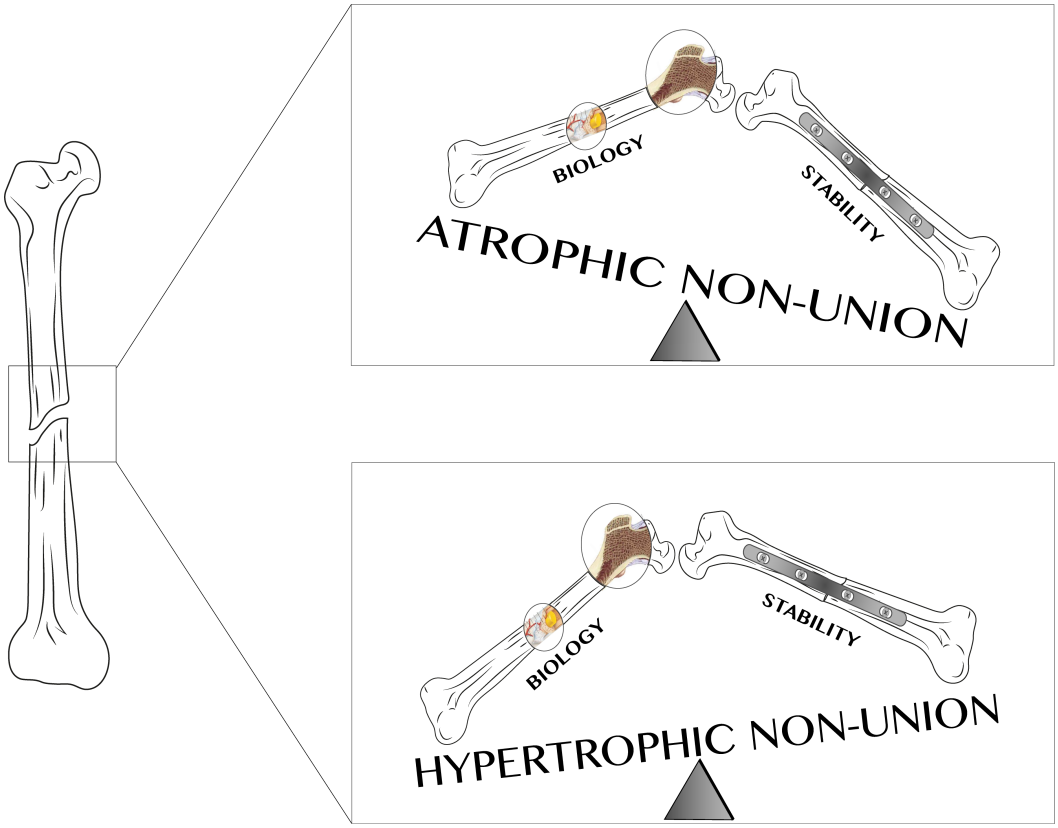

Figure 3. Two different fate of non-union fracture. Atrophic and hypertrophic non-unions as the result of an imbalance between biology and stability.

The hypertrophic non-union is a hypervascularized, viable fracture caused by inadequate fixation; the lack of stability results in the failure of endochondral ossification leading to the deposition of fibrous tissue within the fracture site. In contrast, the atrophic non-union is an avascular, non-viable fracture caused by poor vascularization of the site and subsequent insufficient biological response. The treatment of atrophic non-unions requires the surgical removal of the dead tissue and its replacement with a bone graft, in order to guarantee a prompt biological response in terms of vascularization and cell colonization [10].

It has been estimated that fracture healing is delayed in 600,000 patients per year in the United States alone, and approximately 100,000 of these fractures results in non-unions annually [11]. The percentage of fractures leading to non-union is between 5 and 10% [12] and generally occurs in long bones like tibia, femur, humerus, radius, and ulna, which are characterized by a slower healing process compared to other bones.

These numbers reflect a socio-economic encumbrance, being associated with prolonged hospitalization periods affecting the quality of a patient's life in terms of loss of productivity and earnings, but also in terms of suffering [13]. Nonetheless, these complications result in high

economic impact requiring *ad hoc* health care interventions. In a retrospective study, Antonova and colleagues [14] reported the care costs to treat patients with a non-union and without a non-union (25,555.97 $ vs. 11,686.24 $, $p < 0.001$), underlying the need to prevent or reduce the risks of non-union development. Non-union causative factors have been extensively investigated, and there are some important demographic differences between patients whose fractures will heal and those whose fractures will fail to recover. Niikura and colleagues [15] classified the cause of non-union development as either patient dependent or patient independent factors. Patient dependent factors include comorbidities such as diabetes, vascular and metabolic diseases, genetic disorders, endocrine pathology and immunodeficiency [15, 16]. Moreover, unhealthy habits largely affect the bone healing process. Indeed, it has been recently demonstrated how smoking significantly increases the risk of impaired healing process; orthopedists request patients to quit smoking, as an essential part of fracture treatment [15, 17]. Moreover, dietary behavior also plays a key role in the deficiency of recovery: obesity, alcohol abuse, nutritional deficiency and also the use of nonsteroidal anti-inflammatory drugs are all important causative factors [18, 19]. Conversely, several elements are independent of patient conduct because they are strictly connected to the type of fracture - such as location, displacement - or to the quality of surgical treatment – such as an inadequate or deficient mechanical stability that may lead to impaired biological activity [3]. Finally, infections are considered an independent factor of utmost importance leading to delayed healing or non-union development associated with the loss of function of the affected limb.

Septic non-unions

Septic non-unions occur in the presence of an infection at the fracture site, impairing the bone healing process and affecting the surrounding soft tissues [20].

The incidence of these events has been reported in many independent studies, describing a low infection rate (1%) after the surgical fixation of closed, low-energy fracture, increasing to 30% in complex open fractures [21, 22]. According to the timeline reported in Figure 4, infections after fracture fixation can be classified into three categories: early, delayed and late.

Early infections are mainly caused by high virulence bacteria, like *Staphylococcus aureus*, and usually, they result in an impairment of healing characterized by specific local signs of inflammation such as heat, pain, redness, and swelling leading to systemic symptom such as fever and lethargy [23]. When patients present these unequivocal signs of infection, a prompt diagnosis and treatment of the pathology are provided, ensuing in a quick recovery.

Conversely, delayed infections generally occur 2-10 weeks after fracture fixation and present signs comparable to those of late infections (<10 weeks). These infections are usually due to low-virulence pathogens like *Staphylococcus epidermidis* or *Propionibacterium acnes*, able to adhere to the implant surface and remain protected by the surrounding environment, due to biofilm formation.

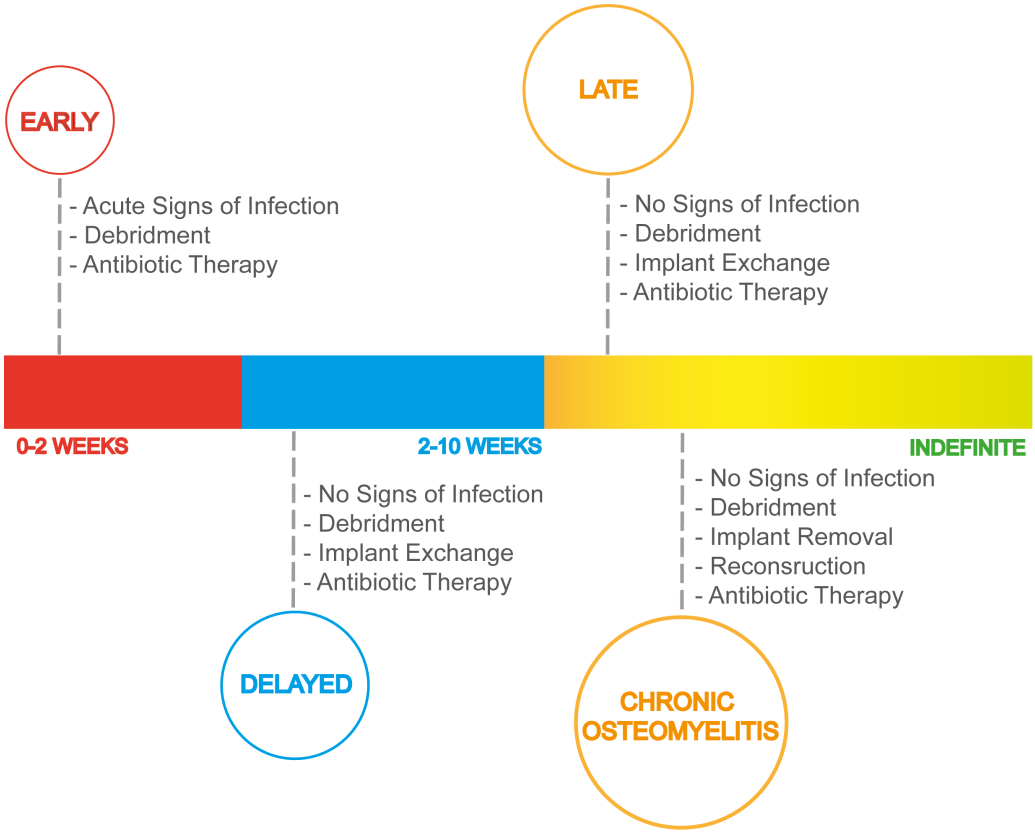

Figure 4. Time course of the progression of infections after fracture fixation. The timeline depicts the progression of the infection according to the progression of time. Along with the temporal steps, the therapeutic strategies of the different stages are reported.

As infection progresses, maturing biofilms provide bacteria the means to evade the host immune defense and to develop antibiotic resistance, thus leading to resistant pathogens (e.g. methicillin-resistant *S. epidermidis*, MRSE). Indeed, this protective environment favors gene transfer among these prokaryotic communities, resulting in an increase in the number of virulence factors [24]. In contrast to early infections associated with specific acute signs, delayed and late infections are clinically silent events hardly distinguishable from aseptic prosthetic failure [22, 25, 26].

Among several pathogens involved in implant-related infections, staphylococci account for two-thirds of the clinical cases [27, 28]. Most of the clinical isolates are highly virulent pathogens, such as *Staphylococcus aureus* (35.5%), *Escherichia coli* (3%) or *Pseudomonas aeruginosa* (4-6%), while the low virulence pathogens usually involved are *S. epidermidis* (27.5%) and *P. acnes* (10%) [29].

In particular, *S. epidermidis* has recently emerged as a common cause of numerous nosocomial infections associated with medical devices (e.g. catheters, pacemaker, metal implants, etc.) particularly in immunocompromised patients and infants [30]. This is mainly due to the presence of *S. epidermidis* on healthy human skin and mucosal flora where it lives as a commensal bacterium. Interestingly, the skin of healthy people is colonized by 10-24 different strains of *S. epidermidis* at any time. The host-bacteria bond is mutually beneficial; it impairs the attachment of more virulent

bacteria through a mechanism called bacterial competition while conferring the ideal habitat for bacterial growth [31]. *S. epidermidis* is a commensal Gram positive, coagulase negative, non-spore-forming bacterial species and, depending on the biological context in which it grows, it could be either a symbiont or a pathogen implicated in delayed infections characterized by the absence of specific clinical signs [29]. Moreover, due to the ubiquitous presence of *S. epidermidis* as a commensal species on human skin, it is often difficult to distinguish whether a clinical isolate represents the causative agent of the infection or an unspecific culture contamination [30]. In contrast to *S. aureus*, *S. epidermidis* does not encode many pathogenicity islands, and its major virulent property is the ability to establish organized communities which regulate the expression of genes involved in survival mechanisms and biofilm formation on implants [31, 32].

Bacterial biofilm

The presence of a foreign body is the triggering event for staphylococcal infections, because it permits bacterial attachment and biofilm formation, making the eradication of the infection difficult [33, 34].

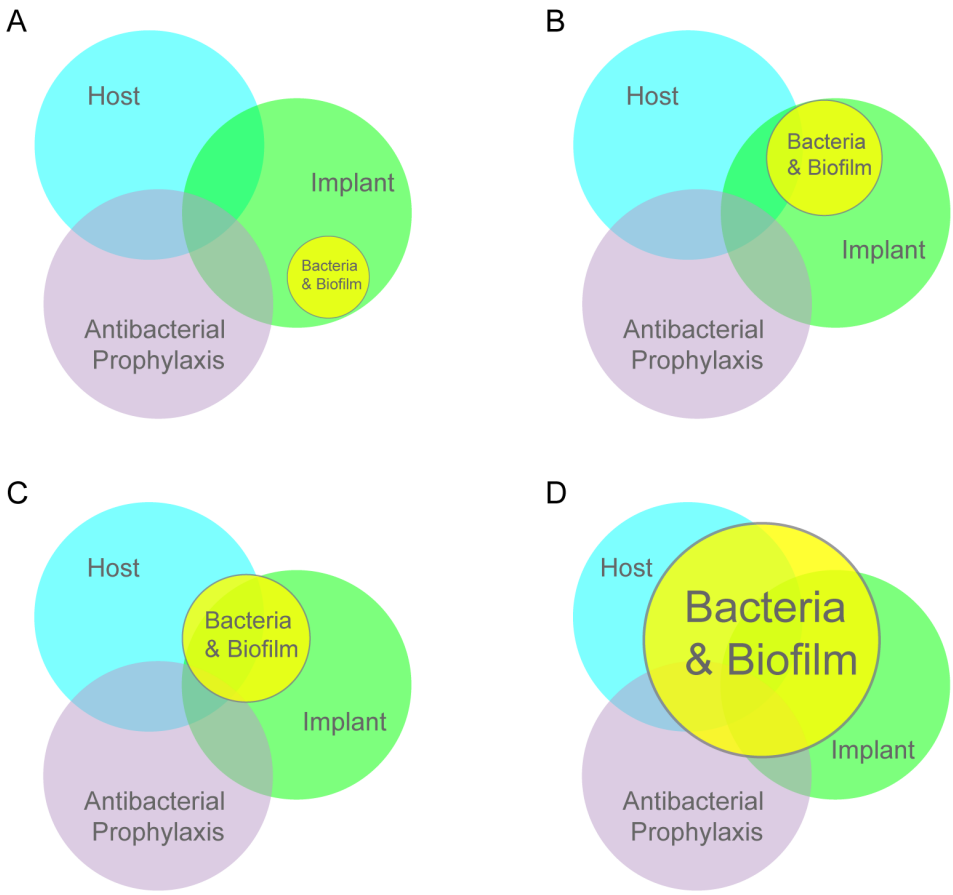

Figure 5. Representation of the clinical interaction between host, implant and antibacterial prophylaxis in the presence of biofilm-forming bacteria. (**A**) Subclinical scenario in which bacteria do not interfere in any detectable way with implant function; (**B**) Implant malfunction defined by minor clinical signs of infection; (**C**) Low-grade infection characterized by a mild host reaction and moderate clinical signs of

infection; (D) High-grade infection. in which acute signs and symptoms of infection and inflammation are present. [Romanò et al., 2017. DOI: 10.1007/5584_2016_158]

Bacteria preferentially adhere and form biofilm on rough surfaces, because surface irregularities maximize contact area while protecting the pathogens from shear forces [35].

Therefore, biofilm plays a crucial role in the pathogenesis of implant-related infections. In Figure 5 clinical scenarios in the presence of an implant contaminated with biofilm-producing microorganisms are outlined.

An early description of bacterial biofilm was presented by Costerton and colleagues in 1978 [36]. in which they described biofilm formation as an evolutionary mechanism that allows bacteria to survive in competitive environments, which favors the selection of pathogens protected from the external ecosystem [36]. Indeed, adhesion to a tissue or to the surface of an implant and subsequent biofilm formation enable bacteria to live in a protected environment with renewed nutrient supply, without being affected by fluid stream shear or by the host immune system. Microbial biofilm is defined as a population of microorganisms attached to a surface and surrounded by extracellular polymeric substance (EPS) matrix, composed of polysaccharides, proteins and nucleic acids [37]. Indeed, sessile bacteria grow as microcolonies enclosed in a thick matrix interspersed with open water channels. The biofilm is a complex dynamic environment and, the process that leads to its formation has been extensively studied and divided into five progressive steps involving bacterial attachment, aggregation, accumulation, maturation, and detachment (Figure 6) [38].

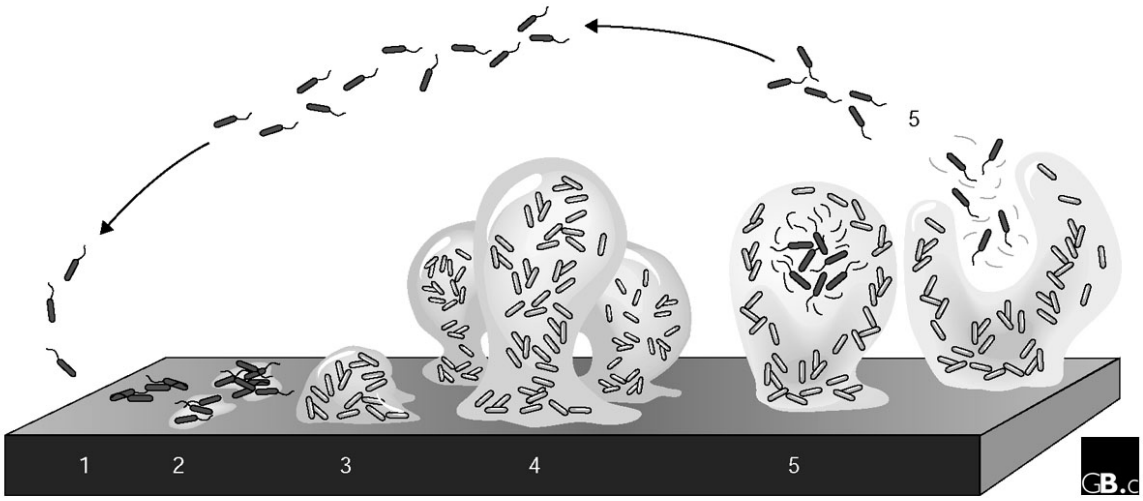

Figure 6. Representative illustration of the phases of biofilm formation. (1) Bacterial attachment; (2) Aggregation; (3) Accumulation; (4) Maturation and (5) Detachment [Sauer, 2003. DOI: 10.1186/gb-2003-4-6-219]

As soon as contamination occurs, the "race to the surface" begins as first described by Gristina and colleagues, determining the fate of the development of the infection [39]. If the race to the surface

is won by cells of the surrounding tissue, the implant surface will be occupied and, therefore, defended. Otherwise, if the race is won by bacteria, they rapidly adhere to the biomaterial and colonize the surface due to several physicochemical interactions (e.g. van der Waals and gravitational forces, electrostatic repulsion, and ionic and dipole interactions). Thereafter, bacteria start to proliferate and aggregate in clusters through cell-to-cell adhesion; guided by molecular signaling, they secrete EPS to form a multi-layered structured biofilm [33, 40].

These micro colonies can remain quietly embedded in biofilm for extended periods of time until the environment allows them to overgrow or until detachment of single cells or larger cell clusters occurs [35]. Biofilm detachment is a crucial evolutionary phase of the infection process since it allows the dissemination of bacteria and, consequently, the colonization of other sites within the host [38]. Several factors may contribute to the detachment of single cells or larger bacterial clusters such as mechanical forces from bloodstream flow or chemical stimuli, such as the transcription of protease or the inhibition of the production of exopolysaccharide [38].

However, the entire pathway that regulates biofilm formation *in vivo* is still unknown due to the complex interaction between the host and microorganisms. For the latter reason, *in vitro* studies cannot entirely mimic the *in vivo* environment. Hence, there is a real need to investigate the pathogenesis of orthopedic infections mediated by biofilm formation through *in vivo* animal models [41].

Animal models of implant-related infections

Several animal models have been established to study osteomyelitis or implant-related infections in terms of pathogenesis, development, and diagnosis. Models have been used also to investigate host response to novel therapeutic or preventive approaches to fight implant-related infections. However, animal models which use low –virulence pathogens, such as *S. epidermidis* and *Propionibacterium acnes*, are poorly described in the literature probably due to their lower incidence in orthopedic infections [29]. Indeed, in 2016 a PubMed search was conducted to review the existing animal models of implant-related low-grade infections published in the last twenty years. Manuscripts were searched using the following keywords: animal model(s) OR preclinical model(s) AND orthopedic infection(s) OR osteomyelitis OR prosthetic infection(s). A total of 764 studies were identified, of which 118 duplicates and 38 non-English studies. As a result, only 45 articles were considered: 39 describing the use of highly virulent pathogens used at low bacterial load and 6 analyzing low virulence pathogens (Figure 7). Of the six articles, only one was focused on infection caused by *P. acnes* and the remaining five on *S. epidermidis*. However, none described or investigated the development of septic non-unions caused by low virulence bacteria, emphasizing the lack of knowledge in this field. Therefore, the creation of a valid animal model of low-grade non-union is crucial to study the complex physiopathology of non-unions in order to optimize both preventive and therapeutic strategies [42].

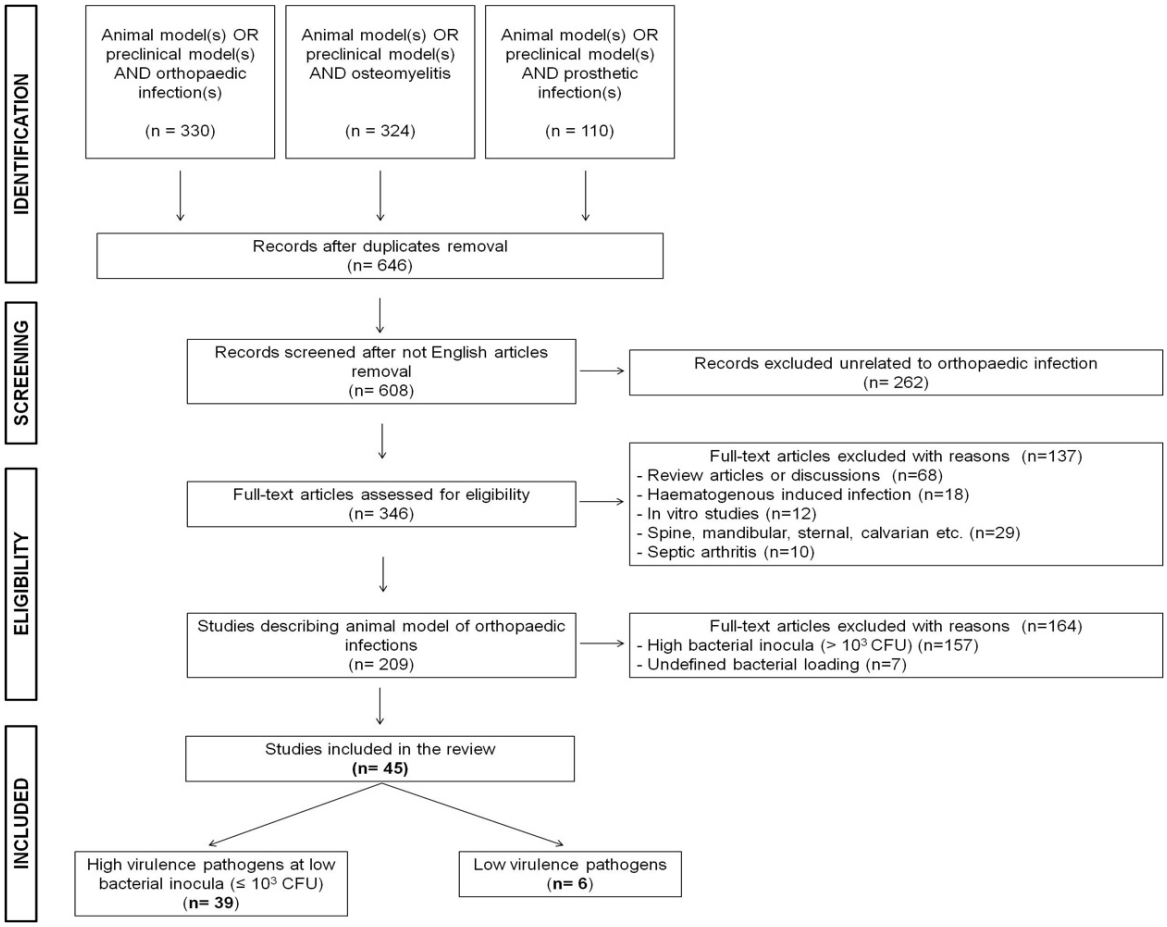

Figure 7. Research strategy. Flow chart of the process of article selection. [Lovati et al., 2017. DOI: 10.1007/5584_2016_157]

Therapeutic approaches to treat septic non-unions

Therapeutic approaches to treat septic non-unions described in the literature, include surgical debridement of the infected tissue, followed by local or systemic antibiotic therapies [20, 34]. Indeed, this two-step procedure is routinely used in clinical practice for the treatment of septic non-unions; primarily, the infected tissue is eradicated through debridement of the affected bone and soft tissues. Then, the resulting gap is reconstructed by means of antibiotic-loaded cement or bone graft [43]. Recently, new protocols in bone tissue engineering propose the use of biological or synthetic scaffolds with osteoinductive and antibacterial proprieties to handle biofilm-mediated infections after surgical debridement [44, 45]. However, most of these innovative materials have some drawbacks, including non-biodegradability, the availability to microbial adhesion and subsequent biofilm formation on their surfaces, restricted range of loadable antibiotics and long-lasting release with a possible increase of antibiotic resistance [46]. These limitations highlight the need for alternative biodegradable biomaterials which can locally deliver and substantial amounts of treatment [47]. Hence, hydrogels represent promising and potential alternative materials to locally convey antibiotics, growth factors or cells, while inducing osteogenesis and forestalling bacterial infections associated with orthopedic devices [48, 49].

Moreover, in the last few years, bone tissue engineering and cell-based therapy achieved some impressive results in the regeneration of organs or tissues, as well as in the treatment of non-septic non-unions [50-52]. This cell therapy approach aims at delivering healthy progenitor cells able to repair the loss of function of damaged tissues. Mesenchymal stromal cells (MSCs) are promising in biomedical research and cell-based therapies due to the ability of these cells to self-renew, differentiate *in vitro* into mesenchymal tissues such as bone, cartilage, or fat and being an readily accessible source of autologous cells [53, 54]. Another advantage in the use of MSCs is represented by the lack of the major histocompatibility complex II (MHC II) which permits the allogeneic transplant of these cells [55]. Furthermore, some recent studies demonstrated the immunomodulatory [56-58] and antimicrobial features [59] of MSCs. Indeed, it has been demonstrated that MSCs are able to suppress the inflammatory response by inhibiting T cell action [60], as well as the inhibition of the maturation of antigen-presenting cells [61]. In particular, MSCs have been shown to be effective in the control of the inflammatory processes within tissues and organs [62, 63]. In the case of infections, the inflammatory process activates macrophages which will produce pro-inflammatory cytokines (e.g. TNFα, IL-1β) [64]. Some authors demonstrated that the systemic or local injection of MSCs could down-regulate the release of pro-inflammatory cytokines, thus inhibiting inflammation development [63, 65, 66]. In addition to the capability of MSCs to modulate pro-inflammatory cytokines, other studies also demonstrated the ability to stimulate the production of anti-inflammatory molecules (e.g. IL-10, IL-4) [57]. Nevertheless, the mechanism of action of MSCs in the modulation of the inflammatory process is still unclear. Finally, recent studies demonstrated that MSCs are able to limit bacterial growth *in vivo* thanks to the aforementioned proprieties which modulate the inflammatory response and macrophage activation at the site of infection [63].

Presently, most tissue engineering strategies aim at discouraging bacterial attachment to the surface of metallic implants thereby impairing the bacterial "race to the surface" [67], while favoring the eradication of the infection and improving the bone healing process. However, the preclinical evaluation of these innovative treatments has some important drawbacks. Indeed, the applied models are unable to elucidate how the infection is suppressed and why bacteria are not able to form biofilm in the presence of the hydrogel or MSCs.

As in other branches of medical science, the synergistic study of the same biological mechanism by dissimilar disciplines helps researchers to evaluate different aspects that, otherwise, would not be taken into consideration

The investigation of the interaction between the host and microorganisms, is difficult due to the enormous number of variables. Therefore, the need to thoroughly understand the mechanisms related to these infections and their pathogenesis as related to the causes of bone healing impairment, starts from the main cause: biofilm producing bacteria.

Molecular approaches to investigate septic non-unions: from genomics to proteomics

Since its development in 1983, polymerase chain reaction (PCR) technology has been employed in microbiological laboratories as an accurate, rapid and sensitive diagnostic tool for the analysis of microorganisms in clinical, environmental and food specimens [68].

In recent years, PCR has been applied to a large number of genome analyses and this technology has been widely optimized and modified, according to scientific demands. Indeed, the versatility of PCR has led to the development of a number of protocols including Real-Time PCR. This quantitative PCR technique analyzes target messenger RNA in a sample, enabling the measurement of the expression of a specific gene [69]. Due to the ability to quantify cellular transcript levels, the focus of molecular biologists shifted from the study of static composition of the genome to functional analysis of the pathways activated by cells under different environmental conditions. Indeed, Real-Time PCR analyses are context-dependent because they measure the number of mRNA copies depending on the physiological or pathological status of cells [70].

Additionally, from the time when the first two complete bacterial sequences were published in 1995 [71, 72], the number of bacterial genome sequences deposited in public databases has increased, as a result of the cost reduction triggered by technological and methodological advancement [73]. The availability of whole bacterial genome sequences in public databases allowed the study of the expression of the entire genome of a microorganism, launching the post-genomic era [74]. Indeed, it is now possible to assay the expression of target genes and to evaluate their modulation under different growth conditions. In particular, proteomic analyses are capable of comparing proteins expressed by microorganisms or cells when they are exposed to various stimuli. Since mRNA levels do not necessarily correlate with protein levels, proteomic analysis quantifies up- or downregulated proteins to determine their abundance, as well as assessing the presence of post-translational modifications (PTMs) enabling the study of their biological roles [75]. Notably, protein activity can be modulated by PTMs now known to be implicated in the pathogenesis of some important neurodegenerative diseases, such as Alzheimer's disease [76].

The aim of the proteomic approach is to extract, separate and identify all the proteins expressed by cells in a given experimental setting. Protein identification requires the availability of genome information in public databases, including the functional annotation of the target genome. Indeed, protein structural information is now available through mass spectrometry (MS), an analytical technique able to convert proteins or peptides into ions and to sort them based on their mass-to-charge ratio [77]. Profiling gene expression patterns in biofilm producing bacteria through omics sciences is crucial to decipher the genetic basis of biofilm formation. Thus, it could provide the groundwork for the development of new drugs against biofilm-related infections, as well as the identification of novel biomarkers [78].

Molecular basis of biofilm formation

Biofilm-forming bacteria have a gene expression pattern that differs from planktonic forms; various genes have been found to be up- or down-regulated during biofilm formation, ranging from 1 to 38% of the total genome [74]. Likewise, the establishment of staphylococcal biofilm is mediated by the activation of different genes, according to the stage of biofilm development. This pathway has been studied and divided into progressive steps involving the expression of specific proteins during attachment, aggregation, accumulation, maturation, and detachment [38]. Staphylococcal attachment is characterized by the expression of proteins related to bacterial adhesion to the surface of the device. In this step, wall teichoic acid (WTA), adhesins/autolysins (AltE and Aea), as well as the Microbial Surface Components Recognizing Adhesive Matrix Molecules (MSCRAMM'S) play a fundamental role in initial attachment [79]. Subsequently, the production of Polysaccharide Intercellular Adhesin (PIA)/poly-N- acetylglucosamine (PNAG) contributes to the cell-to-cell adhesion process. The synthesis of PIA is regulated by the intercellular adhesion (*ica*ADBC) locus, which encodes enzymes able to trigger the synthesis of PNAG in *ica*-dependent biofilm producers. Staphylococci are also capable of producing biofilm through an *ica*-independent pathway, when the *ica*ADBC locus is missing or deleted [33]. In this scenario, biofilm formation in *S. epidermidis* is mediated by adhesive proteins, such as Biofilm Associated Proteins (Bap) and Accumulation Associated Protein (Aap) [33]. It has been described that up to 27% of *S. epidermidis* clinical isolates characterized as being biofilm producers are *ica*-dependent pathogens [79]. The extracellular matrix produced in the accumulation stage is mainly composed of exopolysaccharides (PNAG), proteins (e.g. Bap, Aap, and fibronectin-binding proteins, FnBPs), extracellular DNA and surface proteins (e.g. cell-wall anchored protein, CWA) [79].

Finally, in the detachment stage, bacteria separate from the mature matrix and disperse throughout the host. Bacterial embedded in biofilm secrete signal molecules which permit the cell-to-cell communication, called quorum sensing involved in the control of a large number of biological processes, including the detachment phase [79].

An *in vivo* study demonstrated how this phase depends on a well-characterized quorum-sensing system (accessory gene regulator, *agr*), through *agr* mutant bacteria in a rabbit model of medical device–related infection [80]. Indeed, the quorum-sensing system *agr* is involved in the up-regulation of acute virulence factors and in the simultaneous down-regulation of surface protein expression involved in bacterial attachment [38]. The quorum-sensing system *agr* is modulated by cell-to-cell communication, triggering the synthesis of phenol soluble modulins (PSMs), alpha-helical ampholytes (Figure 8) [81]. The expression of PSMs represents an essential virulence factor of *S. epidermidis*, leading to the shift between an aggressive and silent form during staphylococcal infections [78]. Moreover, PSMs not only are implicated in the spread of the infection due to biofilm detachment but they also are involved in the lysis of red and white blood cells and neutrophils, stimulating the inflammatory response [82].

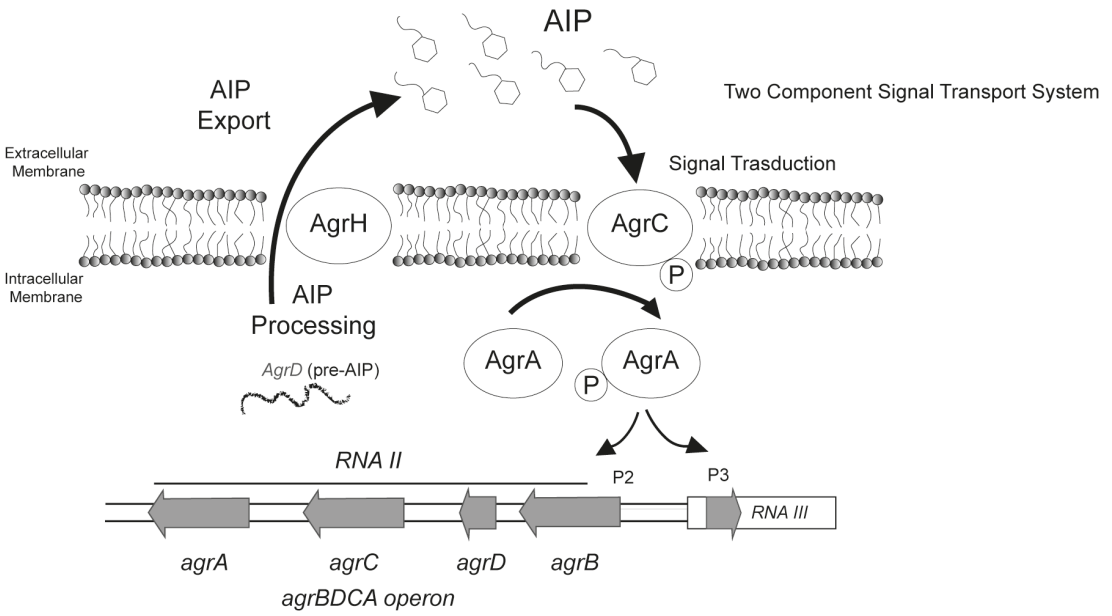

Figure 8. Schematic quorum sensing-agr pathway. [Adapted from Kırmusaoğlu 2016. DOI: 10.5772/62943]

In *S. epidermidis*-mediated infections, biofilm production is strictly related to the environmental conditions in which bacteria grow, such as culture media composition and supplements, the presence of iron ions, salt stress and oxygen [79]. Indeed, both genetic and environmental influences have an impact on biofilm formation; bacteria can adapt to different growing conditions by modulating their biofilm structure [24]. To fully comprehend how nutrients and the mechanical environment (e.g. shear stress) acts or interferes with biofilm formation requires the study of biofilm physiology in greater detail to determine the molecular basis for the development of anti-staphylococcal drugs and treatments.

Future prospective in anti-biofilm therapies

The study of virulence factors and regulatory mechanisms correlated to biofilm-mediated infections may encourage the development of innovative therapeutic strategies, to discourage implant bacterial colonization at the molecular level. Clearly, all the strategies proposed and conceived so far have not been sufficient to reduce this severe complication.

The primary intention of orthopedic devices is to provide mechanical stabilization and osseointegration, to quickly restore the physiological function of the injured limb, while limiting the risk of infections. For this reason, biomaterials used in clinics are rigorously regulated by the International Organization for Standardization (ISO) and the American Society for Testing and Materials (ASTM) [83].

In order to improve implant osseointegration, orthopedic devices have various degrees of surface

roughness. The modification of the surface not only plays a role in implant integration but may also facilitate bacterial adhesion leading to infections [83, 84]. Some studies evaluated the bacterial capability to adhere on metal alloys, identifying a range of roughness and establishing a minimum threshold to avoid colonization. Theoretically, biofilm formation can be impaired by means of smoothing the implant surface [81]. However, this adjustment may delay the integration of the implant, reducing its function.

To overcome this main drawback, many efforts have been devoted to the development of coatings able to interfere with the early stages of biofilm formation by preventing bacterial attachment.

Currently, there is not a universally accepted classification of coating technologies because of the lack of regulatory aspects and standardized validation methods [85]. However, according to their mechanisms of action, coatings can be classified as passive or active surface modifications (PSM and ASM, respectively), or as peri-operative antibacterial local carriers (LCC) (Figure 9).

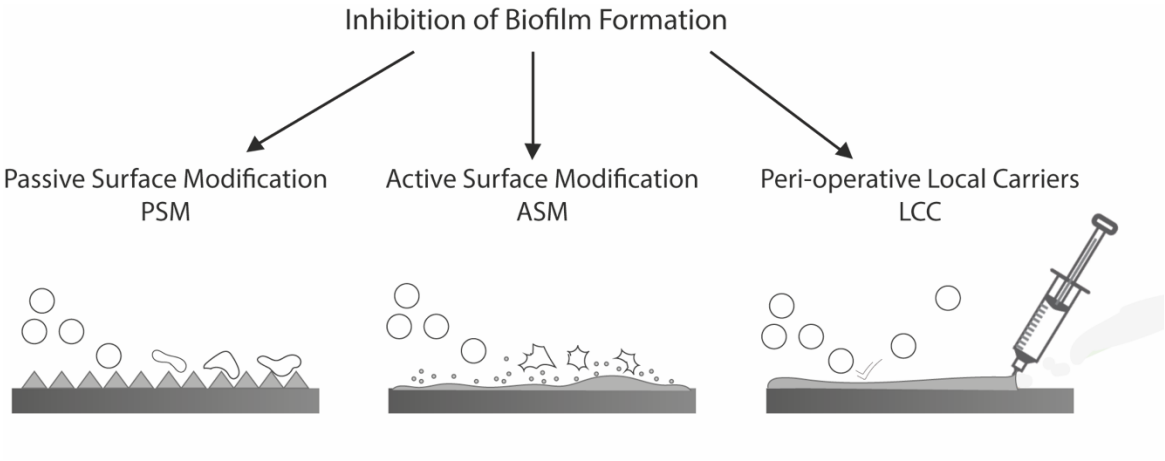

Figure 9. A representative illustration of implant coating mechanisms of action.

Specifically, PSM impedes bacterial adhesion or directly kills pathogens upon contact through chemical or physical alterations of the surface, without the release of antimicrobial agents or antibiotics. In contrast, ASM acts by locally delivering antibiotics or bactericidal agents such as metal ions, or organic and inorganic compounds [86, 87]. Finally, LCC are usually biodegradable barriers able to locally deliver high concentrations of antibacterial in a restricted temporal window [85]. Presently, there are different coatings available in the orthopedic marketplace. However, there are several issues related to their application. Specifically, these include dosage, release kinetics, stability, and biodegradation rates which may lead to antibiotic resistance or alteration in the local microbiologic flora [86].

The development of new molecular techniques, in the last few years make it possible to identify new markers of infections, together with new therapeutic targets or vaccines [88].

This innovation could provide the basis for novel strategies for targeting bacterial biofilm

determinants including blocking the synthesis of PIA/PNAG [79], or developing anti-QS treatments and/or biofilm dispersal agents [88] or identifying new vaccines against MASCRAMMs [89] or PSMs [82]. There are no FDA approved vaccines for the treatment of staphylococcal infections [81]. Thus, there is the need for intensive molecular research focused on biofilm-mediated infection in order to develop a safe, broad-spectrum preventive or therapeutic approach.

Last but not least, the prophylaxis of implant-related infections in hospital settings should be emphasized [81]. Orthopedic operations are an extremely risky surgery, due to prolonged intervention, massive blood loss and due to the implant of foreign bodies, thus requiring an ultra-clean environment [90]. Simple protocols can avoid debilitating consequences, such as the installation of equipment like laminar air flow and/or ultraviolet light can significantly reduce the risks of airborne and non-airborne bacterial contaminations [91]. Moreover, orthopedic surgical teams must reconsider the importance of skin disinfection and decontamination of surgical instruments or orthopedic materials [90]. This central issue could only be accomplished by the surgeons thorough understanding of the factors that may contribute to infection development.

Aim of the study

The introduction section reviewed current knowledge concerning the development of septic non-unions while describing the central role of bacterial biofilm and the need to counteract biofilm formation on orthopedic implants. The mechanisms related to biofilm-mediated infections could be elucidated with the creation of new animal models. However, in the literature, there are few animal models which describe the use of low virulence pathogens, such as *S. epidermidis*.

To address these issues, the first aim of the project was to develop a preclinical model of infected non-union able to resemble the features of a nosocomial implant-associated infection, in order to investigate new preventive or therapeutic options (Chapter 1). We evaluated the incidence of infected non-unions caused by different cell concentrations of methicillin-resistant *S. epidermidis* (MRSE) in rats that underwent femoral fractures synthesized with metal implants.

The development of a valid animal model was crucial for the subsequent experimental phase. Indeed, the second aim was focused on the evaluation of innovative preventive and/or therapeutic strategies using the preclinical model developed in aim 1 above (Chapter 2). In particular, the rat model of the sub-acute onset – infected with 10^5 CFU MRSE - was chosen and used to test the efficacy of a local antibiotic therapy delivered through a hydrogel with osteoinductive and antibacterial proprieties. Moreover, the same model was used to test the feasibility of a cell-based approach, by the systemic or local injection of undifferentiated allogeneic BMSCs. The overall goal of this first part of the project was to examine potential therapeutic strategies for the prevention and the treatment of infected non-unions.

The second aim of the project was to decipher the genetic basis of biofilm formation through the *in vitro* analysis of the proteome of two different strains of *S. epidermidis* growing as sessile or planktonic forms. First, in order to appropriately identify the changes in the proteomic profile of *S. epidermidis* GOI1153754-03-14, the whole genome of this bacterium was sequenced through next generation sequencing analysis and the sequence was deposited in the DDBJ/ENA/GenBank database under the accession number FWCG01000000 (Chapter 3).

Thereafter, the second part of the aim compared the proteomic profiles of *S. epidermidis* ATCC 35984, and the clinical isolate GOI1153754-03-14 statically cultured in their planktonic and sessile forms (Chapter 4). Through this study design, we were able to evaluate the changes in the proteomic profiles as the result of biofilm maturation on titanium in a static environment.

The primary purpose of the final chapter was to define how protein expression varied between two different bacterial strains belonging to the same species while determining how the culture conditions can modulate these differences. Comparative proteomic analyses may enable the scientific community to understand the molecular pathways associated with biofilm formation on implants and identify future therapeutic targets or diagnostic biomarkers.

References

1. Gómez-Barrena E, Rosset P, Lozano D, et al. Bone fracture healing: cell therapy in delayed unions and nonunions. Bone. 2015. 70:93-101.
2. Meling T, Harboe K, Søreide K. Incidence of traumatic long-bone fractures requiring in-hospital management: a prospective age- and gender-specific analysis of 4890 fractures. Injury. 2009. 40(11):1212-1219.
3. Hak DJ, Fitzpatrick D, Bishop JA, et al. Delayed union and nonunions: epidemiology, clinical issues, and financial aspects. Injury. 2014. 45 Suppl 2:S3-7.
4. Schell H, Duda GN, Peters A, et al. The haematoma and its role in bone healing. J Exp Orthop. 2017. 4(1):5.
5. Hankenson KD, Zimmerman G, Marcucio R. Biological perspectives of delayed fracture healing. Injury. 2014. 45 Suppl 2:S8-S15.
6. Sarmiento A, Latta LL. Functional Fracture Bracing. Berlin Heidelberg New York: Springer-Verlag. 1995.
7. Marsell R, Einhorn TA. The biology of fracture healing. Injury. 2011. 42(6):551-555.
8. Claes LE, Heigele CA, Neidlinger-Wilke C, et al. Effects of mechanical factors on the fracture healing process. Clin Orthop Relat Res. 1998. (355 Suppl):S132-147.
9. Marsell R, Einhorn TA. Emerging bone healing therapies. J Orthop Trauma. 2010. 24 Suppl 1:S4-8.
10. Megas P. Classification of non-union. Injury. 2005. 36 Suppl 4:S30-37.
11. Miranda MA, Moon MS. Treatment strategy for nonunions and malunions. Surgical treatment of orthopaedic trauma. 2007. 1:77-100.
12. Zura R, Xiong Z, Einhorn T, et al. Epidemiology of fracture nonunion in 18 human bones. JAMA Surg. 2016. 16;151(11):e162775.
13. Saleh, KJ, Hak DJ, Nierengarten MB. Socioeconomic burden of traumatic tibial fractures: non union or delayed union. Medscape Orthopaedics Clinical Updates. 2001. 1-22.
14. Antonova E, Le TK, Burge R, et al. Tibia shaft fractures: costly burden of nonunions. BMC Musculoskelet Disord. 2013. 26;14:42.
15. Niikura T, Lee SY, Sakai Y, et al. Causative factors of fracture nonunion: the proportions of mechanical, biological, patient-dependent, and patient-independent factors. J Orthop Sci. 2014. 19(1):120-124.
16. Green E, Lubahn JD, Evans J. Risk factors, treatment, and outcomes associated with nonunion of the midshaft humerus fracture. J Surg Orthop Adv. 2005. 14(2):64-72.
17. Hernandez RK, Do TP, Critchlow CW, et al. Patient-related risk factors for fracture-healing complications in the United Kingdom General Practice Research Database. Acta Orthop. 2012. 83:653–660.
18. Yamanaka JS, Yanagihara GR, Carlos BL, et al. A high-fat diet can affect bone healing in growing rats. J Bone Miner Metab. 2017. [Epub ahead of print]
19. Harder AT, An YH. The mechanisms of the inhibitory effects of nonsteroidal anti-inflammatory drugs on bone healing: a concise review. J Clin Pharmacol. 2003. 43(8):807-815.
20. Pelser P. Management of septic non-unions. SA Orthopaedic Journal. 2009. 8.2: 29-34.

21. Boxma H, Broekhuizen T, Patka P, et al. Randomised controlled trial of single-dose antibiotic prophylaxis in surgical treatment of closed fractures: the Dutch Trauma Trial. Lancet. 1996. 27;347(9009):1133-1137.
22. Trampuz A, Widmer AF. Infections associated with orthopedic implants. Curr Opin Infect Dis. 2006. 19:349–356.
23. Metsemakers WJ, Kuehl R, Moriarty TF, et al. Infection after fracture fixation: current surgical and microbiological concepts. Injury. 2016. S0020-1383(16)30470-30473.
24. Gupta P, Sarkar S, Das B, et al. Biofilm, pathogenesis and prevention--a journey to break the wall: a review. Arch Microbiol. 2016. 198(1):1-15.
25. Phillips JE, Crane TP, Noy M, et al. The incidence of deep prosthetic infections in a specialist orthopaedic hospital: a 15-year prospective survey. J Bone Joint Surg (Br). 2006. 88:943–948.
26. Portillo ME, Corvec S, Borens O, et al. Propioni- bacterium acnes: an underestimated pathogen in implant-associated infections. Biomed Res Int. 2013. 2013:804391.
27. Arciola CR, Campoccia D, Ehrlich GD, et al. Biofilm-based implant infections in orthopaedics. Adv Exp Med Biol. 2015. 830:29–46.
28. Campoccia D, Montanaro L, Arciola CR. The significance of infection related to orthopaedic devices and issues of antibiotic resistance. Biomaterials. 2006. 27:2331–2339.
29. Lovati AB, Bottagisio M, de Vecchi E, et al. Animal models of implant-related low-grade infections. A twenty-year review. Adv Exp Med Biol. 2017. 971:29-50.
30. Ziebuhr W, Hennig S, Eckart M, et al. Nosocomial infections by Staphylococcus epidermidis: how a commensal bacterium turns into a pathogen. Int J Antimicrob Agents. 2006. 28(1):14-20.
31. Fey PD, Olson ME. Current concepts in biofilm formation of Staphylococcus epidermidis. Future Microbiol. 2010. 5(6):917-933.
32. Patel R. Biofilms and Antimicrobial Resistance. Clinical Orthop and Relat Res. 2005. 437:41-47.
33. Kirmusaoğlu S. Staphylococcal biofilms: pathogenicity, mechanism and regulation of biofilm formation by quorum-sensing system and antibiotic resistance mechanisms of biofilm-embedded microorganisms. Microbial Biofilms-Importance and Applications. InTech, 2016.
34. Bhatia C, Tiwari AK, Sharma SB, et al. Role of antibiotic cement coated nailing in infected nonunion of tibia. Malays Orthop J. 2017. 11(1):6-11.
35. Ribeiro M, Monteiro FJ, Ferraz MP. Infection of orthopedic implants with emphasis on bacterial adhesion process and techniques used in studying bacterial-material interactions. Biomatter. 2012. 2(4):176-194.
36. Costerton JW, Geesey GG, Cheng KJ. How bacteria stick. Sci Am. 1978. 238(1):86-95.
37. Hall-Stoodley L, Costerton JW, Stoodley P. Bacterial biofilms: from the natural environment to infectious diseases. Nat Rev Microbiol. 2004. 2(2):95-108.
38. Otto M. Staphylococcal Biofilms. Curr Top Microbiol Immunol. 2008. 322:207-228.
39. Gristina AG, Naylor PT, Myrvik Q. The race for the surface: microbes, tissue cells, and biomaterials. In: Switalski L, Höök M, Beachey E. (eds) Molecular Mechanisms of Microbial Adhesion. Springer, New York, NY. 1989.

40. Koseki H, Yonekura A, Shida T, et al. Early staphylococcal biofilm formation on solid orthopaedic implant materials: in vitro study. PLoS One. 2014. 9;9(10):e107588.
41. Tatara AM, Shah SR, Livingston CE, et al. Infected animal models for tissue engineering. Methods. 2015. 84:17–24.
42. Garcia P, Histing T, Holstein JH, et al. Rodent animal models of delayed bone healing and non-union formation: a comparative review. Eur Cell Mater. 2013. 16(26):1-14.
43. Motsitsi NS. Management of infected nonunion of long bones: the last decade (1996-2006). Injury. 2008. 39(2):155-160.
44. Mouriño V, Boccaccini AR. Bone tissue engineering therapeutics: controlled drug delivery in three-dimensional scaffolds. J R Soc Interface. 2010. 6;7(43):209-227.
45. Giavaresi G, Borsari V, Fini M, et al. Preliminary investigations on a new gentamicin and vancomycin-coated PMMA nail for the treatment of bone and intramedullary infections: An experimental study in the rabbit. J Orthop Res. 2008. 26(6):785-792.
46. Kluin OS, van der Mei HC, Busscher HJ, et al. Biodegradable vs non-biodegradable antibiotic delivery devices in the treatment of osteomyelitis. Expert Opin Drug Deliv. 2013. 10(3):341-351.
47. El-Husseiny M, Patel S, Macfarlane RJ, et al. Biodegradable antibiotic delivery systems. Jour of Bone and Joint Surg. 2011. 93(2):151-157.
48. Changez M, Burugapalli K, Koul V, et al. The effect of composition of poly(acrili acid)-gelatin hydrogel on gentamicin sulphate release: in vitro. Biomaterials. 2003. 24(4):527-536.
49. Giavaresi G, Meani E, Sartori M, et al. Efficacy of antibacterial-loaded coating in an in vivo model of acutely highly contaminated implant. Intern Orthop. 2014. 38(7):1505-1512.
50. Quarto R, Mastrogiacomo M, Cancedda R, et al. Repair of large bone defects with the use of autologous bone marrow stromal cells. The New England Journal of Medicine. 2001. 344(5):385–386.
51. Hernigou P, Mathieu G, Poignard A, et al. Percutaneous autologous bone-marrow grafting for nonunions. J Bone Joint Surg Am. 2006. 88(1):322–327.
52. Tseng SS, Lee MA, Reddi AH. Nonunions and the potential of stem cells in fracture-healing. J Bone Joint Surg Am. 2008. 90(1):92–98.
53. Dominici M, Le Blanc K, Mueller I, et al. Minimal Criteria for Defining Multipotent Mesenchymal Stromal Cells. International Society for Cellular Therapy Position Statement. Cytotherapy. 2006. 8(4):315–317.
54. Pittenger MF, Mackay AM, Beck SC, et al. Multilineage potential of adult human mesenchymal stem cells. Science. 1999. 284(5411):143–147.
55. Ryan JM, Barry FP, Murphy JM, et al. Mesenchymal stem cells avoid allogeneic rejection. J Inflam. 2005. 2:8.
56. Frank MH, Sayegh MH. Immunomodulatory functions of mesenchymal stem cells. Lancet. 2004. 363(9419):1411-1412.
57. Aggarwal S, Pittenger MF. Human mesenchymal stem cells modulate allogeneic immune cell response. Blood. 2005. 105:1815-1822.
58. Fibbe WE, Nauta AJ, Roelofs H. Modulation of immune iesponses by mesenchymal stem cells. Ann N Y Acad Sci. 2007. 1106:272–278.

59. Johnson V, Webb T, Dow S. Activated mesenchymal stem cells amplify antibiotic activity against chronic Staphylococcus aureus infection. J Immunol. 2013. 190(1):180.11.
60. Krampera M, Glennie S, Dyson J, et al. Bone marrow mesenchymal stem cells inhibit the response of naive and memory antigen-specific T cells to their cognate peptide. Blood. 2003. 101:3722–3729.
61. Beyth S, Borovsky Z, Mevorach D, et al. Human mesenchymal stem cells alter antigen-presenting cell maturation and induce T-cell unresponsiveness. Blood. 2005.105:2214–2219.
62. Baksh D, Song L, Tuan RS. Adult mesenchymal stem cells: characterization, differentiation, and application in cell and gene therapy. J Cell Mol Med. 2004. 8:301-316.
63. Mei SHJ, Haitsma JJ, Dos Santos CC, et al. Mesenchymal stem cells reduce inflammation while enhancing bacterial clearance and improving survival in sepsis. Am J Respir Crit Care Med. 2010. 182:1047-1057.
64. Zhang JM, An J. Cytokines, inflammation, and pain. Int Anesthesiol Clin. 2007. 45(2):27-37.
65. Xu J, Woods CR, Mora AL, et al. Prevention of endotoxin-induced systemic response by bone marrow-derived mesenchymal stem cells in mice. Am J Physiol Lung Cell Mol Physiol. 2007. 293:131-141.
66. Singer NG, Caplan AL. Mesenchymal stem cells: mechanisms of inflammation. Annu Rev Pathol. 2011. 6:457-478.
67. Gristina AG. Biomaterial-centered infection: microbial adhesion versus tissue integration. Science. 1987. 25;237(4822):1588-1595.
68. Lantz PG, Abu al-Soud W, Knutsson R, et al. Biotechnical use of polymerase chain reaction for microbiological analysis of biological samples. Biotechnol Annu Rev. 2000. 5:87-130.
69. Kralik P, Ricchi M. A basic guide to Real Time PCR in microbial diagnostics: definitions, parameters, and everything. Front Microbiol. 2017. 2;8:108.
70. Bustin SA, Nolan T. Pitfalls of quantitative real-time reverse-transcription polymerase chain reaction. J Biomol Tech. 2004. 15(3):155-166.
71. Fleischmann RD, Adams MD, White O, et al. Whole-genome random sequencing and assembly of Haemophilus influenzae Rd. Science. 1995. 28;269(5223):496-512.
72. Fraser CM, Gocayne JD, White O, et al. The minimal gene complement of Mycoplasma genitalium. Science. 1995. 20;270(5235):397-403.
73. Land M, Hauser L, Jun SR. Insights from 20 years of bacterial genome sequencing. Funct Integr Genomics. 2015. 5(2):141-161.
74. Sauer K. The genomics and proteomics of biofilm formation. Genome Biol. 2003. 4(6):219.
75. Bunnik EM, Le Roch KG. An introduction to functional genomics and systems biology. Adv Wound Care. 2013. 2(9):490-498.
76. Russell CL, Koncarevic S, Ward MA. Post-translational modifications in Alzheimer's disease and the potential for new biomarkers. J Alzheimers Dis. 2014. 41(2):345-364.
77. Graves PR, Haystead TA. Molecular biologist's guide to proteomics. Microbiol Mol Biol Rev. 2002. 66(1):39-63.
78. Yao Y, Sturdevant DE, Otto M. Genomewide analysis of gene expression in Staphylococcus epidermidis biofilms: insights into the pathophysiology of S. epidermidis biofilms and the role of phenol-soluble modulins in formation of biofilms. J Infect Dis. 2005. 15;191(2):289-298.

79. Arciola CR, Campoccia D, Speziale P. Biofilm formation in Staphylococcus implant infections. A review of molecular mechanisms and implications for biofilm-resistant materials. Biomaterials. 2012. 33(26):5967-5982.
80. Vuong C, Kocianova S, Yao Y, et al. Increased colonization of indwelling medical devices by quorum-sensing mutants of Staphylococcus epidermidis in vivo. J Infect Dis. 2004. 15;190(8):1498-1505.
81. Joo HS, Otto M. Molecular basis of in vivo biofilm formation by bacterial pathogens. Chem Biol. 2012. 21;19(12):1503-1513.
82. Peschel A, Otto M. Phenol-soluble modulins and staphylococcal infection. Nat Rev Microbiol. 2013. 11(10):667-673.
83. Yoda I, Koseki H, Tomita M, et al. Effect of surface roughness of biomaterials on Staphylococcus epidermidis adhesion. BMC microbial. 2014. 14(1), 234.
84. Quirynen M, van der Mei HC, Bollen CM, et al. An in vivo study of the influence of the surface roughness of implants on the microbiology of supra- and subgingival plaque. J Dent Res. 1993. 72(9):1304-1309.
85. Romanò CL, Scarponi S, Gallazzi E, et al. Antibacterial coating of implants in orthopaedics and trauma: a classification proposal in an evolving panorama. J Orthop Surg Res. 2015. 10:157.
86. Goodman SB, Yao Z, Keeney M, et al. The future of biologic coatings for orthopaedic implants. Biomaterials. 2013. 34(13):3174-3183.
87. Gallo J, Holinka M, Moucha CS. Antibacterial Surface Treatment for Orthopaedic Implants. Int J Mol Sci. 2014. 15(8):13849-13880.
88. Wu H, Moser C, Wang HZ, et al. Strategies for combating bacterial biofilm infections. Int J Oral Sci. 2015. 23;7(1):1-7.
89. Montanaro L, Speziale P, Campoccia D, et al. Scenery of Staphylococcus implant infections in orthopedics. Future Microbiol. 2011. 6(11):1329-1349.
90. Song Z, Borgwardt L, Høiby N, et al. Prosthesis infections after orthopedic joint replacement: the possible role of bacterial biofilms. Orthop Rev. 2013. 14;5(2):65-71.
91. Evans RP. Current concepts for clean air and total joint arthroplasty: laminar air- flow and ultraviolet radiation: a systematic review. Clin Orthop Relat Res. 2011. 469: 945-953.

Chapter 1

Modeling *Staphylococcus epidermidis*-Induced Non-Unions: Subclinical and Clinical Evidence in Rats

Arianna Barbara Lovati[1]*, Carlo Luca Romanò[2], Marta Bottagisio[1,7], Lorenzo Monti[3], Elena De Vecchi[4], Sara Previdi[5], Riccardo Accetta[3], Lorenzo Drago[4,6]

[1] Cell and Tissue Engineering Laboratory, IRCCS Galeazzi Orthopaedic Institute, Milan, Italy.

[2] Dipartimento di Chirurgia Ricostruttiva e delle Infezioni Osteo-articolari, IRCCS Galeazzi Orthopaedic Institute, Milan, Italy.

[3] Orthopaedics and Traumatology, IRCCS Galeazzi Orthopaedic Institute, Milan, Italy.

[4] Laboratory of Clinical Chemistry and Microbiology, IRCCS Galeazzi Orthopaedic Institute, Milan, Italy.

[5] Laboratory of Cancer Cachexia AIRC Start-Up, Oncology Department, Mario Negri Institute for Pharmacological Research, Milan, Italy.

[6] Department of Biomedical Science for Health, University of Milan, Milan, Italy.

[7] Department of Veterinary Science and Public Health, University of Milan, Milan, Italy.

* Corresponding Author: arianna.lovati@grupposandonato.it

Cite

Lovati AB, Romanò CL, Bottagisio M, Monti L, De Vecchi E, Previdi S, Accetta R, Drago L. Modeling Staphylococcus epidermidis-Induced Non-Unions: Subclinical and Clinical Evidence in Rats. PLoS One. 2016, 21;11(1):e0147447. doi: 10.1371/journal.pone.0147447.

Abstract

S. epidermidis is one of the leading causes of orthopedic infections associated with biofilm formation on implant devices. Open fractures are at risk of *S. epidermidis* transcutaneous contamination leading to higher non-union development compared to closed fractures. Although the role of infection in delaying fracture healing is well recognized, no *in vivo* models investigated the impact of subclinical low-grade infections on bone repair and non-union. We hypothesized that the non-union rate is directly related to the load of this commonly retrieved pathogen and that a low-grade contamination delays the fracture healing without clinically detectable infection. Rat femurs were osteotomized and stabilized with plates. Fractures were infected with a characterized clinical-derived methicillin-resistant *S. epidermidis* (10^3, 10^5, 10^8 colonies forming units) and compared to uninfected controls. After 56 days, bone healing and osteomyelitis were clinically assessed and further evaluated by micro-CT, microbiological and histological analyses. The biofilm formation was visualized by scanning electron microscopy.

The control group showed no signs of infection and a complete bone healing. The 10^3 group displayed variable response to infection with a 67%of altered bone healing and positive bacterial cultures, despite no clinical signs of infection present. The 10^5 and 10^8 groups showed severe signs of osteomyelitis and a non-union rate of 83–100%, respectively. The cortical bone reaction related to the periosteal elevation in the control group and the metal scattering detected by micro-CT represented limitations of this study. Our model showed that an intraoperative low-grade *S. epidermidis* contamination might prevent the bone healing, even in the absence of infectious signs. Our findings also pointed out a dose-dependent effect between the *S. epidermidis* inoculum and non-union rate. This pilot study identifies a relevant preclinical model to assess the role of subclinical infections in orthopedic and trauma surgery and to test specifically designed diagnostic, prevention and therapeutic strategies.

Introduction

Fracture non-unions represent a great clinic and surgical challenge, in particular when associated with bacterial infections. Septic delayed- or non-union fractures have limited and often difficult treatment options, requiring prolonged hospitalization and antibiotic therapy, with a high socioeconomic impact [1, 2]. Although the development of a fracture non-union depends on many factors, including the type and site of fracture, the treatment and host response, open fractures are definitely at higher risk of non-union — 5% to 100%, depending on the degree of exposure and contamination [3] — than those undergoing osteosynthesis for closed, not contaminated fractures (1 – 2%) [4, 5]. Although this observation points out the direct relationship between fracture contamination, infection and non-union development, we currently have no animal models or data from human studies concerning the impact of subclinical, low-grade infections on bone healing and non-union. Sporadic clinical observations showed that low-virulent pathogens, like certain coagulase-negative staphylococci, might be related to non-unions or pain at the fracture site even in the absence of clinical signs of infection [6]. *Staphylococcus aureus* and *Staphylococcus epidermidis* are the most common pathogens involved in orthopaedic infections and account for 70 – 90% of the cases after elective surgery [7]. *S. epidermidis* is a harmless commensal inhabitant of human skin lacking the capability to penetrate the host [8]. Therefore, the *S. epidermidis*-related infection is caused by its delivery from the skin to the host tissues in case of open fractures and surgical procedures [9]. *S. epidermidis* is also one of the leading causes of infections associated with biofilm formation because of its high ability to adhere and colonize implant medical devices, such as catheters, heart valves and orthopaedic prosthesis [10-12]. The biofilm formation in *S. epidermidis* orthopaedic infections makes less effective the antimicrobial treatment and increases the emergence of antibiotic-resistant strains such as methicillin-resistant *S. epidermidis* (MRSE), a common osteomyelitis-inducing pathogen [13].

Concerning the consequence of *S. epidermidis*-associated infections in orthopaedic implants, animal models are mandatory to investigate the pathogenesis of non-union-related infections, with particular reference to subclinical infections. To our knowledge, there are many rodent models of osteomyelitis and septic arthritis, but only few studies did investigate the fracture repair in the presence of *S. aureus* infection by performing critical defects in long bones [1, 14-17], while no modeling of *S. epidermidis* implant-related infection in osteosynthesis has been described so far. Specifically, a few studies did investigate clinical MRSE strains in developing intravascular or urinary tract infections [18-20] as well as in wound healing and in subcutaneous models [9, 21]. Animal models of prosthetic joint and medullary canal infections have also been studied associating a clinical MRSE strain to stainless steel implants [22-24]. To the best of our knowledge, there is not a suitable animal model to mimic MRSE-induced non-union fractures. Moreover, there

are no data concerning the effect of low bacteria inocula on fracture healing after osteosynthesis. Our hypothesis is that the rate of non-union, induced by a commonly isolated pathogen, like *S. epidermidis*, is directly related to the inoculated bacterial load and that very low bacterial inocula may be associated with a higher rate of non-union development compared to uninfected controls, despite the absence of local or general signs or symptoms of a post-surgical infection.

For the first time, we propose a rat model of dose-dependent MRSE-induced non-union synthesized with metal implants both to demonstrate the role of subclinical infections in impairing the fracture healing and to create a model useful to investigate novel treatments for non-unions.

Materials and Methods

Ethics Statement

The whole study was approved by the Mario Negri Institute for Pharmacological Research (IRFMN) Animal Care and Use Committee (IACUC) (Permit N. 06/2014-PR). The animals were housed at the Institute's Animal Care Facilities that meet international standards. The IRFMN adheres to the principles set out in the following laws, regulations, and policies governing the care and use of laboratory animals: Italian Governing Law (D.lgs 26/2014; Authorization n.19/2008-A issued March 6, 2008 by Ministry of Health); Mario Negri Institutional Regulations and Policies providing internal authorization for persons conducting animal experiments (Quality Management System Certificate–UNI EN ISO 9001:2008 –Reg. N° 6121); the NIH Guide for the Care and Use of Laboratory Animals (2011 edition) and EU directives and guidelines (EEC Council Directive 2010/63/UE). The Statement of Compliance (Assurance) with the Public Health Service (PHS) Policy on Human Care and Use of Laboratory Animals has been recently reviewed (9/9/2014) and will expire on September 30, 2019 (Animal Welfare Assurance #A5023-01). The animals were regularly checked by a certified veterinarian responsible for health monitoring, animal welfare supervision, experimental protocols and procedure revision. All surgeries were performed under general anesthesia, and all efforts were made to minimize suffering.

Study design

Twenty-four 12-weeks-old Wistar male rats weighing 300–350 g (Harlan, Italy) were included in this study. The rats were randomly assigned to one of the experimental groups (n = 6 each group): the control group (CTRL) was injected with 30 µl phosphate-buffered saline (PBS); the 10^3 MRSE, 10^5 MRSE, and 10^8 MRSE groups were injected with 30 µl of a bacterial suspension containing 10^3, 10^5, and 10^8 colonies forming units (CFU) of MRSE, respectively. After 8 weeks, micro-CT scanning, microbiological and histological analyses were performed to assess the bone healing and infection, and Scanning Electron Microscopy (SEM) was carried out to visualize the biofilm formation.

Bacterial strain characterization

The MRSE strain GOI1153754-03-14 used in this study was isolated at the Laboratory of Clinical Chemistry and Microbiology (IRCCS Galeazzi Orthopaedic Institute, Milan, Italy). The strain derived from infected knee prosthesis of a patient undergone implant revision at the Center for Reconstructive Surgery of Osteoarticular Infections (IRCCS Galeazzi Orthopaedic Institute, Milan, Italy). This strain was selected for its antibiotic susceptibility pattern and its capacity to produce

biofilm on prosthetic materials *in vitro*.

Identification and antibiotic susceptibility testing

Microbiological identification was performed at a phenotypic and genotypic level. Phenotypic identification carried out on VITEK2 System (Biomerieux, France) was subsequently confirmed by pyrosequencing analysis (PSQ96RA, Diatech, Italy) of DNA of variable regions V1 and V3 of the 16S rRNA gene by using primers reported in a previous study [25]. Amplified sequences (about 60–80 bp) were compared with sequences available in BLAST search. Antimicrobial susceptibility testing and determination of the minimum inhibitory concentration (MIC) were carried out on Vitek2 System using the card AST 632 specific for staphylococci.

Biofilm formation assay by crystal violet staining

Biofilm production was evaluated according to spectrophotometric assay [26] that was repeated in triplicate. Briefly, the MRSE strain was grown on blood agar plates. After overnight incubation at 37°C in aerobiosis, a 0.5 McFarland suspension was prepared and 20µl aliquots were inoculated in 96-well plates containing 180 µl of Tryptose Soy Broth (TSB; BioMérieux). After an overnight incubation at 37° C in aerobiosis, the medium was refreshed and plates were incubated for a further 48 hours at 37° C. Un-inoculated wells containing only TSB were used as negative control. At the end of incubation, the wells were washed with PBS (Gibco, Italy) to remove bacteria not included in biofilm. Once dried, wells were stained with 200 µl of 5 % crystal violet solution (Merck, Germany) for 10 minutes, and then washed. After air-drying, 200 µl of absolute ethanol were added to solubilize the dye attached to the biofilm. The optical density (OD) of each well was measured at 595 nm by using a microplate reader (Multiskan FC, Thermo Scientific, Italy). Strains were classified as strong, moderate or weak producers of biofilm, according to criteria defined by Stepanovic et al [27], which are based on the comparison between the OD of strain under testing and a cut-off value (ODc) defined as three standard deviation above the mean OD of the negative control (un-inoculated broth). In particular, if the sample OD (ODs) is less than the ODc, the strain is considered as a non-biofilm producer. If the ODs value is comprised between 1 and 2 ODc, the strain is classified as a weak producer. If the ODs values is comprised between 2 and 4 ODc, the strain is classified as a moderate producer. Finally, if the ODs value is greater than 4 ODc, the strain is classified as a strong producer.

Preparation of MRSE for inoculation into the femur fracture

Previously characterized MRSE strain was cultured onto Mannitol Salt Agar (BioMérieux) at 37° C overnight. To prepare the inoculum, a selected colony was cultured into Brain Heart Infusion Broth (BHI, BioMérieux) and incubated for 16 hours at 37°C. The bacterial suspension was washed

twice and the obtained pellet was suspended in sterile saline to obtain a 10 McFarland turbidity equal to about 3×10^8 CFU/ml. The bacterial suspension was then serially diluted with sterile saline solution to obtain the desired bacterial load of $1x10^3$, $1x10^5$ and $1x10^8$ CFU/30 µl. Bacterial inocula were verified and confirmed by agar plate counting procedures. The bacterial suspension was used within 2 hours and stored at 4° C until use.

In vivo surgical procedures

Twenty-four 12-weeks old male Wistar rats (mean body weight 337.6 ± 10.2 g) were used for the experiments. The rats were maintained in controlled conditions of temperature and lightning and fed with autoclaved food and water provided ad libitum. All pre-surgical and surgical procedures on the animals were performed under a laminar flow hood. The rats were anesthetized via inhalation of isoflurane (3 %; Merial, Italy) and maintained with an intraperitoneal injection of ketamine hydrochloride (80 mg/kg; Imalgene, Merial) and medetomidine hydrochloride (1 mg/kg; Domitor, Pfizer, Italy). All animals received a preoperative intramuscular single injection of cefazolin (30 mg/kg; Cefamezin, Teva, Italy) and a subcutaneous treatment with carprofen (5 mg/kg; Rimadyl, Pfizer). Using aseptic technique, all rats were submitted to a midshaft osteotomy of the right femur. Briefly, after shaving and disinfection, a longitudinal 2.5 cm skin incision was performed through a lateral approach to expose the femoral shaft by blunt dissection between the lateral vastus muscle and the femoral biceps muscle. Using the distal screw as a pivot, the plate was diverted from the femur and a 1 mm non-critical midshaft full-thickness defect was created after a localized periosteal elevation with an electric circular saw under continuous sterile saline irrigation (Figure 1A). A compression stainless steel four-hole-mini-plate (length 20 mm, width 4 mm, height 1 mm) (Mini Fragment plate) was fixed on the anterolateral surface of the femoral diaphysis using four 1.5 mm Ø bicortical screws (all from Zimmer, Germany). In the infected groups, a volume of 30 µl of the bacterial suspension, corresponding to an inoculum of about $1x10^3$, $1x10^5$ and $1x10^8$ CFU/rat was injected into the femoral defect and the suspension was allowed to spread throughout the medullary canal. The sham-inoculated control group received an inoculum of 30 µl sterile PBS. Then the muscular planes were closed with a continuous suture with Vycril 4/0 and the skin with separated stitches with Prolene 4/0 (Johnson&Johnson, Italy). The stability of the fracture was firstly manually assessed, then confirmed by fluoroscopic examination (Figure 1B). Atipamezole (1 mg/kg; Antisedan, Pfizer) was administered subcutaneously to recover the animals from general anesthesia.

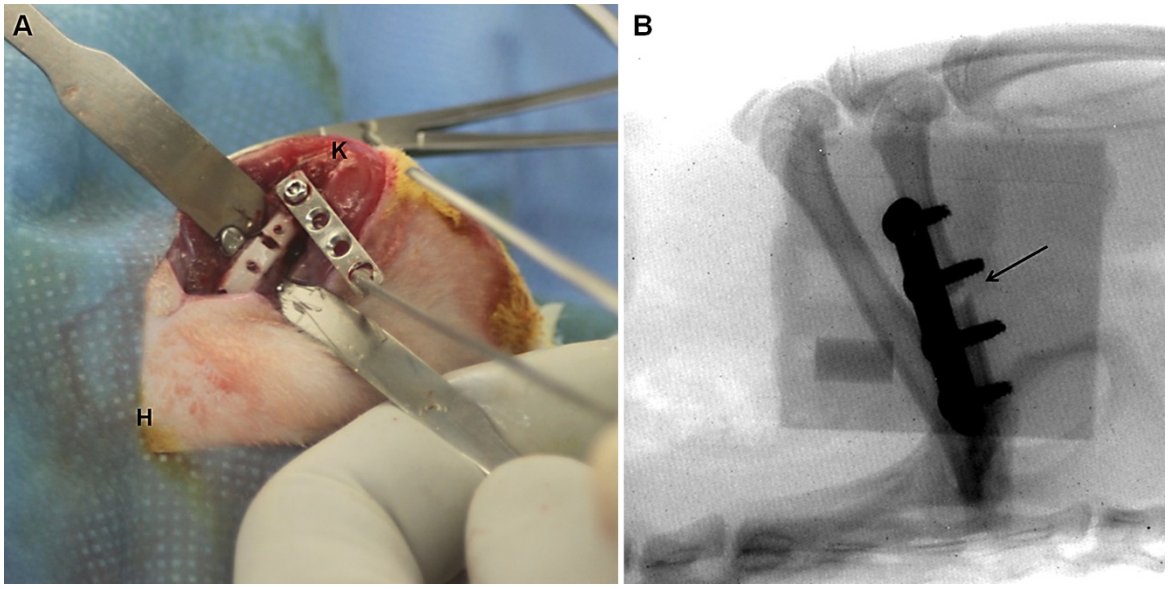

Figure 1. Plate positioning and postoperative analysis. (**A**) Plate diversion from the femur and the creation of a 1 mm non-critical midshaft full-thickness defect. The anatomical sites are reported as knee (K) and hip (H) joints. (**B**) Fluoroscopic examination of the femoral fracture and the correct plate position. The fracture of the femoral midshaft is shown by a black arrow.

The animals were then housed in separate cages under an infrared lamp and monitored until the effects of anesthesia had worn off. About 24 hours later, animals were couple caged, monitored daily for general status and welfare, clinical signs of infection, lameness, weight bearing, swelling, local hyperemia, wound healing, serous exudate, hematoma, pain and suffering. The pain was controlled with buprenorphine (0.1 mg/kg SC; Temgesic, Schering Plough, Italy) immediately after surgery. After 8 weeks, the rats were euthanized by CO_2 inhalation to perform the investigations. Anatomical dissection was performed under a laminar flow hood and in sterile conditions; the soft tissues were inspected for gross appearance, then stripped off the cortical bone surface, and the femurs were aseptically retrieved.

Animal weight and blood analyses

The body weight was measured in all animals at day 0 (day of operation) and weekly until the explantation. As an indicator of infection, hematology for each rat was performed on blood samples. Blood samples were collected from the tail vein on day 0 and day 14, and directly from the left ventricle immediately after sacrifice (day 56) to determine the peripheral neutrophil count, acting as first defenders against infections (n = 6 per group). The blood was promptly transferred to centrifuge tubes containing the appropriate anticoagulants for cell counting. Blood samples in 0.5 M EDTA (Sigma Aldrich, Italy) were processed with an automatic cell counter (Sysmex XT-1800, Dasit, Italy) to obtain the white blood count and leukocyte formula.

Micro-CT imaging and data analysis

Micro-CT imaging analysis was performed with an Explore Locus micro-CT scanner (GE Healthcare, Canada), without contrast agents. Immediately after sacrifice, the femurs (n = 6 per group) were removed, placed into a culture dish and scanned *en bloc*. A micro-CT lower-resolution (Bin-2) protocol was performed using 80kV voltage, 400 μA current with 400 msec exposure time per projection and 720 projections over 360° for a total scan time of approximately 24 minutes. The isotropic resolution of this protocol is 45 μm. The 3D reconstructed images were viewed and analyzed using the MicroView software (version 2.1.2; GE Healthcare). Individual micro-CT images were qualitatively scored for osteomyelitis by two blinded observers according to the Odekerken's grading scale [28]: 0, no abnormalities; 1, mild periosteal reaction, cortical thickening; 2, evident periosteal reaction, cortical thickening, and mild osteolysis; 3, extensive cortical thickening, cortical focal loss, evident osteolysis; 4, extensive cortical thickening, osteolysis, loss of cortical morphology. Bony bridging > 75% of the fracture gap was considered as healed fractures and bridging < 75% was seen as nonunion fracture, according to others [1]. Furthermore, a histogram-based isosurface rendering was performed on the fracture region. Then, after scan calibration, using a phantom made of an epoxy-based resin that mimics hydroxyapatite and contains water and air inclusion, a cylindrical volume of interest (VOI, 780 mm^3) including the fracture site was designed between the proximal and distal screw to quantitatively measure the bone formation. The bone volume (BV, mm^3) and tissue mineral density (TMD, mg/cc) were measured within the identified VOI as highest sensitive parameters in early stage of fracture healing [29].

Microbiological analysis

After 56 days, bacteria were recovered from samples (n = 5 per group) consisting in the plate, screws and peri-implant tissue. Samples were weighed and treated with dithiothreitol (DTT) to detach bacteria from the biofilm, as previously described [30]. Briefly, samples were immersed in a 0.1% w/v DTT (Sigma) solution in PBS and mechanically stirred for 15 min at RT. Samples were centrifuged and pellets suspended in 1 ml of the DTT eluate, 0.1 mL was then plated onto blood agar plates and inoculated in BHI broth. Plates were incubated for 48 hours at 37°C while incubation of broths at 37°C was prolonged for 15 days. Broths were daily checked for microbial growth. Then, 10 μL from positive broths were plated onto blood agar plates which were incubated for 24 at 37°C. Gram-positive stained colonies were assessed for catalase test and for growth on Mannitol salt agar. Mannitol negative, coagulase negative, white, smooth, not hemolytic colonies on blood agar, resembling *S. epidermidis* were identified by pyrosequencing and counted. The (Log CFU)/g explant was determined by dividing the CFU number by the initial total weight of the sample. The limit of detection was set at 1 (Log CFU)/g. Phenotypic characteristics (biochemical and antibiotic susceptibility profiles) and sequences obtained by pyrosequencing were also compared with that of

the *in vivo* injected *S. epidermidis* to confirm strain identity.

Histological analysis

Femoral specimens (n = 5 per group) were fixed in 10% formalin for 24 hours. The bones were decalcified in Osteodec (Bio-Optica, Italy) for 7 days and dehydrated in alcohol scale before embedding the specimens in paraffin and cutting into 5 µm longitudinal sections. The slides were stained with haematoxylin and eosin (H&E) to assess morphology and with Gram staining for bacterial examination. Photomicrographs were captured using an Olympus IX71 light microscope and an Olympus XC10 camera (Japan). The samples were evaluated by two blinded observers to assess the percentage of the fracture healing and signs of osteomyelitis according to a grading score proposed in our previous study [31]. The Gram-positive staining was evaluated as present or absent.

Scanning Electron Microscopy analysis

After explantation, one sample per group was fixed in 2.5 % paraformaldehyde and 2.5 % glutaraldehyde in 0.1 M Na-Cacodylate buffer (pH 7.4; all from Sigma) for 24 hours. After fixation, the samples were fixed for 1 hour in 1 % osmium tetroxide (Sigma) in 0.1 M Cacodylate buffer, then prepared to expose the plate surfaces and dehydrated in ethanol scale, mounted on aluminum stubs and sputter-coated with gold using a SEMPREP 2 Sputter Coater (Nanotech Ltd, UK). Observations were performed with a LEO 1400 EVO Scanning Electron Microscope (Zeiss, Germany) mixing secondary and backscattered electrons detectors. Images were acquired at 10kV at a working distance of 7 mm.

Statistical analysis

The normal distribution of data was ascertained with the Shapiro-Wilk test. Comparisons among groups and time points were analyzed with two-way analysis of variance (ANOVA) (GraphPad Prism v5.00 Software, USA) coupled with Bonferroni's post hoc test. Comparisons among groups were analyzed with one-way ANOVA corrected with Dunnett's post hoc test. The interrater reliability of the examiners' scores for micro-CT and histology were calculated with intraclass correlation coefficient (ICC): ICC = 1, perfect reliability; ICC > 0.75, excellent reliability. All data are expressed as means ± standard error (SE), unless specified otherwise. Values of $P<0.05$ were considered statistically significant.

Results

In vitro antibiotic susceptibility and biofilm production

The strain of *S. epidermidis* used in our infected non-union model was susceptible to gentamicin, vancomycin and fusidic acid (MIC ≤ 0.5 μg/ml), erythromycin and daptomycin (MIC ≤ 0.25 μg/ml), clindamycin and tigecycline (MIC ≤ 0.12 μg/ml), linezolid and tetracycline (MIC ≤ 1 μg/ml), teicoplanin (MIC = 4 μg/ml), trimethoprim/sulfamethoxazole (MIC ≤ 10 μg/ml). The strain was resistant to benzylpenicillin (MIC ≥ 0.5 μg/ml), oxacillin, cefazolin, rifampicin and levofloxacin (MIC ≥ 4 μg/ml). Based on the OD value (ODs vs ODc ratio: 6.38), the isolated strain was classified as a strong biofilm producer.

Clinical examination

During the follow-up period, none of the animals included in any group died or had clinical evidence of implant or systemic infection, such as local signs of peri-implant inflammation (hyperemia or exudation), diarrhea and behavioral alterations.

At day 0 and weekly, the body weight (b.w.) was determined and reported as numerical data for all groups (Figure 2A). During the acute phase (7 days after surgery), infection induced anorexia associated with a b.w. loss in all infected groups, particularly in the 10^8 MRSE group compared to the control group ($P<0.01$). At the same time point, no b.w. loss occurred in the control group. Thereafter, in the control group, b.w. recovered progressively consistent with the standard Wistar rat-growing curve from day 14 until the end of the experiment. On the contrary, infected animals showed a less marked b.w. recovery during the same period; in particular, infected rats of the 10^8 MRSE group recovered less b.w. than other infected groups from day 14 to day 35 after infection. A significant difference was found in the 10^8 MRSE group compared to the controls at different time points ($P<0.001$ at 14, 28 and 56 days; $P<0.01$ at 21, 35, 42 and 49 days). Unexpectedly, after 35 days, the 10^8 MRSE group showed a sensible b.w. regain reaching values similar to the 10^3 MRSE group. Conversely, the 10^5 MRSE group showed a permanent slow recovery of b.w. compared to other infected groups as well as to the control group with a significant difference at different time points ($P<0.0001$ at 35, 42, 49 and 56 days; $P<0.01$ at 14 and 28 days; $P<0.05$ at 21 days).

Blood laboratory tests

The peripheral neutrophil count is reported as number of neutrophils $x10^3/\mu l$ compared to the baseline (day of surgery, day 0) at 14 and 56 days after surgery (Figure 2B). Two weeks after infection, all animals exhibited an increase of the neutrophil count with respect to the basal values. In particular, both the 10^5 and 10^8 MRSE groups showed a significant increase of neutrophils

compared to the basal values (P<0.01 and P<0.001, respectively) and compared to the control group (P<0.05 and P<0.001, respectively). A significant difference in neutrophil count was also found in the 10^8 MRSE group compared with the 10^3 MRSE group at two-weeks post-operatively (P<0.01). Interestingly, the post-operative neutrophil count of the 10^3 MRSE group did not significantly differ from both the pre-operative basal values and from the control group at any time. In all groups, the peripheral neutrophil count almost normalized after eight weeks without showing any significant differences compared to the baseline. Interestingly, the 10^8 MRSE group showed the most significant decrease also compared to the same group at 2 weeks (P<0.001). No significant differences were detected among the experimental groups at 8 weeks.

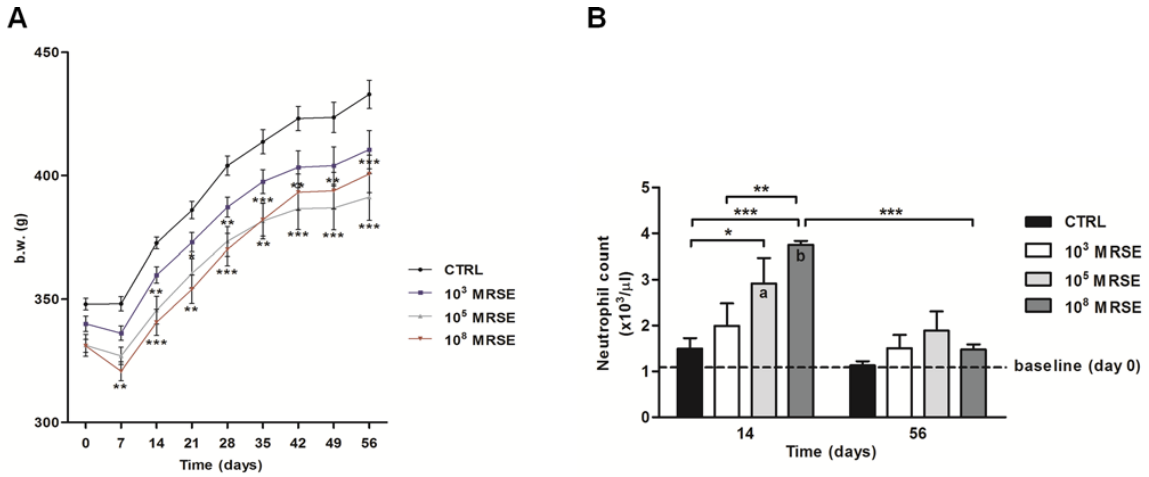

Figure 2. Clinical data. (**A**) The graph shows the numerical values of body weight (g) in the experimental groups over time. (**B**) The histogram shows the neutrophil count among experimental groups at day 14 and 56 after surgery. The dotted line represents the baseline at day 0 before surgery. Comparisons between groups and time points were analyzed with two-way ANOVA and Bonferroni's post-hoc. Statistical significance was P<0.05 (*, a, b), P<0.01 (**) and P<0.001 (***), n = 6.

Imaging diagnosis

The micro-CT qualitative analysis showed no signs of osteomyelitis in the control group in all the analyzed planes (Figure 3A, sagittal, coronal, and axial). Some animals displayed a restricted cortical bone reaction, whereas a well-organized bone callus, remodeling, and a good bone encapsulation of the screws were present in all cases. One sample of the control group was not evaluated due to the mechanical loss of the proximal screws followed by a fracture dislocation because of a surgical inaccuracy. Thus, this subject was excluded from quantitative analyses and dedicated to SEM investigation. All valuable samples (100%) showed a fracture healing > 75% with mineralized cortices and bony bridging across the medullary canal (Figure 3B).

The 10^3 MRSE group displayed variable response to bacterial infection. The 67% of samples showed signs of altered bone healing. In particular, they exhibited both a diffuse cortical bone thickening associated with focal loss of the cortical wall and mild osteolysis around the screws near

to the fracture site (Figure 3C, sagittal, coronal, and axial). The fracture healing was < 75% and displayed mainly fibrous non-union (Figure 3D).

The 10^5 MRSE group presented extensive signs of osteomyelitis both near the fracture site and extending to the metaphysis regions associated with severe osteolysis around the screws and resorption of the cortex, with a quite complete disruption of the bone integrity (Figure 3E, sagittal, coronal, and axial). Moreover, most of the samples demonstrated the presence of subcortical abscesses (Figure 3E, axial). The 83% of the samples showed a fracture healing < 75%, with absence of bony bridging, frequently associated with deformity of the femoral diaphysis (Figure 3F). One animal showed no signs of osteomyelitis and a fracture healing around 75%.

The 10^8 MRSE group showed extensive cortical thickening, severe periosteal reaction, loss of cortical wall and severe osteolysis around the screws near to the fracture site (Figure 3G, sagittal, coronal, and axial). All samples (100%) showed a fracture healing < 75%, and displayed nonunion extended across the entire bone (Figure 3H).

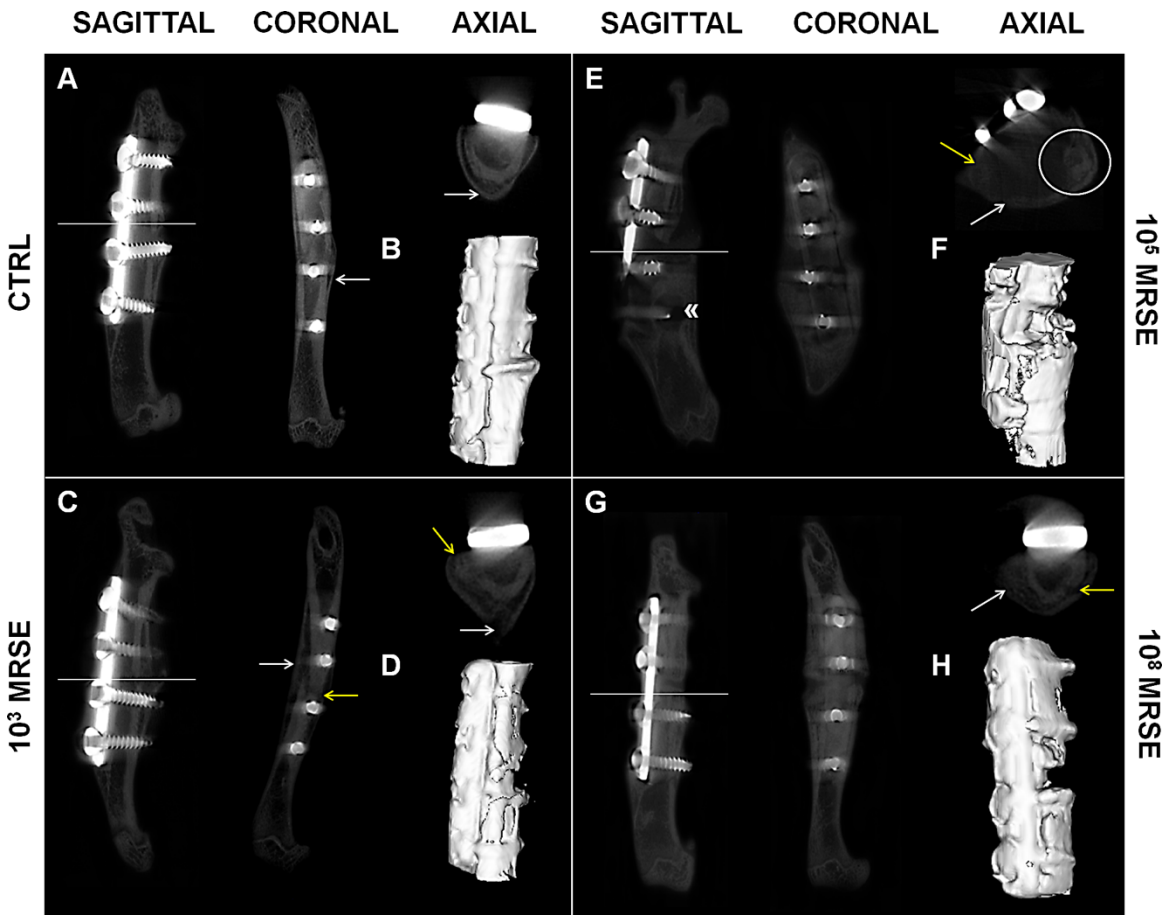

Figure 3. Qualitative micro-CT imaging and isosurface. The representative panel shows micro-CT images on the day of explantation. The sagittal, coronal and axial planes (**A**, **C**, **E**, **G**), as well as a three-dimensional isosurface reconstruction (**B**, **D**, **F**, **H**) were presented for the control (CTRL), and the 10^3, 10^5, and 10^8 MRSE groups. Symbols indicate: cortical reaction (white arrows); loss of cortical wall and osteolysis (yellow arrows); peri-implant osteolysis («); presence of abscesses (white circle).

Assessing the percentage of bony bridging, no significant difference was measured between the 10^3 MRSE group and the control group or the10^5 and 10^8 MRSE groups, as well as between the 10^5 and 10^8 MRSE group. The control group significantly differed from the 10^5 and 10^8 MRSE groups for $P<0.05$ and $P<0.01$, respectively.

The interrater reliability of blind scoring based on the Odekerken's scale was excellent—ICC 0.83 (95% CI 0.51, 0.94)—and highlighted a significant higher osteomyelitis grade in the 10^5 and 108 MRSE groups, but not for the 10^3 MRSE group, compared to the controls ($P<0.05$) (Figure 4A). The quantifications of BV and TMD were reported as percentage of decrease with respect to the control group in which, despite no significant difference was found, a lower BV was measured for all the infected groups with a higher trend in the 10^5 MRSE group (Figure 4B) as well as for the TMD with the exception of the 10^8 MRSE group (Figure 4C).

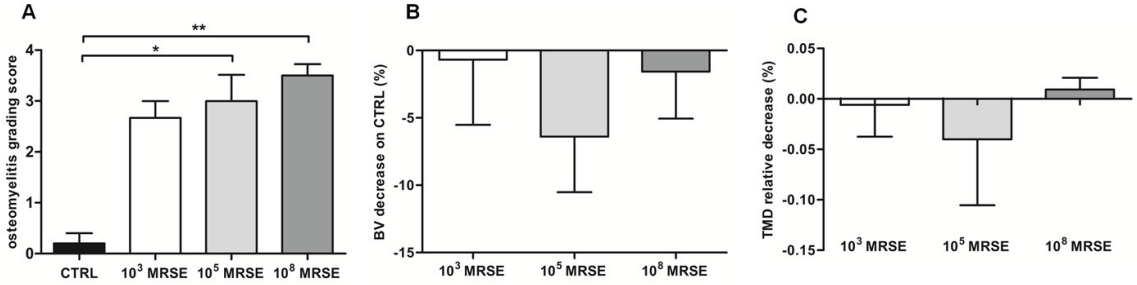

Figure 4. Micro-CT-based semiquantitative and quantitative analyses of bone structure. (**A**) Osteomyelitis grading score based on Odekerken's scale. (**B**) Bone volume (BV) quantitative analysis of the infected groups normalized on the control group, reported as a percentage. (**C**) Tissue mineral density (TMD) quantitative analysis of the infected groups normalized on the control group, reported as a percentage. Comparisons among groups were analyzed by one-way ANOVA. Statistical significance for $P<0.05$ (*), n = 6.

Microbiological tests

No bacterial growth was observed in the control group (non-detectable values, n.d., L.o.D.). There was not a significant difference between the control group (n.d.) and the 10^3 MRSE group (1.5±1 CFU/g explant, mean ± standard deviation), in which bacteria were found in three animals out of five. Considerable bacterial counts were found in samples of the 10^5 and 10^8 MRSE groups (10.33±9.5 and 20.33±27.4 CFU/g explant, respectively) with a significant difference compared to the control group ($P<0.05$ and $P<0.01$, respectively), as well as between the 10^3 and 10^8 MRSE groups a difference was measured ($P<0.05$). No significant differences in DNA sequences between strains isolated from animal explants and the parental strain were observed. In particular, all the isolated bacteria from rat explants were susceptible to gentamicin, vancomycin and fusidic acid (MIC ≤ 0.5 μg/ml), erythromycin and daptomycin (MIC ≤ 0.25 μg/ml), clindamycin and tigecycline (MIC ≤ 0.12 μg/ml), linezolid and tetracycline (MIC ≤ 1 μg/ml), teicoplanin (MIC = 4 μg/ml), trimethoprim/sulfamethoxazole (MIC ≤ 10 μg/ml) while they were resistant to benzylpenicillin

(MIC ≥ 0.5 μg/ml), oxacillin, cefazolin, rifampicin and levofloxacin (MIC ≥ 4 μg/ml). As far as biofilm production was concerned, all the isolated bacteria were classified as strong biofilm producers as well as the parental strain, without significant differences among 10^3, 10^5 and 10^8 CFU inoculum groups, as reported in Table 1.

Table 1. Biofilm production of *S. epidermidis* isolated from the infected rats (ODs vs ODc ratio).

Groups	Explants				
	A	**B**	**C**	**D**	**E**
10^3	6.26	6.37	n.d.	6.47	n.d.
10^5	6.28	6.58	5.67	6.54	6.14
10^8	6.53	6.48	5.78	6.28.	6.21

n.d. = non detectable

Histological analysis

The histological analysis confirmed the results obtained by micro-CT scans in terms of percentage of fracture healing and bone structure in the control group (Figure 5A). Specifically, fractures appeared closed with a great amount of new bone formation in a remodeling phase, sometimes associated with a mild cortical thickening (woven bone) (Figure 5B, upper box). The small portion of unclosed fracture displayed a well-organized fibrocartilaginous tissue (Figure 5B, lower box). No signs of osteomyelitis were detected as also displayed by the absence of bacteria reported by the Gram-positive staining. As aforementioned, animals of the 10^3 MRSE group showed a variable response to bacterial infection. Animals with a microbiological detectable infection showed an incomplete bone healing (Figure 5C) characterized by a great formation of fibrovascular tissue disseminated with scarce inflammatory cells (Figure 5D, upper box) and only sporadically replaced by cartilaginous tissue (Figure 5D, lower box). The cortices appeared uniformly enlarged with few areas of bone remodeling. Gram staining detected areas disseminated with Gram-positive cocci. Differently, infected rats, in which no bacteria were microbiologically retrieved, showed histological features resembling the findings of the control group. The 10^5 MRSE group showed a complete disorganization of the bone structure, the missing of cortical bridging with non-union establishment (Figure 5E). Severe signs of osteomyelitis were found: extensive periosteal reaction, cortical thickening, myeloid hyperplasia, a diffuse presence of polymorphonuclear cells in the granulation tissue (Figure 5F, upper box), multiple subperiosteal, intracortical and medullary abscesses and hematomas, and bone sequestra (Figure 5F, lower box). The severe osteomyelitis was also sustained by the presence of gram-positive bacteria in the bone and granulation tissue.

The histology of the 10^8 MRSE group confirmed the results obtained by micro-CT scans. The analysis depicted a great deposition of fibrovascular tissue permeating from the cortical margin to the medullary canal, surrounding screws and embedding numerous polymorphonuclear cells

(Figure 5G). The severe osteomyelitis led to a massive cortical and endosteal osteolysis (Figure 5H, upper box). Subperiosteal sequestra were found together with a moderate periosteal reaction (Figure 5H, lower box). Gram staining identified a massive presence of bacteria both intraosseous and within the periosteal and subperiosteal area.

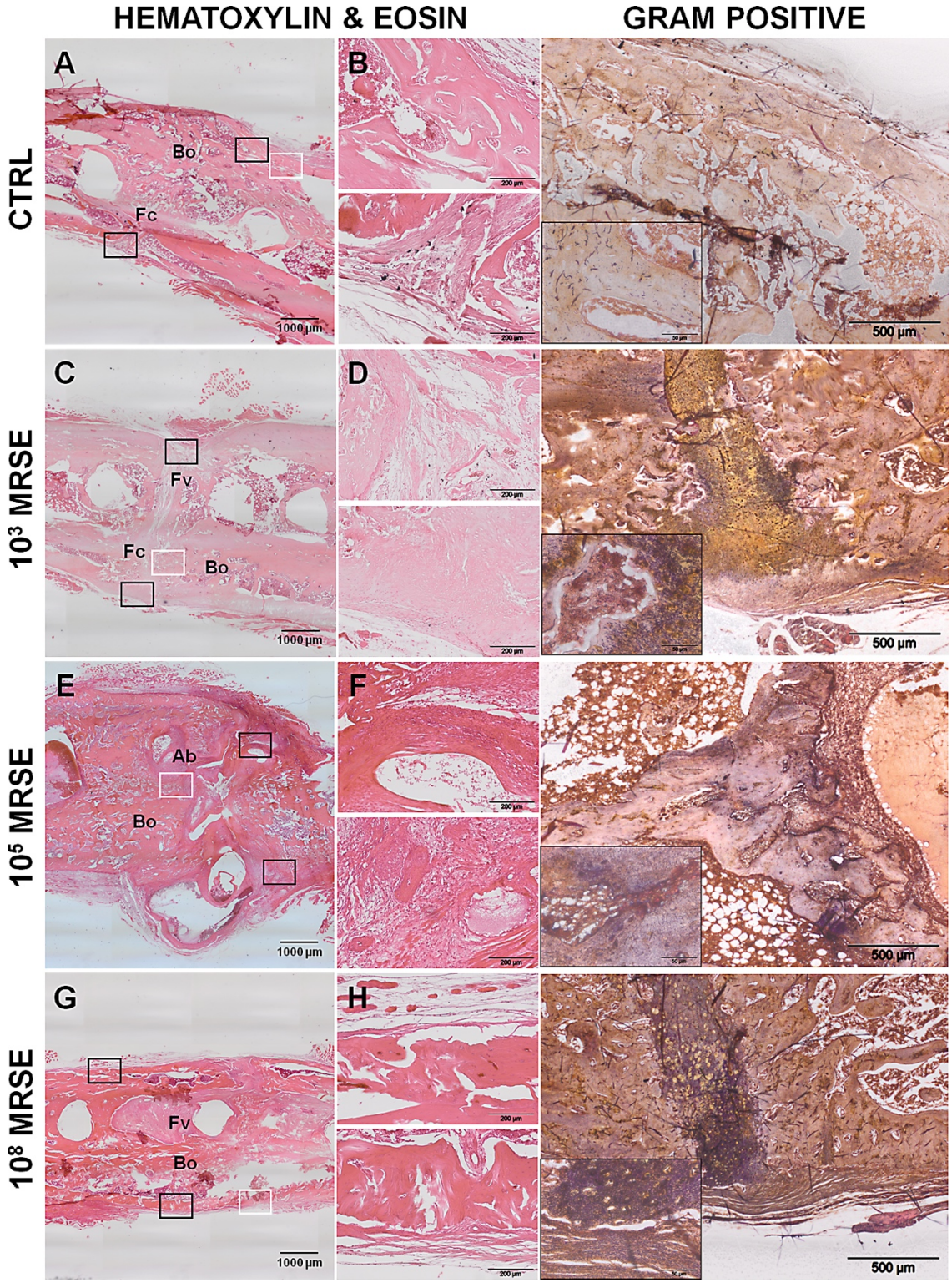

Figure 5. Histological analysis at the day of explantation. The representative panel shows H&E and Gram

staining in the four groups. The panels depict an overview of the samples, magnification 2x, scale bar 1000 µm (**A**, **C**, **E**, **G**). The panels depict areas of interest of the black boxes, magnification 10x, scale bar 200 µm (**B**, **D**, **F**, **H**). The Gram staining depicts bacterial colonies identified by the white boxes, magnification 4x, scale bar 500µm and specific regions within the small boxes, magnification 40x, scale bar 50 µm. Bo, bone; Fc, fibrocartilaginous callus; Fv, fibrovascular tissue; Ab, abscesses

The interrater reliability of blind scoring based on the Petty's scale was excellent—ICC 0.82 showed no signs of bone infection and the 10^3 MRSE group displayed only a mild inflammatory reaction with particular reference to the cortex, as shown in Figure 6B. A moderate to severe osteomyelitis was found in the 10^5 and 10^8 MRSE groups with a significant difference with respect to the control group for $P<0.01$ and 0.05, respectively. Moreover, a significant difference was found in terms of periosteal reaction between the 10^3 MRSE group and both the 10^5 and 10^8 MRSE groups for $P<0.001$ and $P<0.01$, respectively.

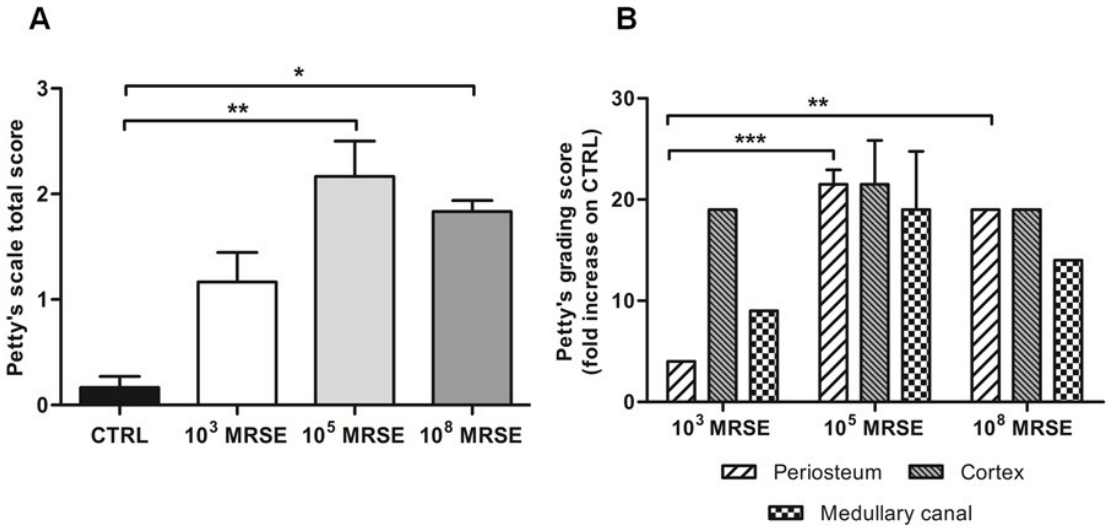

Figure 6. Histological score based on Petty's scale. The histogram compares the semiquantitative score performed on the periosteum, cortex and medullary canal regarding the osteomyelitis signs. (**A**) Total score analysis. (**B**) Fold increase of the grading scale of the infected groups with respect to the control group. Comparisons among groups were analyzed by one-way ANOVA. Statistical significance for $P<0.05$ (*), $P<0.01$ (**), $P<0.001$ (***), n = 5.

Scanning electron microscopy analysis

The control group without *S. epidermidis* contamination was completely free from biofilm formation on the surface of the implanted stainless-steel plate both on its top (Figure 7A) and bottom side (Figure 7B), where the presence of bony bridging on the bone-implant interface was detected (Figure 7B, small box). A little presence of free cocci, ranging from 1–2 µm of diameter, was detected on the plate surface in the 10^3 MRSE group, in which a scarce mucoid material occasionally coated cocci (Figure 7C and 7D).

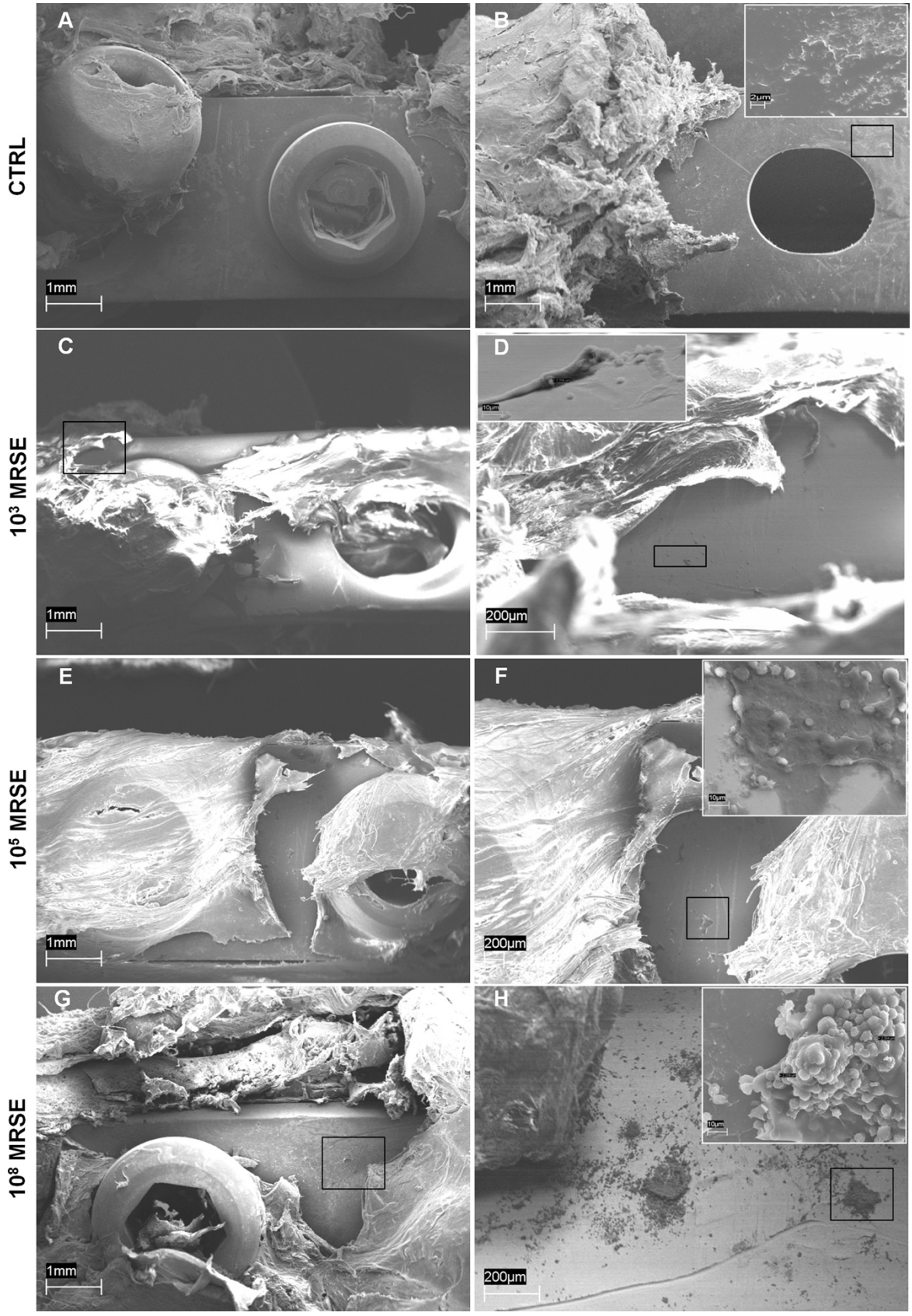

Figure 7. Representative photographs of SEM analysis of biofilm formation. Absence of biofilm formation in the control group either on the top (**A**) or on the bottom (**B**) of the implanted plate (magnification 40x, scale bar 1mm) with the presence of bony bridging structure on the bone-implant interface (B small box, magnification 6700x, scale bar 2µm). Presence of few coccidal bacteria on the top of the plate (**C**, **D**,

magnifications 40x and 250x, scale bars 1mm and 200μm, respectively) occasionally coated with mucoid material in the 10^3MRSE group (D small box, magnification 3000x scale bar 10μm). Presence of cocci within the peri-implant fibrous tissues covering the plate and on the top of the plate (**E**, magnification 40x, scale bar 1mm), free or partially embedded into mucous-gelatinous matrix in the 10^5MRSE group (**F**, magnification 70x, scale bar 200μm; F small box, magnification 3000x scale bar 10μm). Clusters of cocci adhering to the top of the plate surface (**G**, **H**, magnifications 40x and 90x, scale bars 1mm and 200μm, respectively) completely embedded in a well- organized biofilm matrix in the 10^8MRSE group (**H** small box, magnification 3000x, scale bar 10μm).

Differently, in the 10^5 MRSE group, bacteria were mainly present on the plate surface and within the peri-implantar fibrous tissues covering the plate, free or partially embedded into mucous-gelatinous matrix (Figure 7E and 7F). As expected, in the 10^8 MRSE group, several clusters of cocci were identified adherent at the top and bottom of the plate surface (Figure 7G and 7H) completely embedded in a well-organized and three-dimensional self-produced extracellular polymer structure, the biofilm, able to entrap also platelets, erythrocytes and polymorphonucleated cells (Figure 7H, small box).

Discussion

Postoperative infections and invasive trauma causing septic non-union are still a major clinical problem that requires specific preclinical models. An interesting model has been proposed by Chen and colleagues [17] combining a critical bone defect in the rat femur with a local injection of *S. aureus*. This model may not effectively characterize the clinical condition in which septic non-unions develop. Actually, critical bone defects do not heal spontaneously, thus *in vivo* non-union models should avoid the combination of critical defect and bacterial inoculation to better understand the pathogenesis of infection in fractures, as also suggested by others [32, 33]. In our study, we proposed a standardized osteotomy model devoid of a critical bone defect associated with a local infection. This approach aims to better understand the role of bacteria in the non-union development with particular reference to subclinical contaminations and to generate a useful preclinical model of non-union-related infection for future therapeutic approaches. Similarly, Alt and colleagues [1] established a model of *S. aureus* non-unions of the tibia after intramedullary fixation. To resemble human procedures for complicated femoral fractures, we provided a direct fracture fixation with plates, we used a pathogen commonly involved in implant colonization and we administered routine antimicrobial prophylaxis. *S. epidermidis* biofilm formation is a well-known virulence factor in the development of implant infection [34]. Thus, to better recreate a human clinical setting, we developed a model taking advantage of a prosthetic-derived MRSE-strain selected for its ability to produce biofilm. The antibiotic susceptibility of the selected MRSE-strain was comparable to that of collection numbered ATCC35984, particularly referred to daptomycin and vancomycin [18]. Despite similar antibiotic susceptibility to ATCC35984, MIC values for vancomycin and daptomycin of our clinical strain were lower than the referenced one [18].

Moreover, we treated animals with a preoperative systemic, broad-spectrum cephalosporin (cefazolin), since it is considered the first choice in orthopaedic prophylaxis according to the specific guidelines [35]. Thus, we tried to prevent other than MRSE contaminations by using cefazolin to have a deeper insight in this specific bacterial infection. Again, male animals were selected to avoid the influence of hormonal cycles on bone repair and turnover, as also suggested by others [33]. In the literature scenario, there are several studies on osteomyelitis or septic arthritis animal models, but few studies report models of infections during the fracture healing by employing *S. aureus* as main strain [1,16, 17, 36–38]. Differently, we proposed a dose-dependent *S. epidermidis*-induced non-union model, belonging *S. epidermidis* to the normal skin flora and being responsible for most of the metal implant infections [13, 39]. To our best knowledge, there are not currently animal models simulating a *S. epidermidis*-related nonunion of the femur after internal plate stabilization. In fact, only few studies describe the MRSE-related orthopaedic infections mainly focused on prosthetic joint infection [22] or intramedullary osteomyelitis [24].

In our results, the changes in b.w. and neutrophil count were correlated with the host response to infection. The b.w. loss reflected the dose-dependent trend in the infected rats, as well as the increase of the neutrophils during the acute phase of infection. Overall, most of the analyses highlighted a worse condition in the 10^5 MRSE group compared to the others. The recovery of the 10^8 MRSE group in terms of both b.w. and the systemic neutrophil count could be related to the capability of the formed biofilm to locally attract activated neutrophils reducing their presence in the circulating blood. This finding was histologically supported by the abundant presence of local polymorphonuclear cells and severe host tissue damages. Hence, this suggested a quicker, stronger and mature biofilm formation induced by the higher dose of injected bacteria (10^8 MRSE) with respect to the other infected groups, as demonstrated by Gram staining, microbiological and SEM analyses. Thus, the greater amount of biofilm with a high mechanical stability allowed bacteria to escape from neutrophil assault. This supported the low susceptibility to phagocytic destruction by neutrophils of the *S. epidermidis* [40]. The inability to kill bacteria associated with a great amount of protective biofilm slowed the cocci metabolic rate leading to a chronic osteomyelitis development and eventually delaying the fracture bone healing [13]. *S. epidermidis* autolysin (AltE) has been suggested to mediate the primary attachment to the implant surface and to bind vitronectin, an abundant glycoprotein found in serum, extracellular matrix and bone, promoting cocci spreading [41]. The autolysin/adhesin system binds fibrinogen, fibronectin, and vitronectin in a bacterial dose-dependent fashion [41], explaining the greater amount of biofilm formation in the 10^8 MRSE group compared to the 10^5 MRSE one. Moreover, *S. epidermidis* embedded in biofilm commonly produces quorum-sensing controlled virulence factors as the one encoded by the accessory gene regulator (agr) system. In addition, the transcription of Agr gene is also induced by the presence of neutrophils and regulates biofilm formation in *S. epidermidis* by acting on AtlE and toxin expression that cause a rapid lysis of local polymorphonuclear cells [10, 42]. Therefore, the vicious circle of neutrophils promoted the biofilm formation and aggravated the local inflammatory response. Although *S. epidermidis* has a lower pathogenic potential, most staphylococcal infections are chronic especially in patients with associated predisposing factors such as diabetes or peripheral vascular disease, as we have previously demonstrated [31].

Differently, the 10^5 MRSE group showed a more severe condition in terms of osteomyelitis signs and non-union establishment, as properly supported by micro-CT and histological analysis, despite a lower detection of bacterial growth. In this group, subacute osteomyelitis was characterized by abscesses at the site of bacterial colonization frequently associated with vascular and bone damages, like cortical resorption and sequestra. Sequestra represent foci of recurrent infection that could lead to the chronic osteomyelitis development over time. Accordingly, in these rats, the subacute infection was also related to a higher symptomatic status in terms of b.w. decrease and circulating neutrophils, as also supported by others [43]. Reducing the bacterial load and consequently the biofilm production in the 10^5 MRSE respect to the 10^8 MRSE group could be responsible of a higher

presence of free cocci in the fracture site. In fact, this lower microbial dose induced a subacute host response fighting against cocci, with both maintenance of high levels of circulating neutrophils and local cellular immune reaction (abscess formation). This phenomenon could be reasonably controlled by using appropriate antimicrobial treatment for MRSE, considering that bacteria in such specific case are poorly embedded in a weak and immature extracellular matrix. More interestingly, the 10^3 MRSE group displayed an inconsistent grade of infection and fracture healing. This could be related to the specific host immune system that was able to spontaneously eradicate the infection determined by a low-grade of MRSE injection in 33% of rats, as demonstrated also by other authors [28]. According to our experience, this group showed subclinical features of infected fractures, in which the bone repair or damages are filtered by the host immune defense and bacteria did not trigger signs or symptoms of a post-surgical infection. Findings of our study, in which a low grade of *S. epidermidis* administration in the presence of metal implants seems to be a good model for subclinical perioperative infections, are consistent with those supported by Qin and colleagues in an implant-related osteomyelitis in a rat model [24]. The spontaneous eradication of infection occurred in some cases of the 10^3 MRSE group suggests the inadequacy of low grade infection in creating a reliable and reproducible model of infected non-unions, supporting another study on *S. epidermidis* graft infections [44]. Conversely, it may represent a useful approach to have a deeper insight of the subclinical event in terms of pathogens and host response.

The control group was free of clinical and diagnostic signs of infection and showed a quite complete fracture healing, as expected. The restrict cortical bone reaction detected by micro-CT is due to the periosteal elevation performed during surgery to properly create the fracture by means of a circular saw. According to some authors, the cautery-induced periosteal damage induced an atrophic nonunion [45]. In our study, we carried out a simple periosteal cut and elevation without provoking necrotic damages. This variability was adopted in all animal groups. In the development of our models, some limitations were encountered in the micro-CT imaging related to the scattering artifacts of the stainless-steel plates and screws. This phenomenon was particularly limiting for the quantitative analyses. To overcome this limit, the use of titanium implants could be helpful to reduce scattering artifacts and to apply validated protocols for micro-CT acquisition. Anyway, thanks to the combination of several diagnostic techniques, our bone analysis provided adequate information on fracture healing and osteomyelitis associated to microbial infections. Our modeling is reliable for the assessment of osteomyelitis and fracture healing, offering a good correlation of their typical features. Moreover, the small number of animals included in this research could be also considered a limitation, despite offering an innovative and interesting preclinical model. Indeed, at this writing, there are not available rodent models describing the use of *S. epidermidis* to determine an orthopaedic infection associated with non-union fractures. This is also the first time that the impact of bacterial load has been investigated with regard to bone healing after fracture and osteosynthesis and that the effect on bone healing of a subclinical infection due to *S. epidermidis*

contamination of a metallic plate is shown. Although this research is a pilot study, the model appears both as a more traditional tool, designed to study implant-related infections due to a common pathogen, like *S. epidermidis*, and as a more innovative way to investigate the underestimated effect of subclinical contamination of bone due to trauma or surgery.

Conclusions

Our models of subclinical and evident orthopaedic infection constitute clinically relevant tools for studying prophylactic and therapeutic strategies or biofilm pathogenesis in infected nonunion establishment as well as models for the assessment of sophisticated diagnostic approaches. Importantly, our modeling could be used in the next feature to characterize by proteomics the adaptation and changes of bacteria during the different stages of the infective process and biofilm formation.

Acknowledgements

The authors wish to thank the Engineers M. Cabrini and S. Lorenzi for their technical assistance in Scanning Electron Microscopy at the Engineering Department, University of Bergamo (Dalmine, Italy).

The financial support for this study was provided by the Italian Ministry of Health (RC 2014, Research Line 4, #62). The funders had no role in study design, data collection and analysis, decision to publish, or preparation of the manuscript.

References

1. Alt V, Lips KS, Henkenbehrens C, et al. A new animal model for implant-related infected non-unions after intramedullary fixation of the tibia in rats with fluorescent in situ hybridization of bacteria in bone infection. Bone. 2011. 48:1146–1153.
2. Trampuz A, Zimmerli W. Diagnosis and treatment of implant associated septic arthritis and osteomyelitis. Curr Infect Dis Rep. 2008. 10:394–403.
3. Kim PH, Leopold SS. Gustilo-Anderson classification. Clin Orthop Relat Res. 2012. 470:3270–3274.
4. Ostermann PA, Henry SL, Seligson D. Timing of wound closure in severe compound fractures. Orthopedics. 1994. 17:397–399.
5. Seligson D, Klemm K. Adult posttraumatic osteomyelitis of the tibial diaphysis of the tibial shaft. ClinOrthop Relat Res .1999. 360:30–36.
6. Esteban J, Sandoval E, Cordero-Ampuero J, et al. Sonication of intramedullary nails: clinically-related infection and contamination. Open Orthop J. 2012. 6:255–260.
7. Montanaro L, Speziale P, Campoccia D, et al. Scenery of Staphylococcus implant infections in orthopedics. Future microbial. 2011. 6:1329–1349.
8. Rupp ME, Fey PD, Heilmann C, et al. Characterization of the importance of Staphylococcus epidermidis autolysin and polysaccharide intercellular adhesin in the pathogenesis of intravascular catheterassociated infection in a rat model. J Infect Dis. 2001. 183:1038–1042.
9. Sacar M, Sacar S, Kaleli I, et al. Linezolid alone and in combination with rifampicin prevents experimental vascular graft infection due to methicillin-resistant Staphylococcus aureus and Staphylococcus epidermidis. J Surg Res. 2007. 139:170–175.
10. Vuong C, Gerke C, Somerville GA, et al. Quorum-sensing control of biofilm factors in Staphylococcus epidermidis. J Infect Dis. 2003. 188:706–718.
11. Rupp ME, Archer GL. Coagulase-negative staphylococci: pathogens associated with medical progress. Clin Infect Dis. 1994. 19:231–243.
12. Romanò CL, Manzi G, Logoluso N, et al. Value of debridement and irrigation for the treatment of peri-prosthetic infections. A systematic review. Hip international. 2012. 22 (Suppl 8):S19–24.
13. Ciampolini J, Harding KG. Pathophysiology of chronic bacterial osteomyelitis. Why do antibiotics fail so often? Postgrad Med J. 2000. 76:479–483.
14. Chen X, Schmidt AH, Mahjouri S, et al. Union of a chronically infected internally stabilized segmental defect in the rat femur after debridement and application of rhBMP-2 and systemic antibiotic J Orthop Trauma. 2007. 21:693–700.
15. Chen X, Schmidt AH, Tsukayama DT, et al. Recombinant human osteogenic protein-1 induces bone formation in a chronically infected, internally stabilized segmental defect in the rat femur. J Bone Joint Surg [Am]. 2006. 88A:1510–1523.
16. Sanchez CJ Jr, Prieto EM, Krueger CA, et al. Effects of local delivery of D-amino acids from biofilm-dispersive scaffolds on infection in contaminated rat segmental defects. Biomaterials. 2013. 34:7533–7543.

17. Chen X, Tsukayama DT, Kidder LS, et al. Characterization of a chronic infection in an internally-stabilized segmental defect in the rat femur. J Orthop Res. 2005. 23:816–823.
18. Van Praagh AD, Li T, Zhang S, Arya A, et al. Daptomycin antibiotic lock therapy in a rat model of staphylococcal central venous catheter biofilm infections. Antimicrob Agents Chemother. 2011. 55:4081–4089.
19. Chauhan A, Lebeaux D, Decante B, et al. A rat model of central venous catheter to study establishment of long-term bacterial biofilm and related acute and chronic infections. PLoS One. 2012. 7:e37281.
20. Hou Z, Da F, Liu B, et al. R-thanatin inhibits growth and biofilm formation of methicillin-resistant Staphylococcus epidermidis in vivo and in vitro. Antimicrob Agents Chemother. 2013. 57:5045–5052.
21. Bracho DO, Barsan L, Arekapudi SR, et al. Antibacterial properties of an iron-based hemostatic agent in vitro and in a rat wound model. Acad Emerg Med. 2009. 16:656–660.
22. Zhai H, Pan J, Pang E, et al. Lavage with Allicin in Combination with Vancomycin Inhibits Biofilm Formation by Staphylococcus epidermidis in a Rabbit Model of Prosthetic Joint Infection. PLoS ONE. 2014. 9: e102760.
23. Del Pozo JL, Rouse MS, Euba G, et al. The electricidal effect is active in an experimental model of Staphylococcus epidermidis chronic foreign body osteomyelitis. Antimicrob Agents Chemother. 2009. 53:4064–4068.
24. Qin H, Cao H, Zhao Y, et al. In vitro and in vivo anti-biofilm effects of silver nanoparticles immobilized on titanium. Biomaterials. 2014. 35:9114–9125.
25. Jonasson J, Olofsson M, Monstein HJ. Classification, identification and subtyping of bacteria based on pyrosequencing and signature matching of 16s rDNA fragments. APMIS. 2007. 15:668–677.
26. Christensen GD, Simpson WA, Younger JJ, et al. Adherence of coagulase-negative staphylococci to plastic tissue culture plates: a quantitative model for the adherence of staphylococci to medical devices. J Clin Microbiol. 1985. 22:996–1006.
27. Stepanovic S, Vukovic D, Dakic I, et al. A modified microtiter-plate test for quantification of staphylococcal biofilm formation. Microbiol Methods. 2000. 40:175–179.
28. Odekerken JCE, Arts JJC, Surtel DAM, et al. A rabbit osteomyelitis model for the longitudinal assessment of early post-operative implant infections. J Orthop Surg Res. 2013. 3:38.
29. O'Neill KR, Stutz CM, Mignemi NA, et al. Micro-computed tomography assessment of the progression of fracture healing in mice. Bone. 2012. 50:1357–1367.
30. Drago L, Romano CL, Mattina R, et al. Does dithiothreitol improve bacterial detection from infected prostheses? A pilot study. Clin Orthop Relat Res. 2012. 470:2915–2925.
31. Lovati AB, Drago L, Monti L, et al. Diabetic Mouse Model of Orthopaedic Implant-Related Staphylococcus Aureus Infection. PLoS One. 2013. 8:e67628.
32. Garcia P, Histing T, Holstein JH, et al. Rodent animal models of delayed bone healing and non-union formation: a comprehensive review. Eur Cell Mater. 2013. 26:1–12.
33. Mills LA, Simpson AH. In vivo models of bone repair. J Bone Joint Surg Br. 2012. 94:865–874.
34. Fey PD, Olson ME. Current concepts in biofilm formation of Staphylococcus epidermidis. See comment in PubMed Commons belowFuture Microbiol. 2010. 5:917–933.

35. Lima AL, Oliveira PR, Carvalho VC, et al. Recommendations for the treatment of osteomyelitis. Braz J Infect Dis. 2014. 18:526–534.
36. Andriole VT, Nagel DA, Southwick WO. A paradigm for human chronic osteomyelitis. J Bone Joint Surg [Am]. 1973. 55-A:1511–1515.
37. Worlock P, Slack R, Harvey L, et al. An experimental model of posttraumatic osteomyelitis in rabbits. Br J Exp Pathol. 1988. 69:235–244.
38. Southwood LL, Frisbie DD, Kawcak CE, et al. Evaluation of Ad-BMP-2 for enhancing fracture healing in an infected defect fracture rabbit model. J Orthop Res. 2004. 22:66–72.
39. Lowy FD, Hammer SM. Staphylococcus epidermidis infections. Ann Intern Med. 1983. 99: 834–839.
40. Hirschfeld J. Dynamic interactions of neutrophils and biofilms. J Oral Microb. 2014. 6:26102.
41. Heilmann C, Hussain M, Peters G, et al. Evidence for autolysinmediated primary attachment of Staphylococcus epidermidis to a polystyrene surface. Mol Microbiol. 1997. 24:1013–1024.
42. Rohde H, Burdelski C, Bartscht K, et al. Induction of Staphylococcus epidermidis biofilm formation via proteolytic processing of the accumulation-associated protein by staphylococcal and host proteases. Mol Microbiol. 2005. 55:1883–1895.
43. Horst SA, Hoerr V, Beineke A, et al. A novel mouse model of Staphylococcus aureus chronic osteomyelitis that closely mimics the human infection: an integrated view of disease pathogenesis. Am J Pathol. 2012. 181:1206–1214.
44. Agalar C, Ozdogan M, Agalar F, et al. A rat model of polypropylene graft infection caused by Staphylococcus epidermidis. ANZ J Surg. 2006. 76:387–391.
45. Kokubu T, Hak DJ, Hazelwood SJ, et al. Development of an atrophic nonunion model and comparison to a closed healing fracture in rat femur. J Orthop Res. 2003. 21:503–510.

Chapter 2

Systemic and Local Administration of Antimicrobial and Cell Therapies to Prevent Methicillin-Resistant *Staphylococcus epidermidis*-Induced Femoral Nonunions in a Rat Model

Arianna Barbara Lovati[1]*, Lorenzo Drago[2,3], Marta Bottagisio[1,4], Matilde Bongio[1], Marzia Ferrario[5], Silvia Perego[6], Veronica Sansoni[6], Elena De Vecchi[2], Carlo Luca Romanò [7]

[1] Cell and Tissue Engineering Laboratory, IRCCS Galeazzi Orthopaedic Institute, Milan, Italy.

[2] Laboratory of Clinical Chemistry and Microbiology, IRCCS Galeazzi Orthopaedic Institute, Milan, Italy.

[3] Department of Biomedical Science for Health, University of Milan, Milan, Italy.

[4] Department of Veterinary Medicine (DiMeVet), University of Milan, Milan, Italy.

[5] MAP Laboratory, Fondazione Filarete, Milan, Italy.

[6] Laboratory of Experimental Biochemistry & Molecular Biology, IRCCS Galeazzi Orthopaedic Institute, Milan, Italy.

[7] Department of Reconstructive Surgery of Osteoarticular Infections, CRIO Unit, IRCCS Galeazzi Orthopaedic Institute, Milan, Italy.

* Corresponding Author: arianna.lovati@grupposandonato.it

Cite

Lovati AB, Drago L, Bottagisio M, Bongio M, Ferrario M, Perego S, Sansoni V, De Vecchi E, Romanò CL. Systemic and Local Administration of Antimicrobial and Cell Therapies to Prevent Methicillin-Resistant Staphylococcus epidermidis-Induced Femoral Nonunions in a Rat Model. Mediators Inflamm. 2016;2016:9595706. doi: 10.1155/2016/9595706.

Abstract

This study compares the response to *S. epidermidis*-infected fractures in rats systemically or locally injected with vancomycin or bone marrow mesenchymal stem cells (BMSCs) in preventing the nonunion establishment. The 50% of rats receiving BMSCs intravenously (s-rBMSCs) died after treatment. A higher cytokine trend was measured in BMSCs locally injected rats (l-rBMSCs) at day 3 and in vancomycin systemically injected rats (l-VANC) at day 7 compared to the other groups. At day 14, the highest cytokine values were measured in l-VANC and in l-rBMSCs for IL-10. Micro-CT showed a good bony bridging in s-VANC and excellent both in l-VANC and in l-rBMSCs. The bacterial growth was lower in s- VANC and l-VANC than in l-rBMSCs. Histology demonstrated the presence of new woven bone in s-VANC and a more mature bony bridging was found in l-VANC. The l-rBMSCs showed a poor bony bridging of fibrovascular tissue. Our results could suggest the synergic use of systemic and local injection of vancomycin as an effective treatment to prevent septic nonunions. This study cannot sustain the systemic injection of BMSCs due to high risks, while a deeper insight into local BMSCs immunomodulatory effects is mandatory before developing cell therapies in clinics.

Introduction

Open fractures are notorious to be at high risk of bacterial contaminations, mainly supported by the osteosynthesis devices that induce the biofilm development and a delayed bone healing [1]. *S. epidermidis* is one of the most involved pathogens in bone infections and nonunions [2] creating a protective niche from antimicrobial treatments [3]. At present, the standard therapy for orthopaedic infections implicates the systemic administration of antibiotics [4]. However, the long-term use of antibiotics, insufficient to reach bacteria within the biofilm matrix, generates a multidrug resistance leading to methicillin-resistant *S. epidermidis* (MRSE) [5]. Moreover, the antibiotic prophylaxis could be inadequate in case of fractures associated with vascular injuries, which reduce the local drug concentration. Hence, alternative prophylaxis strategies need to be assessed not only to prevent bacterial infections but also to support the bone repair. Many antimicrobial agents have been incorporated into biomaterials to be locally delivered [6]. Specifically, a novel bioresorbable hydrogel was in vitro and in vivo validated as an orthopaedic implant coating and antibiotic slow-releasing delivery to impair the bacterial colonization through an antimicrobial competitive inhibition [7-9]. Nowadays, cell therapies have also been proposed to promote the bone repair [10]. Mesenchymal stem cells (MSCs) are claimed to be one of the most frequently used cell types thanks to their high proliferative ability and easy accessibility. MSCs have unique immunologic features that support their viability and proliferation in nonself environments [11]. The use of allogeneic MSCs may drastically reduce the waiting time to obtain a relevant cell amount for clinical use [12], as supported by orthopaedic clinical trials (ClinicalTrial.gov #NCT02307435 and #NCT01586312). Furthermore, MSCs ability to restrain bacterial infections has been hypothesized having both proangiogenic and immunomodulatory characteristics that promote the release of mediators (cytokines and chemokines) [13, 14]. In a recent study, we provided evidence of dose-dependent MRSE-induced nonunions in rats [15], demonstrating that subclinical orthopaedic infections are diagnosed with a significant delay. Typically, in clinics, the C reactive protein remains the most used biomarker of infection, despite a scarce sensitivity and specificity [16]. To supportmedical treatments for infections, identifying reliable predictive markers is urgency. Cytokines play an important role during the host response to infections inflammation and tissue repair by recruiting the cell mediated immunity, before any clinical appearance [17]. Importantly, the inflammation associated with fractures induces a precocious cytokine release that is essential during the early stage of bone healing [18]. However, a prolonged release of inflammatory cytokines fails to stimulate the osteogenic differentiation of resident MSCs recruited on the fracture site leading to an impaired healing [18], and the presence of bacteria highly influences the inflammatory cytokines and bone healing. In the present study, we compare the host response to MRSE-related infections of femoral fractures in rats treated with cell therapies, conventional systemic antibiotic prophylaxis,

and antibacterial-coated implant devices. We hypothesize that transplanted MSCs in a nonunion rat model could have benefits on bone healing and prevention of septic nonunion development thanks to MSC immuonomodulatory effects. Moreover, we hypothesize a role of circulating cytokines in the MRSE-related infections presuming a different activity, according to the received treatments.

Materials and Methods

Study Design and Procedures

This study on animals was approved by the Mario Negri Institute for Pharmacological Research (IRFMN) Animal Care and Use Committee (IACUC) (Permit number 06/2014-PR).The IRFMN adheres to the principles set out in the following laws, regulations, andpolicies governing the care anduse of laboratory animals: Italian Governing Law (D.lgs 26/2014; Authorization number 19/2008-A issued March 6, 2008, by Ministry of Health); Mario Negri Institutional Regulations and Policies providing internal authorization for persons conducting animal experiments (Quality Management System Certificate—UNI EN ISO 9001:2008—Reg. number 6121); the NIH Guide for the Care and Use of Laboratory Animals (2011 edition); and EU directives and guidelines (EEC Council Directive 2010/63/UE). TheStatement of Compliance (Assurance) with the Public Health Service (PHS) Policy on Human Care and Use of Laboratory Animals has been recently reviewed (9/9/2014) and will expire on September 30, 2019 (Animal Welfare Assurance #A5023-01).

Thirty 12-week-old maleWistar rats (body weight 373.56 ± 24.82 g) (Harlan Laboratories SRL) were used in this study. Briefly, rats were maintained under general anesthesia and received a preoperative intramuscular single injection of cefazolin (30 mg/kg, Cefamezin, Teva) and a subcutaneous treatment with carprofen (5 mg/kg, Rimadyl, Pfizer). The rats were osteotomized on the right femur and the fracture was synthesized with stainless steel plate and bicortical screws (all from Zimmer®, Germany). All animals were injected into the femoral defect with an inoculum of $1x10^5$ CFU/30 µl of MRSE strain #GOI1153754-03-14, as validated and widely described in our previous study [15]. Briefly, to prepare the inoculum, a colony of the MRSE strain was cultured into Brain Heart Infusion Broth (BioMérieux) and incubated at 37°C for 16 hours. The bacterial pellet was suspended in sterile saline to obtain a 10 McFarland turbidity equal to about 3 x 10^9 CFU/ml; then the bacterial suspension was diluted with sterile saline solution to obtain a bacterial load of 1×10^5 CFU/30 µl. The bacterial inocula were confirmed by agar plate counting procedures and stored at 4°C until use. After the bacterial inoculum, the muscular planes were closed with Polysorb 4/0 and the skin with Monosof 4/0 (Covidien).The rats were randomly divided into five groups (n = 6 each group): the positive control group (PC) did not receive any therapeutic treatment (Figure 1A); the systemically treated groups received intravenousl vancomycin (15 mg/kg, Hikma) (s-VANC) or allogeneic rat bone marrow MSCs (s-rBMSCs) immediately after surgery; the locally treated groups received a local injection of rBMSCs (l-rBMSCs) (Figure 1B) 24 hours after surgery or a local layering of a vancomycin-enriched hydrogel (l-VANC) (Figure 1C and 1D) during surgery. Atipamezole (1 mg/kg, Antisedan, Pfizer) was administered subcutaneously to recover rats from general anesthesia. The animals were monitored daily for general status and welfare, clinical signs of infection, lameness, weight bearing, swelling, local hyperemia, wound healing, serous

exudate, hematoma, pain, and suffering. The pain was controlled with buprenorphine (0.1mg/kg SC, Temgesic, Schering Plough, Italy) immediately after surgery. Three animals of the s-rBMSCs group died within 6–10 hours after surgery for respiratory complications. Their lungs and hearts were explanted and histologically analyzed. From here on, the investigations regarding the s-rBMSCs group were performed on the remaining three animals. Overall, the animals were monitored for body weight changes, neutrophil counts, and circulating cytokines during the follow-up period. After 6 weeks, rats were euthanized by CO_2 and micro-CT scans; microbiological and histological analyses were performed to assess the bone healing and infection.

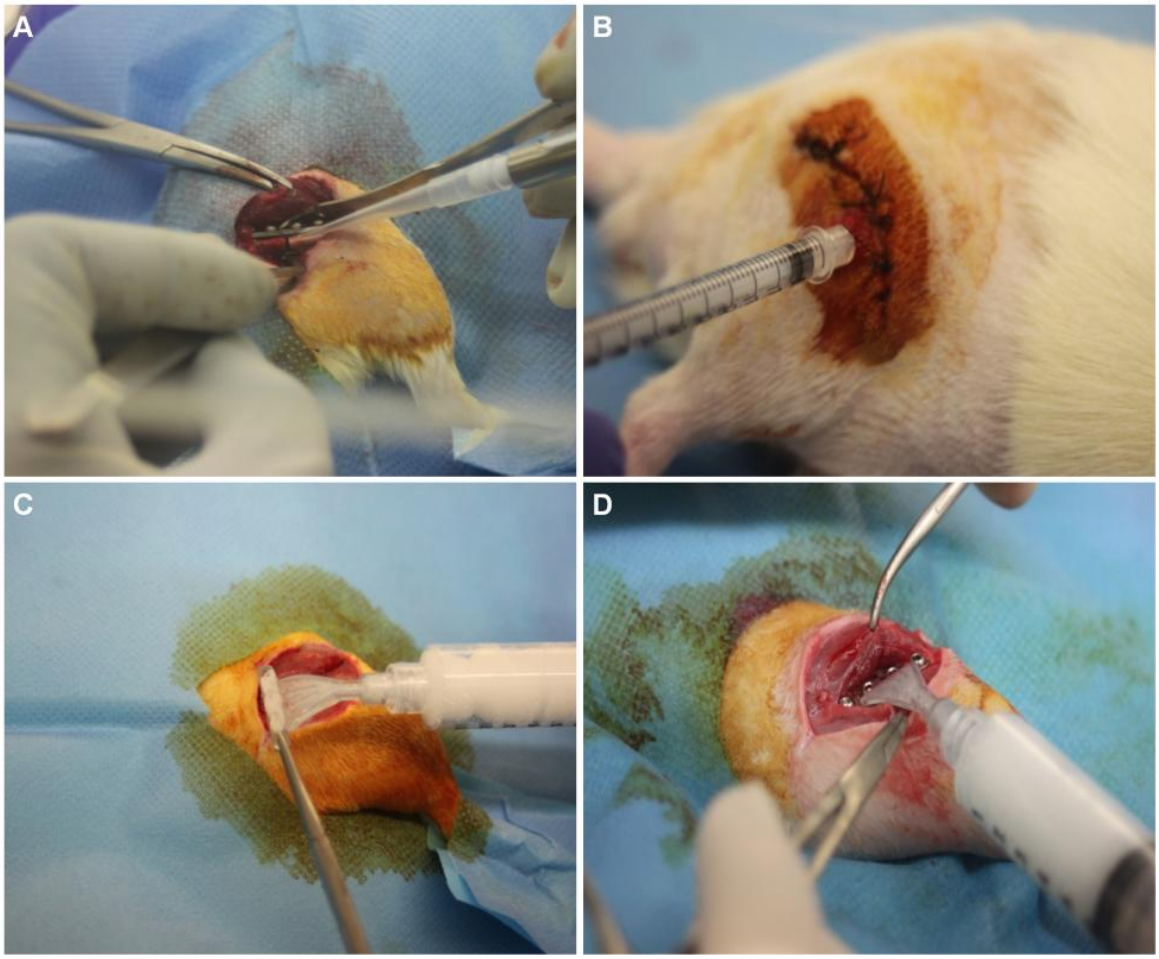

Figure 1. Treatments in the experimental groups. (**A**) All animals received MRSE locally. The picture represents the injection of the bacterial suspension within the site of the fracture. (**B**) Representative picture of the local treatment with rBMSCs in the site of the fracture 24 h after surgery. e picture represents the transcutaneous injection of rBMSCs after disinfection within the site of the fracture. (**C**) e l-VANC group received a vancomycin-enriched hydrogel locally layered on the plate surface before the fracture stabilization and (**D**) within the site of the osteosynthesis after the plate fixation. e pictures represent the distribution of 250 µl of the vancomycin-enriched hydrogel on the bottom (**C**) and top side of the plate (**D**).

Culture and Preparation of Rat BMSCs

Allogeneic Wistar rBMSCs (Oricell®, Cyagen Biosciences, Cat. Number RAWMX-01001, passage 2) were used. Cells were expanded in medium composed of 4.5 g/L glucose Dulbecco's

Modified Eagle's Medium, 100 U/mL penicillin-streptomycin, 2 mM L-glutamine, 1% sodium pyruvate, 1% HEPES (all from Gibco), and 10% fetal bovine serum (Hyclone). At passage 5, undifferentiated rBMSCs were differently injected in the rats at concentration of 2 x 10^6 cells/kg.

Antimicrobial Coating Preparation

A resorbable hydrogel called DAC (Defensive Antibacterial Coating, Novagenit Srl) was enriched with vancomycin at 5% (v/w), according to manufacturer's guidelines and others [8], and then distributed on plates and screws during the osteosynthesis of the l-VANC group. Briefly, to prepare the vancomycinenriched hydrogel, 500 mg of vancomycin was diluted in 10 ml of sterile water, and then 5 ml of this suspension was used to solubilize the hydrogel, thus obtaining an enriched hydrogel containing 50 mg/ml of vancomycin. In the l-VANC group, plates and screws implanted were coated with 250 µl of enriched hydrogel, thus delivering locally 35 mg/kg of vancomycin.

Body Weight and Blood Analyses

The rat body weight was measured before surgery and weekly until the day of explantation (day 42) and reported as relative b.w. increase on the baseline (day of surgery). On days 0, 14, and 42 (n = 6 per group; n = 3 s-rBMSCs), venous blood was harvested from the tail vein under general anesthesia and then transferred into K_2 EDTA tubes (Microtainer MAP, Becton Dickinson) to determine the neutrophil count. On days 3, 7, and 14 after surgery, plasma was obtained by centrifuging the samples (n = 4 per group; n = 3 s-rBMSCs) at 1200 xg for 10min at RT and stored at −80◦C until use for the cytokine analysis (IL-1α/β, IL-6, IL-10, TNF-α, and IFN-γ) by means of the Luminex assay kit (Bio-Plex Pro® Rat Cytokine Assay, Bio-Rad) according to the manufacturer's instructions. Measurement was performed in duplicate by using a Bio-Plex 200 system based on the Luminex xMAP technology (Bio-Rad, Hercules). Cytokine levels are reported as pg/ml.

Micro-CT Imaging

The qualitative and quantitative micro-CT analyses on femurs were performed with an Explore Locus micro-CT scanner (GE Healthcare), as previously described elsewhere [15]. Bony bridging percentage of >75%, 50–75%, or <75% of the fracture gap was evaluated and scored. The bone volume (BV, mm^3) and tissue mineral density (TMD, mg/cc) were calculated within the volume of interest, as described by others [19]. Data were reported as fold increase of the treated groups on the PC group.

Microbiological Analysis

After 42 days, bacteria were recovered from explanted femurs (n = 6 per group; n = 3 s-rBMSCs)

by treating samples with dithiothreitol to dislodge bacteria from the biofilm and analyzed as previously described [15, 20]. Data were reported as Log (CFU/g) explant.

Histological Analysis

Femurs (n = 6 per group; n = 3 srBMSCs) were fixed in 10% formalin, decalcified in Osteodec (Bio-Optica), embedded, and cut into 5 μm sections. Haematoxylin and eosin (H&E) staining was performed to assess morphology, fracture healing, and signs of osteomyelitis. The Gram-positive staining was evaluated for presence or absence of bacteria. Olympus IX71 light microscope and Olympus XC10 camera (Japan) were used to obtain images.

Statistical Analysis

After verifying the normal distribution of data with the Shapiro-Wilk test, comparisons among groups and time points were analyzed with two-way analysis of variance (ANOVA) and comparisons among groups were analyzed with one-way ANOVA (GraphPad Prism v5.00 Software) and then coupled with Bonferroni's post hoc test. All data are expressed as means ± standard error (SE). Values of $p < 0.05$ were considered statistically significant.

Results

Clinical Examination

The histological analysis of the organs of the s-rBMSCs treated rats did not show any cardiac alteration but assessed the presence of acute hyperemia associated with multifocal alveolar edema and hemorrhage in the lungs (Figure 2). Despite emboli within pulmonary arteries were not evident, the interlobular septa were markedly inflated with fluid and diffuse diffuse congestion (Figure 2, asterisk), presence of macrophages and polymorphonucleated cells within the parenchyma indicating a severe inflammatory reaction. During the follow-up period, no other animals of any group died or presented peri-implant inflammation. From days 3 to 7, three PC rats showed a partial load bearing on the operated limb without any clinical evidence of infection.

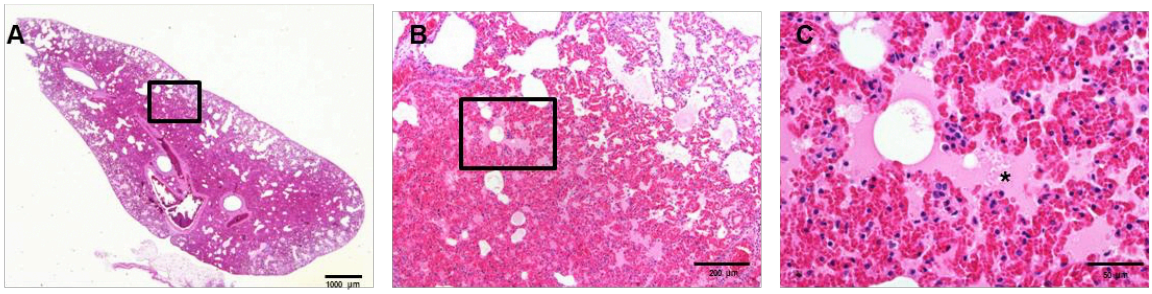

Figure 2. Representative histological panel of the rat lungs reporting the effects of the acute intravenous administration of allogeneic BMSCs in the s-rBMSCs group. The lung sections are stained with haematoxylin and eosin. (**A**, **B**) Presence of acute and diffuse hyperemia within the lung parenchyma. (**C**) Presence of multifocal alveolar edema (∗). (A) scale bar 1000 μm; (B) scale bar 200 μm; (C) scale bar 50 μm.

Body Weight and Blood Analyses

The relative b.w. increase on the baseline was represented in Figure 3(a). At day 7, a b.w. loss was recorded in all groups. At day 14, lrBMSCs and l-VANC showed a b.w. decrease and a slower b.w. recovery throughout the experimental follow-up compared to the other treated groups. Differently, s-VANC depicted a significant b.w. increase compared to l-VANC, l-rBMSCs, and PC over time. In Figure 3B, the neutrophil count is reported as number of neutrophils ×103/μl compared to the baseline (day 0). After 14 days, PC showed a significant neutrophil increase compared to the basal values and to l-VANC. After 42 days, the neutrophil count almost normalized in all groups without any significant differences compared to the basal values and among the experimental groups.

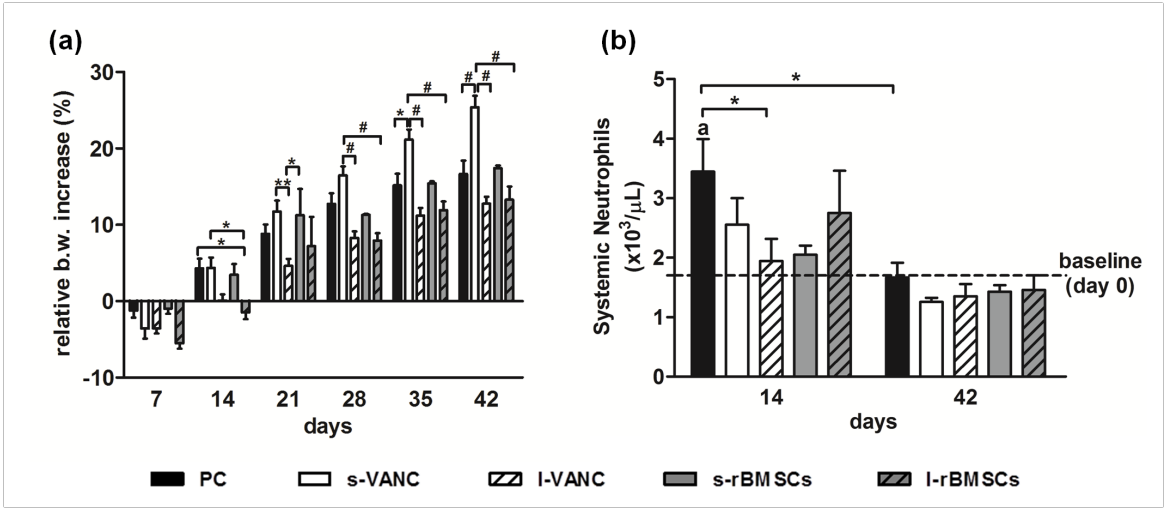

Figure 3. Clinical data. (**A**) e histogram shows the relative changes in body weight in the experimental groups over time. (**B**) e histogram shows the systemic neutrophil count in the experimental groups at days 14 and 42 after surgery. Comparisons between groups and time points were analyzed with two-way ANOVA and Bonferroni's post hoc test. Statistical significance was $p < 0.05$ (∗),$p < 0.01$ (A, ∗∗), and $p < 0.001$ (#); n = 6, n = 3 s-rBMSCs.

Pro- and Anti-Inflammatory Cytokines

Plasma levels of pro inflammatory (IL-1α/β, TNF-α, and IFN-γ), anti-inflammatory (IL-10), and regulatory (IL-6) cytokines were assessed at days 3, 7, and 14 (Figure 4). In most of the groups, all cytokines showed the same changes with time. Overall, at day 3, PC and l-rBMSCs had a higher cytokine trend with respect to the other groups. At day 7, PC and s-VANC showed a higher cytokine trend compared to the other groups. Similarly, this trend was found for IL-1β in s-rBMSCs, for IL-10 in l-rBMSCs, and for IFN-γ in l-VANC. At day 14, the highest cytokine values were measured in PC and l-VANC and just for IL-10 in the l-rBMSCs group. Particularly, PC had a higher trend for all the analyzed cytokines compared to the other groups at day3 and peaked at 7 days after injection. Moreover, PC demonstrated the highest cytokine activity compared to the treated groups. Mainly at day 7, PC had increased values of the acute phase cytokines (IL-1α/β and TNF-α) with significant differences compared to l-VANC, s-rBMSCs, and l-rBMSCs. This trend was found also on day 3 for TNF-α in the PC group. Moreover, s-VANC showed a higher trend compared to l-VANC. Differently, the anti-inflammatory cytokines (IL-10) and the late phase (IFN-γ and IL-6) did not show a significant difference in PC compared to all the treated groups. At day 3, l-rBMSCs showed higher values for IL-1α/β, TNF-α, and IFN-γ with respect to s-VANC and l-VANC. At day 14, l-VANC showed a higher trend with respect to the other groups in all the analyzed cytokines, with a significant difference for TNF-α and IL-6 with respect to s-VANC.

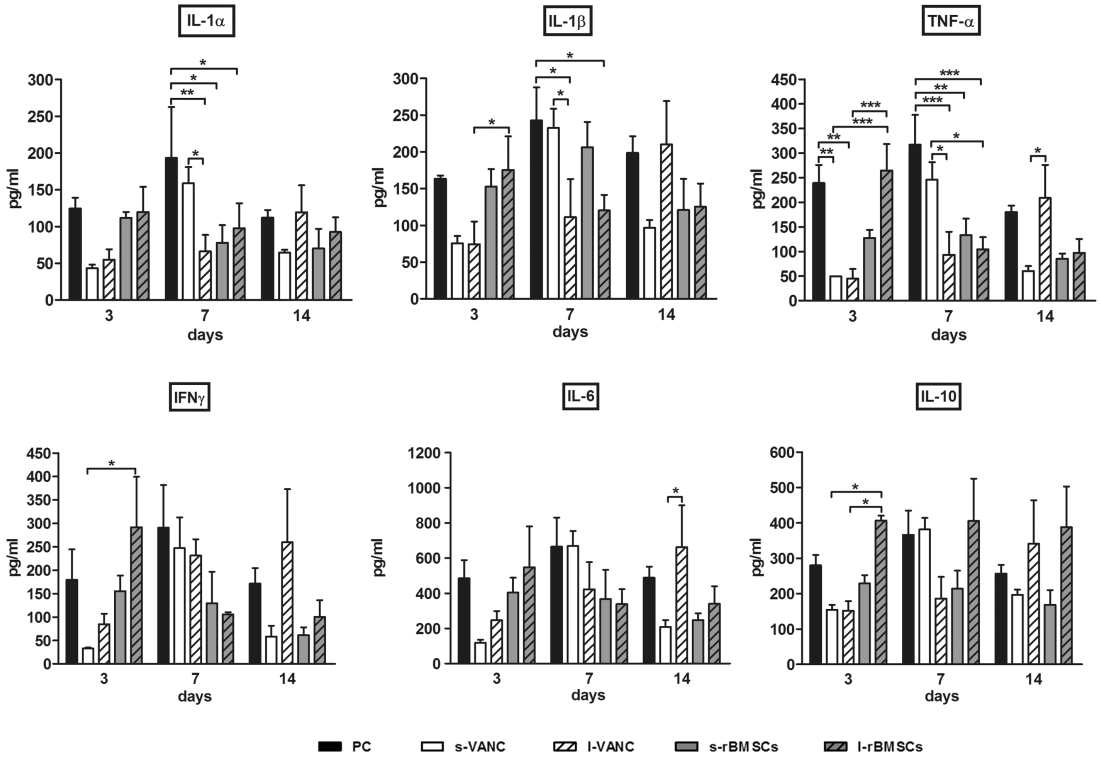

Figure 4. Cytokine analysis. The histograms show the cytokine values of the experimental groups at 3, 7, and 14 days after surgery and bacterial injection. Comparisons between groups and time points were analyzed with two-way ANOVA and Bonferroni's *post hoc* test. Statistical significance was $p < 0.05$ (*), $p < 0.01$ (**), and $p < 0.001$ (***); n = 4, n = 3 s-rBMSCs.

Micro-CT Imaging Diagnosis

The micro-CT qualitative analysis depicted a variable percentage of bony bridging in the experimental groups (Table 1).

Table 1. Percentage of bony bridging of the fracture site.

	Bony bridging		
	< 75% Nonunion fracture	50-75% Partial fracture healing	> 75% Fracture healing
PC	83% (5/6)	17% (1/6)	n.d. (0/6)
s-VANC	n.d. (0/6)	67% (4/6)	33% (2/6)
l-VANC	33% (2/6)	17% (1/6)	50% (3/6)
s-rBMSCs	n.d. (0/6)	n.d. (0/6)	100% (3/3)
l-rBMSCs	33% (2/6)	17% (1/6)	50% (3/6)

The osteomyelitis grading score for this group showed significant difference with respect to all the treated groups, while no significant differences were found between the treated groups (Figure 5K).

BV and TMD were reported as fold increase with respect to the PC group in Figure 6A and 6B. No significant differences were found for BV between the treated groups; differently, the fold increase of TMD was higher in s-rBMSCs with respect to both l-VANC and l-rBMSCs.

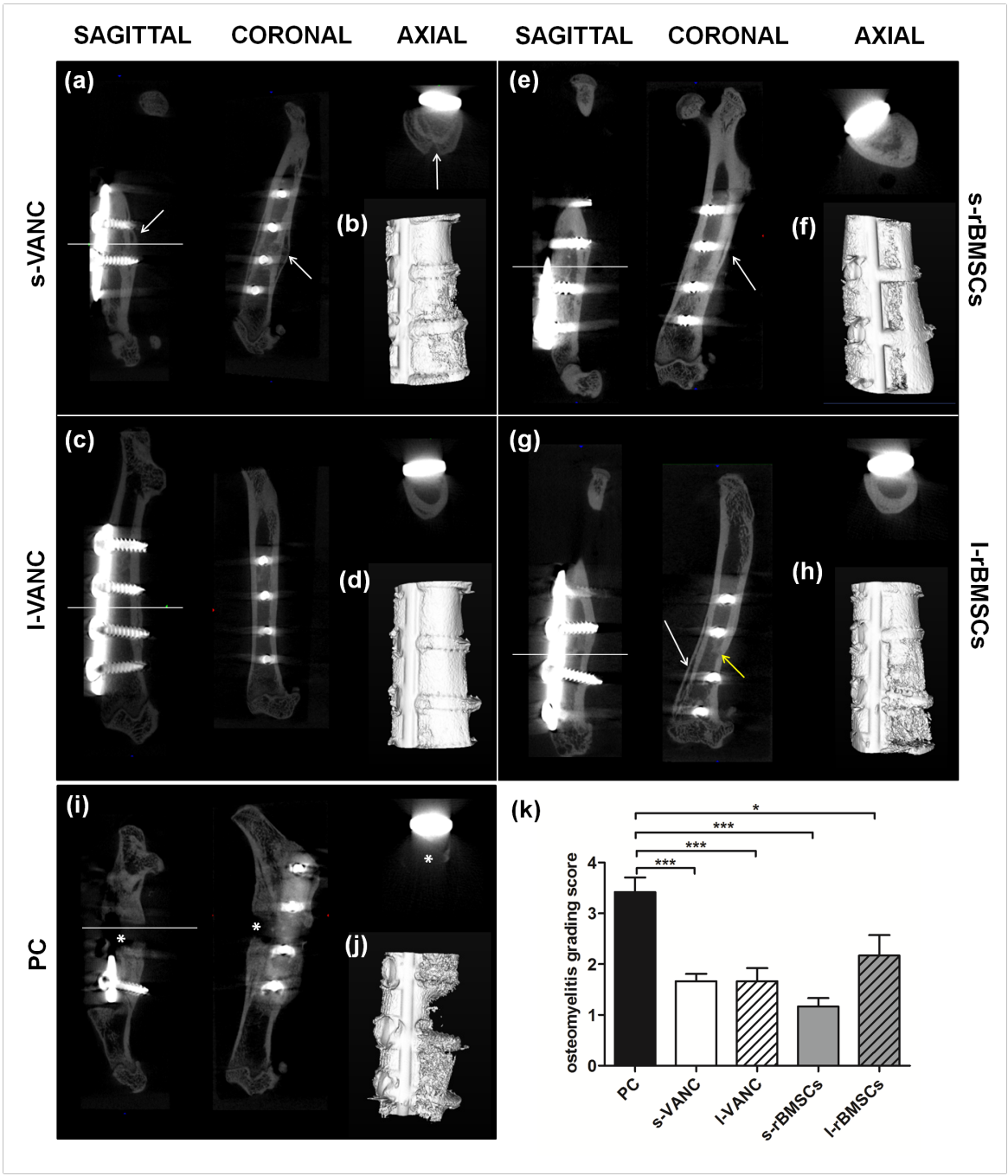

Figure 5. Qualitative micro-CT imaging, isosurface, and semiquantitative osteomyelitis score. The representative panel shows micro-CT images on the day of explantation. (**A**, **C**, **E**, **G**, **I**) Sagittal, coronal, and axial planes. (**B**, **D**, **F**, **H**, **J**) 3D isosurface reconstruction is presented for the s-VANC, s- rBMSCs, l-VANC, l-rBMSCs, and PC groups. Symbols indicate cortical reaction (white arrows); medullary reaction (yellow arrow); and loss of cortical wall and osteolysis (asterisks). (**K**) Osteomyelitis grading score based on Odekerken's scale is reported in the histogram. Comparisons among groups were analyzed with one-way ANOVA corrected with Bonferroni's *post hoc* test. Statistical significance was $p < 0.05$ (*) and $p < 0.001$ (***); n = 6, n = 3 s-rBMSCs.

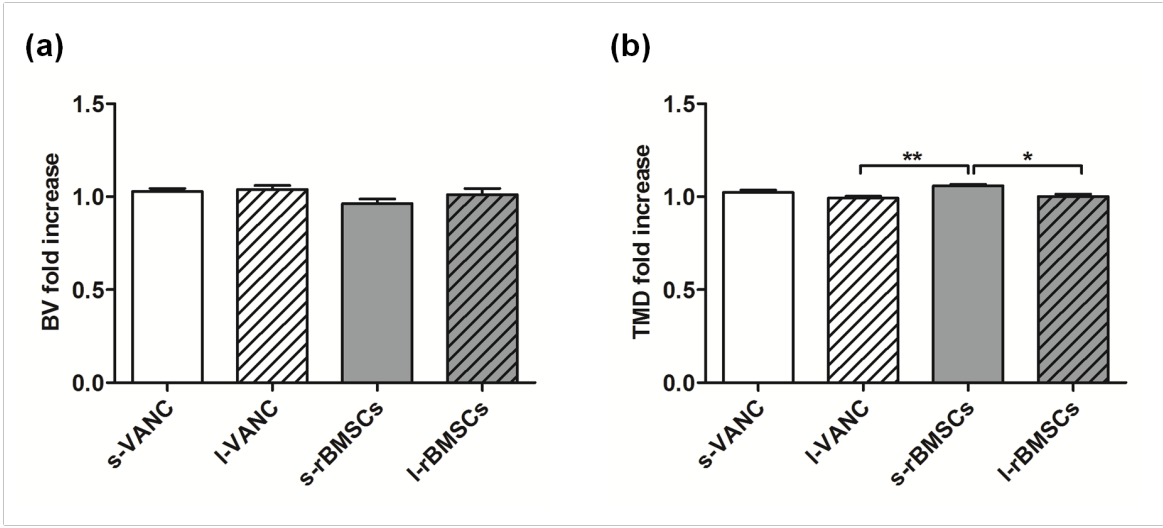

Figure 6: micro-CT quantitative analyses of bone structure. (**A**) Bone volume (BV) and (**B**) tissue mineral density (TMD) quantitative analysis of the treated groups normalized on the PC group, reported as fold increase. Comparisons among groups were analyzed with one-way ANOVA corrected with Bonferroni's *post hoc* test. Statistical significance was $p < 0.05$ (*) and $p < 0.01$ (**); n = 6, n = 3 s-rBMSCs.

Microbiological Analysis

The microbiological analysis reported in Figure 7 detected a significant higher bacterial growth between PC and both s-VANC and l-VANC. Moreover, l-VANC showed a lower bacterial growth with respect to l-rBMSCs. The limit of detection was set at 0.18 Log (CFU/g) explant.

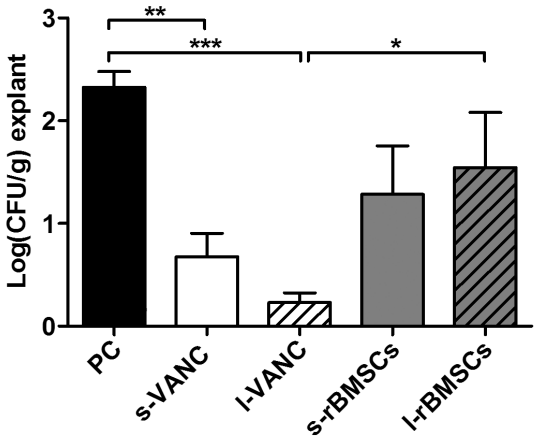

Figure 7. Microbiological detection of bacterial growth on the explanted specimens. The limit of detection (L.o.D.) was set at 0.18 Log(CFU/g)/explant. Comparisons among groups were analyzed with one-way ANOVA corrected with Bonferroni's *post hoc* test. Statistical significance was $p < 0.05$ (*),$p < 0.01$ (**), and $p < 0.001$ (***); n = 6, n = 3 s-rBMSCs.

Histological Analysis

The H&E staining confirmed the results obtained by micro-CT in terms of percentage of fracture healing and absence of osteomyelitis in s-VANC, l-VANC, and s-rBMSCs (Figure 8).

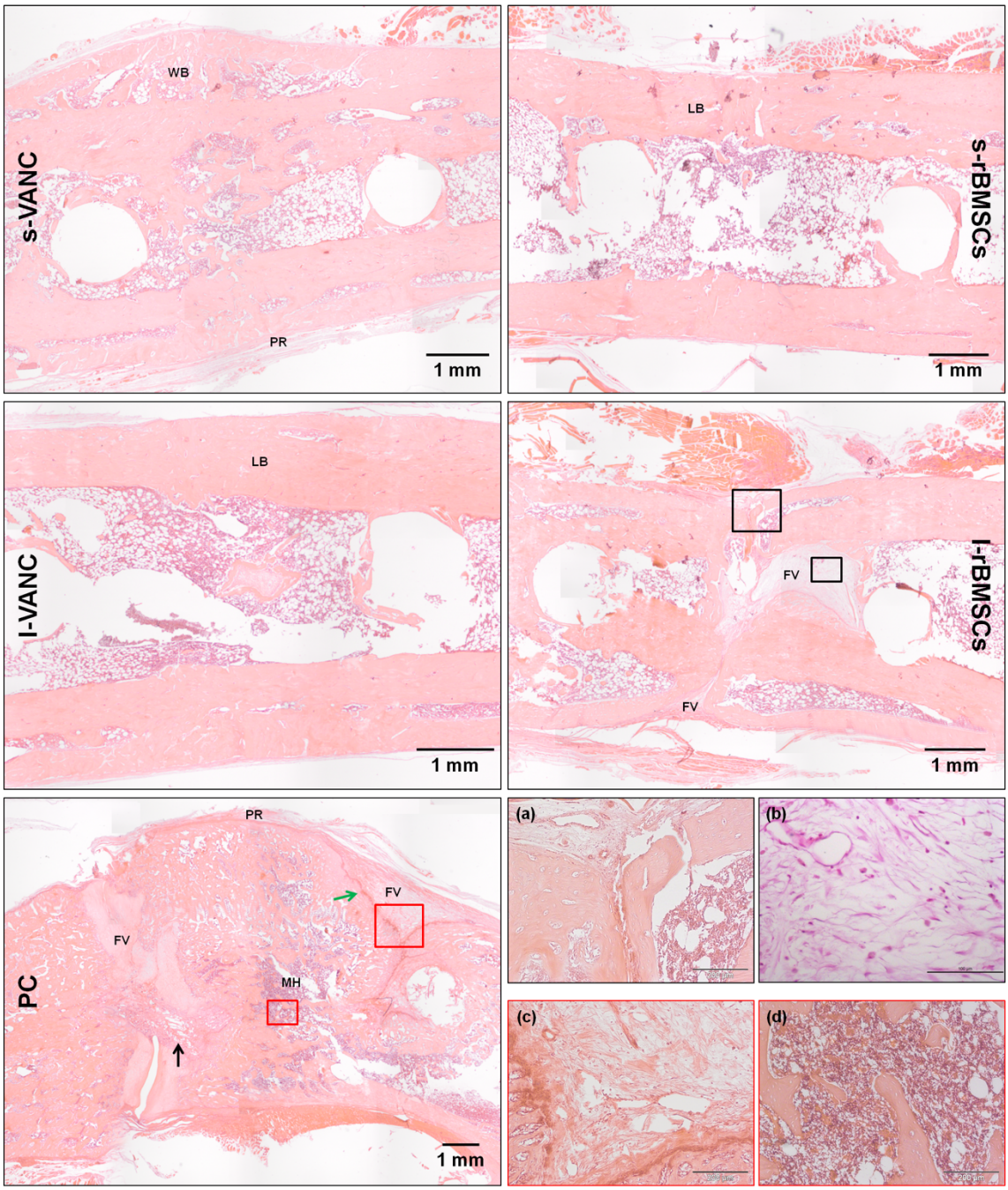

Figure 8. Histological analysis (H&E) at the day of explantation. The representative panel shows H&E staining of the femurs in all the experimental groups. The panels depict an overview of the samples, scale bar 1 mm. WB: woven bone; LB: lamellar bone; PR: periosteal reaction; FV: fibrovascular tissue; MH: myeloid hyperplasia; vascular infiltrates (black arrow); alteration of cortical bone (green arrow). For the l-rBMSCs group, (**A**) a specific area containing fibrovascular tissue and polymorphonucleated cells is reported in the big black box (scale bar 200 µm) and (**B**) the presence of giant cells in the small black box (scale bar 100 µm) is reported. For the PC group, (**C**) a specific area with fibrovascular tissue is reported in the big red box (scale bar 200 µm) and (**D**) the myeloid hyperplasia is shown in the small red box (scale bar 200 µm).

Specifically, in s-VANC, the fractures appeared repaired by a great amount of newly bone deposition in a remodeling phase (woven bone), coupled with a mild cortical thickening and

periosteal reaction. Both in l-VANC and s-rBMSCs, a complete closure of the fracture was found and the new bone appeared more mature and lamellar than in s-VANC. The l-VANC group showed uniformly enlarged cortices with areas of bone remodeling.

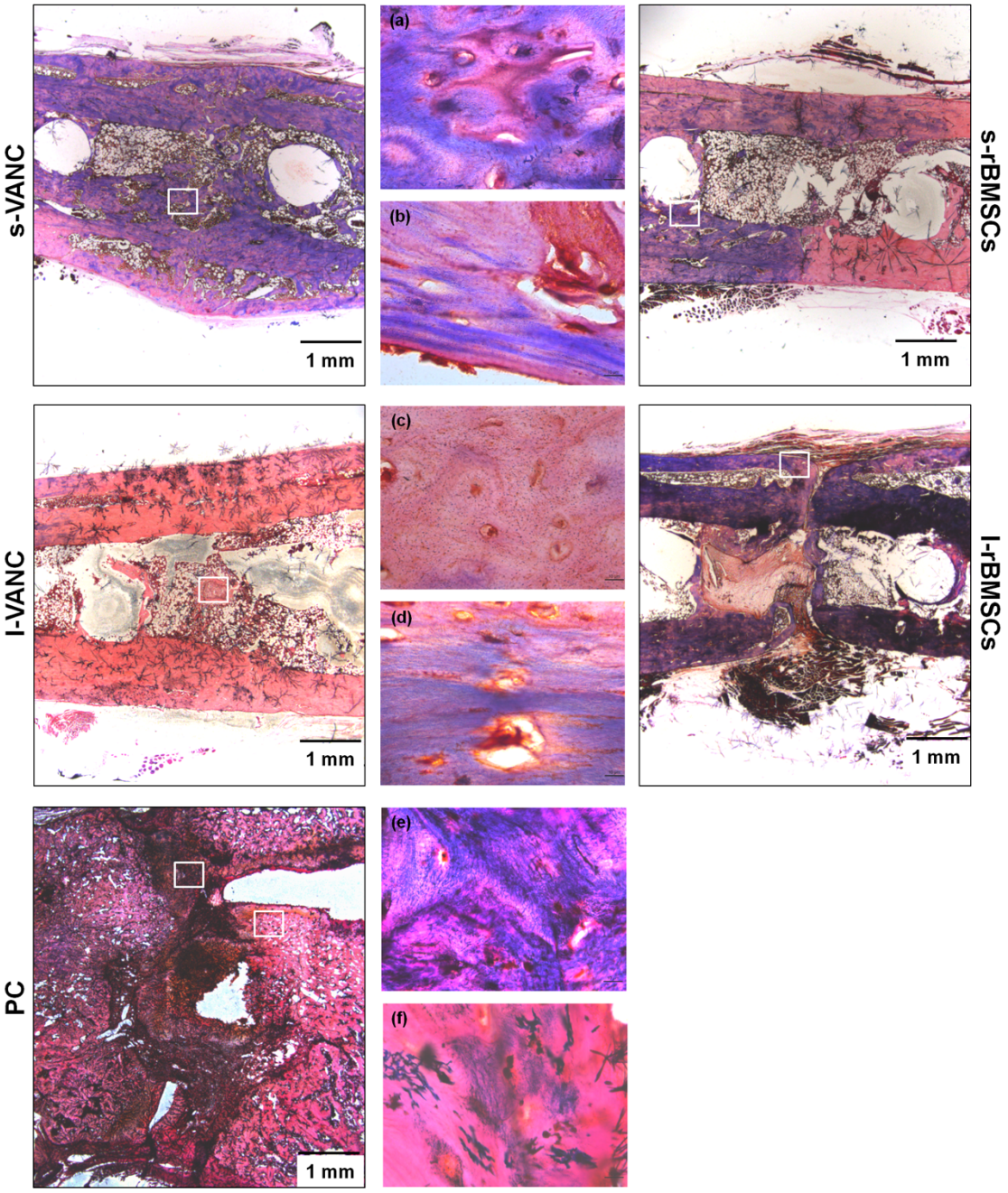

Figure 9. Gram staining of the femurs at the day of explantation. The representative panel shows the Gram staining of the femurs in all the experimental groups. The panels depict an overview of the samples, scale bar 1 mm. In each group, the white boxes have a scale bar 10 μm and represent (A) detail of the s-VANC group; (B) detail of the s-rBMSCs group; (C) detail of the l-VANC group; (D) detail of the l-rBMSCs group; (E, F) details of the PC group.

In l-rBMSCs, 17% of samples presented only a partial bony bridging characterized by a great deposition of fibrovascular tissue invading the fracture site and surrounding the screws

disseminated with giant cells. In all the aforementioned groups, a moderate presence of polymorphonucleated cells was found within the medullary canal. The PC group showed disorganized bone architecture, a lot of fibrovascular tissues, and nonunion establishment. The periosteal reaction, myeloid hyperplasia, and presence of intact and fragmented polymorphonucleated cells in the granulation tissue associated with several vascular vessels represented signs of osteomyelitis. The Gram staining confirmed the quantitative data obtained from the microbiological tests (Figure 9). Indeed, in all groups, the presence of cocci was detected. In particular, s-VANC, s-rBMSCs, l-rBMSCs, and PC showed several cocci assembled in clusters and diffuse within the bone and periosteal tissue. Differently, l-VANC showed scarce dispersed cocci within areas of new bone formation in the fracture site.

Discussion

This comparative study analyzes for the first time the efficacy of systemic antimicrobial prophylaxis and antibacterial coating of orthopedic implants and cell therapy on MRSE-induced nonunions in rats. We hypothesized that the use of allogeneic MSCs could improve the host response to bacterial infections based on the potential immunomodulatory effects directly on the injured site [21]. In our study, the amount of systemically or locally injected rBMSCs was concordant with the dosage used in the literature for cardiovascular or autoimmune diseases [22, 23], as demonstrated to reach damaged sites. However, in our series, we had a 50% of animal death when intravenously injected with rBMSCs (s-rBMSCs). The histological analysis supported the "pulmonary first-pass theory," in which a scarce cellular delivery has been demonstrated due to the lung filter in either animals or humans [24-27]. This phenomenon should be related to the cell adhesion, the activation of the coagulation pathway, and anaphylactic reactions promoted by the allogeneic MSCs causing pulmonary embolisms [23, 28]. Hereon, it is worth taking into account that the data obtained in the s-rBMSCs group considered only three animals and they cannot offer a good sample sizing to properly sustain our results, representing a limit of our study. The pathogenesis of bone infections after severe fractures is strictly related to the biofilm formation, making difficult both the diagnosis and the efficacy of treatments. Thus, identifying specific biomarkers would be crucial to early detection of the grade of infection. In our study, we evaluated cytokines produced in both the acute (IL-1α/β and TNF-α) and the chronic phases (IFN-γ, IL-10, and IL-6) of inflammation/infection and involved in the bone remodeling (IL-6). Specifically, IL-6 has a bivalent function depending on the mode of expression: persistently high (even moderate) levels are associated with a pro-inflammatory activity whilst a peaking behavior is associated with an anti-inflammatory pro regenerative effect [29]. However, the inability to discriminate between changes from postsurgical trauma and MRSE induced infection could represent a limitation. Overall, we demonstrated significant differences among groups after 7 days of infection. Due to the staphylococcal toxin release, TNF-α showed difference already at day 3, being the primary involved cytokine [30]. Moreover, we demonstrated the simultaneous activation of both pro- and anti-inflammatory cytokines. At day 7, higher IL-1α/β and TNF-α values in the PC group with respect to the others may have been in response to inflammatory stimuli because of bacterial growth and biofilm formation. This correlates with the greater neutrophil count at 14 days, when neutrophils mediate the recruitment of macrophages maintaining high levels of cytokines [31, 32]. Similarly, on day 7, s-VANC showed increased IL-1α/β and TNF-α values compared to the other treated groups, relating to a reduced efficacy of one-shot injected vancomycin. It is known that vancomycin acts both directly against bacteria and as an immunomodulatory drug, inhibiting the cytokine production during the early stages [33], as we also demonstrated at day 3. On day 14, higher cytokine levels in

l-VANC compared to the other groups could be caused by the local inflammatory response through the activation of macrophages that intervene against the material debris and could affect the bone repair, as also demonstrated by others [34]. Moreover, we detected high levels of IL-6 in l-VANC after 14 days, predicting a lower systemic efficacy of this treatment with respect to the conventional prophylaxis therapy [35]. However, IL-6 is involved in the modulation of bone cells during repair by suppressing the differentiation of the osteoclast progenitors [36, 37]. The increase of IL-1β, IFN-α, and TNF-γ found in l-rBMSCs at day 3 could be related to the antiapoptotic activity of MSCs on neutrophils in the microenvironment of a damaged and infected tissue [38, 39]. These data were also confirmed by the neutrophil analysis and were consistent with those described by Seebach et al. [13]. Furthermore, these inflammatory cytokines can stimulate the MSCs to release a large amount of growth factors promoting the tissue repair [40]. Again, we detected an up regulation of IL-10 in l-rBMSCs at days 7 and 14. Specifically, IL-10, produced by the macrophages present in the histological sections of l-rBMSCs, has a regulatory role in immunological and inflammatory responses by decreasing the production of pro-inflammatory cytokines, as demonstrated here and by others [41]. Indeed, the interaction between MSCs and macrophages secretes prostaglandin E2 that reprograms the macrophages to release IL-10 [39]. The increase of IL-10 in l-rBMSCs suggests that MSCs can modulate the host immune response to infection. Otherwise, a similar behavior for the s-rBMSCs group could not be supported by this study because of the small number of survived animals. Thus, the clinical results in the s-rBMSCs group (micro-CT and histology) cannot be considered representative for the efficacy of this treatment. Concerning the other groups, the semi-quantitative Odekerken's score for osteomyelitis was supported by the BV and TMD measurements, in which no significant differences were found among s-VANC, l-VANC, and l-BMSCs groups. The micro-CT and histological analyses of the PC group generated results consistent with those of our previous study [15], demonstrating the development of septic nonunions. The same analyses highlighted a worse osteomyelitis score in the l-rBMSCs group compared to the antibiotic treated groups, as also supported by Seebach et al. [13]. This is potentially due to the release of cellular proteases by dead MSCs that could negatively act on bone repair and support the bacterial colonization. This was also demonstrated by the microbiological tests measuring a greater bacterial growth in l-rBMSCs compared to the antibiotic treated groups. Overall, our study demonstrated a good response in terms of bone healing and absence of osteomyelitis in s-VANC and l-VANC.

Conclusions

Through our results, we could suggest the synergic use of systemically injected vancomycin and its local delivery as an effective treatment to prevent the bacterial spread in orthopedic infections. The hydrogel, used in this study, could also ameliorate the bone repair towards a more mature bone thanks to its capability in stimulating bone specific cytokine (IL-6). Otherwise, our study cannot definitely sustain the use of cell therapy for this purpose. Indeed, the intravenous injection of MSCs should be considered a highly risky treatment with a high rate of mortality. However, based on our preliminary results on the local injection of MSCs, a deeper insight into their immunomodulatory mechanisms in a large experimental design should be helpful to develop novel strategies for the clinical use of MSCs.

Acknowledgements

The financial support for this study was provided by the Italian Ministry of Health (RC 2014, Research Line 4, #62). The authors thank Dr. Anna Sacchetta for her technical advice concerning hydrogel (DAC) chemical and physical aspects and for providing the product used in this study.
The Authors have no conflict of interest to declare.

References

1. Moore RE, Baldwin K, Austin MS, et al. Asystematic review of open reduction and internal fixation of periprosthetic femur fractures with or without allograft strut, cerclage, and lockedplates. Journal ofArthroplasty. 2014. 29(5):872-6.
2. Ribeiro M, Monteiro FJ, Ferraz MP. Infection of orthopedic implants with emphasis on bacterial adhesion process and techniques used in studying bacterial-material interactions. Biomatter. 2012. 2(4):176-94.
3. Namvar AE, Bastarahang S, Abbasi N et al. Clinical characteristics of Staphylococcus epidermidis: a systematic review. GMS Hygiene and Infection Control. 2014. 30;9(3).
4. Reiter KC, Villa B, Paim TG, et al. Inhibition of biofilm maturation by linezolid in meticillin-resistant Staphylococcus epidermidis clinical isolates: comparison with other drugs. Journal of Medical Microbiology. 2013. 62(Pt 3):394-9.
5. Sahal G, Bilkay IS. Multi drug resistance in strong biofilm forming clinical isolates of Staphylococcus epidermidis. Brazilian Journal of Microbiology. 2014. 45(2):539-44.
6. ter Boo GJA, Grijpma, DW, Moriarty TF, et al. Antimicrobial delivery systems for local infection prophylaxis in orthopedic-and trauma surgery. Biomaterials. 2015. 52:113–125.
7. Drago L, Boot W, Dimas K, et al. Does implant coating with antibacterial-loaded hydrogel reduce bacterial colonization and biofilm formation in vitro? Clinical Orthopaedics and Related Research. 2014. 472(11):3311-23.
8. Giavaresi G, Meani E, Sartori M, et al. Efficacy of antibacterial-loaded coating in an in vivo model of acutely highly contaminated implant. International Orthopaedics. 2014. 38(7):1505-12.
9. Romanò CL, Giammona G, Giardino R, Meani E. Antibiotic-loaded resorbable hydrogel coating for infection prophylaxis of orthopaedics implants: preliminary studies. J Bone Joint Surg Br. 2011. 93-B:337–338.
10. Gómez-Barrena E, Rosset P, Lozano D, et al. Bone fracture healing: cell therapy in delayed unions and nonunions. Bone. 2015. 70:93-101.
11. Sharma RR, Pollock K, Hubel A, et al. Mesenchymal stem or stromal cells: a review of clinical applications and manufacturing practices. Transfusion. 2014. 54(5),1418-1437.
12. Wu T, Liu Y, Wang B, et al. The roles of mesenchymal stem cells in tissue repair and disease modification. Current Stem Cell Research and Therapy. 2014. 9(5):424-31.
13. Seebach E, Holschbach J, Buchta N, et al. Mesenchymal stromal cell implantation for stimulation of long bone healing aggravates Staphylococcus aureus induced osteomyelitis, Acta Biomaterialia. 2015. 21:165-77.
14. Yuan Y, lin S, Guo N, et al. Marrow mesenchymal stromal cells reduce methicillin-resistant Staphylococcus aureus infection in rat models. Cytotherapy. 2014. 16(1):56-63
15. Lovati AB, Romanò CL, Bottagisio M et al. Modeling staphylococcus epidermidis-induced non-unions: subclinical and clinical evidence in rats. PLoS ONE. 2016. 11(1):e0147447.
16. Lelubre C, Anselin S, Zouaoui Boudjeltia K, et al. Interpretation of C-reactive protein concentrations in critically ill patients. BioMed Research International. 2013. 2013:124021.

17. Shah K, Mohammed A, Patil S, et al. Circulating cytokines after hip and knee arthroplasty: A Preliminary Study. Clinical Orthopaedics and Related Research. 2009. 467(4):946-51.
18. Bastian O, Pillay J, Alblas J, et al. Systemic inflammation and fracture healing. Journal of Leukocyte Biology. 2011. 89(5):669-73.
19. O'Neill KR, Stutz CM, Mignemi NA, et al. Micro-computed tomography assessment of the progression of fracture healing in mice. Bone. 2012. 50(6):1357-67.
20. Drago L, Romanò CL, Mattina R, et al. Does dithiothreitol improve bacterial detection from infected prostheses? A pilot study infection. Clinical Orthopaedics and Related Research. 2012. 470(10):2915-25.
21. Klier U, Maletzki C, Göttmann N, et al. Avitalized bacteria mediate tumor growth control via activation of innate immunity. Cellular Immunology. 2011. 269(2):120-7.
22. Freyman T, Polin G, Osman H, et al. A quantitative, randomized study evaluating three methods of mesenchymal stem cell delivery following myocardial infarction. European Heart Journal. 2006. 27(9):1114-22.
23. Kean TJ, Lin P, Caplan AI, et al. MSCs: delivery routes and engraftment, cell-targeting strategies, and immunemodulation. Stem Cells International. 2013. 2013:732742
24. Barbash IM, Chouraqui P, Baron J, et al. Systemic delivery of bone marrow-derived mesenchymal stem cells to the infarcted myocardium: feasibility, cell migration, and body distribution. Circulation. 2003. 108(7):863-8.
25. Kyriakou C, Rabin N, Pizzey A, et al. Factors that influence short-term homing of human bone marrow-derived mesenchymal stem cells in a xenogeneic animal model. Haematologica. 2008. 93(10):1457-65.
26. Furlani D, Ugurlucan M, Ong L, et al. Is the intravascular administration of mesenchymal stem cells safe? Mesenchymal stem cells and intravital microscopy. Microvascular Research. 2009. 77(3):370-6.
27. Jung JW, Kwon M, Choi JC, et al. Familial occurrence of pulmonary embolism after intravenous, adipose tissue-derived stem cell therapy. Yonsei Medical Journal. 2013. 54(5):1293-6.
28. Moll G, Le Blanc K. Engineering more efficient multipotent mesenchymal stromal (stem) cells for systemic delivery as cellular therapy. ISBT Science Series. 2015. 10(S1),357-365.
29. Lombardi G, Sanchis-Gomar F, Perego S, et al. Implications of exercise-induced adipo-myokines in bone metabolism. Endocrine. 2015. 54(2):284-305.
30. Müller-Alouf H, Carnoy C, Simonet M, et al. Superantigen bacterial toxins: state of the art. Toxicon. 2001. 39(11):1691-701.
31. Chung R, Cool JC, Scherer MA, et al. Roles of neutrophil-mediated inflammatory response in the bony repair of injured growth plate cartilage in young rats. Journal of Leukocyte Biology. 2006. 80(6):1272-80.
32. Andrew JG, Andrew SM, Freemont AJ, et al. Inflammatory cells in normal human fracture healing. Acta Orthopaedica. 1994. 65(4):462-6.
33. Bode C, Muenster S, Diedrich B et al. Linezolid, vancomycin and daptomycin modulate cytokine production, Toll-like receptors and phagocytosis in a human in vitro model of sepsis. Journal of Antibiotics. 2015. 68(8):485-90.

34. Goodman SB, Yao Z, Keeney M, et al. The future of biologic coatings for orthopaedic implants. Biomaterials. 2013. 34(13):3174-83.
35. Pierrakos C, Vincent JL. Sepsis biomarkers: a review. Critical Care. 2010. 14(1):R15.
36. Yoshitake F, Itoh S, Narita H, et al. Interleukin-6 directly inhibits osteoclast differentiation by suppressing receptor activator of NF-kappaB signaling pathways. The Journal of Biological Chemistry. 2008. 283(17):11535-40.
37. Lombardi G, Sanchis-Gomar F, Perego S, et al. Implications of exercise-induced adipo-myokines in bone metabolism. Endocrine. 2015. 54(2):284-305.
38. Wei X, Yang X, Han ZP, et al. Mesenchymal stem cells: a new trend for cell therapy. Acta Pharmacologica Sinica. 2013. 34(6):747-54.
39. Tyndall A, Pistoia V. Mesenchymal stem cells combat sepsis. Nature Medicine. 2009. 15(1):18-20.
40. Ma S, Xie N, Li W, et al. Immunobiology of mesenchymal stem cells. Cell Death and Differentiation. 2014. 21(2):216-25.
41. de Waal Malefyt R, Abrams J, Bennett B, et al. Interleukin 10 (IL-10) inhibits cytokine synthesis by humanmonocytes: an autoregulatory role of IL-10 produced by monocytes. The Journal of Experimental Medicine. 1991. 174(5):1209-20.

Chapter 3

Draft genome sequence of *Staphylococcus epidermidis* clinical strain GOI1153754-03-14 isolated from an infected knee prosthesis

Marta Bottagisio[1,2*], Alessio Soggiu[2], Arianna B. Lovati[1], Marco Toscano[3], Cristian Piras[2], Carlo L. Romanò[4], Luigi Bonizzi[2], Paola Roncada[5], Lorenzo Drago[3,6].

[1] Cell and Tissue Engineering Laboratory, IRCCS Galeazzi Orthopedic Institute, Milan, Italy.

[2] Department of Veterinary Medicine (DiMeVet), University of Milan, Milan, Italy.

[3] Department of Biomedical Science for Health, University of Milan, Milan, Italy.

[4] Center for Reconstructive Surgery of Osteoarticular Infections, C.R.I.O., IRCCS Galeazzi Orthopedic Institute, Milan, Italy.

[5] Istituto Sperimentale Italiano Lazzaro Spallanzani, Cremona, Italy.

[6] Laboratory of Clinical Chemistry and Microbiology, IRCCS Galeazzi Orthopedic Institute, Milan, Italy.

[*] Corresponding Author: marta.bottagisio@grupposandonato.it

Cite

Bottagisio M, Soggiu S, Lovati AB, Toscano M, Piras C, Romanò CL, Bonizzi L, Roncada P, Drago L. Draft genome sequence of *Staphylococcus epidermidis* clinical strain GOI1153754-03-14 isolated from an infected knee prosthesis. Genome announcements. 2017. 5:e00378-17. https://doi.org/10.1128/ genomeA.00378-17.

Abstract

We announce the draft genome sequence of *Staphylococcus epidermidis* clinical strain GOI1153754-03-14 isolated for an infected orthopedic prosthesis. The reported genomic sequence will provide valuable information concerning the mechanisms of the biofilm formation on metallic implants.

Implant-related infections are the most severe complications following joint arthroplasty and represent a socioeconomic burden. Consequently, it is important to pore over the interaction between pathogens and the host immune response along with the mechanisms leading to prosthetic infections [1]. This complex process starts with bacterial contamination, adhesion and biofilm formation on the implant surface, thus conferring to bacteria a protection from both the host immune system and antibiotics [2].

Among several pathogens involved in implant-related infections, staphylococci account for 82.3% of clinically isolated bacteria. In the presence of medical devices, *S. aureus* infection accounts for 31.7 % of all isolates, while *S. epidermidis* accounts for 39 % [3].

Staphylococcus epidermidis is a commensal gram positive, coagulase negative pathogen responsible for delayed, low-grade nosocomial infections characterized by the absence of specific clinical signs and hardly distinguishable from aseptic prosthetic loosening [4, 5].

In this work, we announce the draft genome sequence of *S. epidermidis* clinical strain GOI1153754-03-14 derived from an infected knee prosthesis of a patient undergone implant revision at the Center for Reconstructive Surgery of Osteoarticular Infections (C.R.I.O., IRCCS Galeazzi Orthopedic Institute, Milan, Italy), and isolated at the Laboratory of Clinical Chemistry and Microbiology (IRCCS Galeazzi Orthopedic Institute, Milan, Italy).

The antimicrobial susceptibility and minimum inhibitory concentration (MIC) of this strain were carried out on Vitek2 System (Biomerieux, Craponne, France), displaying resistance to benzylpenicillin (MIC $\geq$ 0.5 μg/ml), oxacillin, cefazolin, rifampicin and levofloxacin (MIC $\geq$ 4 μg/ml) [6].

Genomic DNA from bacterial culture was extracted using the Bacterial Genomic DNA Isolation Kit (Norgen Biotek Corp., Thorold, ON, Canada) according to the manufacturer's guidelines, and quantified through the NanoDrop 2000 UV-Vis Spectrophotometer (Thermo Fisher Scientific Inc., Waltham, MA, USA).

Libraries were prepared by means of the ThruPLEX DNA-seq (Rubicon Genomics, Ann Arbor, MI, USA). The isolate was sequenced on the Illumina MiSeq platform through the MiSeq Reagent Kit v3 (600-cycles) to produce 300 bp paired-end reads (Illumina Inc., San Diego, CA, USA).

The outputs were quality-trimmed using ERNE-Filter [7] into 51 contigs (Average = 50,720.6 Mb; Max = 280,473 Mb; Min = 633 Mb) with 396X fold average coverage. The combined length of the

contigs was 2,586,753 bp with a GC content of 31.84% and an N50 value of 7 bp. Gene annotations were performed thorough the RAST software [8], resulting in a total of 2,467 protein-encoding genes and 64 RNAs (55 tRNAs and 9 rRNAs).

Since the ability of *S. epidermidis* GOI1153754-03-14 to colonize implants and to cause septic non-unions was already validated in a recent in vivo study [6], the deposition of the draft genome sequence will enable to have a deeper insight into the mechanisms of prosthetic joint infections.

Accession number(s). The genome shotgun has been deposited in DDBJ/ENA/GenBank under the accession no. FWCG01000000. The version described in this paper is the first version, FWCG01000000.

Acknowledgements

This study was supported by the Italian Ministry of Health (# RC 2016, L4083).

The Authors have no conflict of interest to declare.

References

1. Song Z, Borgwardt L, Høiby N, et al. Prosthesis infections after orthopedic joint replacement: the possible role of bacterial biofilms. Orthop Rev (Pavia). 2013. 5(2):65-71.
2. Romanò CL, Romanò D, Morelli I, et al. The Concept of Biofilm-Related Implant Malfunction and "Low-Grade Infection". Adv Exp Med Biol. 2016. in press.
3. Arciola CR, Campoccia D, Ehrlich GD, et al. Biofilm-based implant infections in orthopaedics. Adv Exp Med Biol. 2015. 830:29-46.
4. Otto M. Staphylococcus epidermidis-the 'accidental' pathogen. Nat Rev Microbiol. 2009. 7(8):555-567.
5. Trampuz A, Widmer AF. Infections associated with orthopedic implants. Curr Opin Infect Dis. 2006. 19(4):349-356.
6. Lovati AB, Romanò CL, Bottagisio M, et al. Modeling Staphylococcus epidermidis-Induced Non-Unions: Subclinical and Clinical Evidence in Rats. PLoS One. 2016. 11(1):e0147447.
7. Vezzi F, Del Fabbro C, Tomescu AI, et al. rNA: a fast and accurate short reads numerical aligner. Bioinformatics. 2012. 28(1):123-124.
8. Aziz RK, Bartels D, Best AA, et al. The RAST server: Rapid Annotations using Subsystems Technology. BMC Genomics. 2008. 9:75.

Chapter 4

Comparative proteomic analysis of *Staphylococcus epidermidis* strains in planktonic and sessile forms

- Cell and Tissue Engineering Laboratory, IRCCS Galeazzi Orthopedic Institute, Milan, Italy.
- Department of Veterinary Medicine (DiMeVet), University of Milan, Milan, Italy.
- Department of Biomedical Science for Health, University of Milan, Milan, Italy.
- Center for Reconstructive Surgery of Osteoarticular Infections, C.R.I.O., IRCCS Galeazzi Orthopedic Institute, Milan, Italy.
- Istituto Sperimentale Italiano Lazzaro Spallanzani, Cremona, Italy.
- Laboratory of Clinical Chemistry and Microbiology, IRCCS Galeazzi Orthopedic Institute, Milan, Italy.

In Progress

Introduction

Prosthetic joint replacements are widely performed orthopedic procedures, being effective therapeutic options in the case of severe osteoarthritis. Indeed, arthroplasties are characterized by high rates of success by giving long-term pain relief and by restoring joint function [1]. As population age increases, the incidence of total hip and knee arthroplasties also increase along with this global trend. In the USA alone, the number of joint replacements is currently over one million and are expected to reach four million by 2030 [1].

Despite excellent clinical results, prosthetic joint replacements have complications including persistent pain, implant loosening and infections that lead to revision surgery.

In particular, prosthetic joint infections (PJI) are one of the major causes of failure that requires the replacement of the implant and has a burdensome impact on patient quality of life and hospitalization costs [2]. PJI are usually caused by an accidental bacterial contamination which occurs in the operating room. The pathogens involved in are those able to colonize orthopedic devices and to form biofilm on the implant surface, include *Staphylococcus aureus*, *Staphylococcus epidermidis* and *Pseudomonas aeruginosa* [3]. In particular, staphylococci account for 82.3% of clinically isolated bacteria and, in the presence of medical devices, *S. aureus* isolates account for 31.7 %, while *S. epidermidis* accountfor 39 % of all isolates [4].

Recently, *S. epidermidis* has been identified as an emergent low virulence pathogen implicated in numerous nosocomial infections associated with medical devices (e.g. catheters, pacemakers, metal implants etc.) [5]. *S. epidermidis* is a commensal Gram positive, coagulase negative bacteria and, depending on the biological context in which it grows, it could be either a symbiont or a pathogen implicated in delayed infection characterized by the absence of specific clinical signs barely distinguishable from aseptic prosthetic failure [6]

In contrast to *S. aureus*, *S. epidermidis* does not encode many pathogenicity islands and its major virulent property is the ability to establish organized communities which regulate the expression of genes involved in survival mechanisms and biofilm formation on implants [7, 8]. Indeed, biofilm confers a protective niche to *S. epidermidis* in which sessile bacteria can grow and evade host immune defenses and antimicrobial treatments, leading to the development of antimicrobial-resistant strains, such as methicillin-resistant *S. epidermidis* (MRSE) [8]. The complete pathway that regulates biofilm formation *in vivo* has been studied and divided in to four progressive steps involving the expression of specific proteins: attachment, accumulation, maturation and detachment [9]. The attachment phase is characterized by the expression of proteins related to bacterial adherence to the surface of the device (e.g. adhesins/autolysins AltE and Aea, Microbial Surface Components Recognizing Adhesive Matrix Molecules MSCRAMMs etc.). The accumulation and maturation steps are characterized by the synthesis of proteins responsible for intercellular adhesion

(Polysaccharide Intercellular Adhesin, PIA), formation of fibril-like structures (Accumulation Associated Protein, Aap) and also formation of channels to ensure the supply of nutrients and oxygen to bacteria throughout the thick biofilm (Phenol-soluble Modulins, PSMs) [7, 10]. The last phase is detachment, in which bacteria separate from the mature matrix and disperse throughout the host: this phase has a crucial evolutionary importance for the spread of the infection. An *in vivo* study demonstrated how the detachment phase depends on a well-characterized quorum-sensing system (accessory gene regulator, *agr*), through an *agr* mutant bacterial strain in a rabbit model of medical device–related infection [11].

The purpose of the present study was to analyze proteins expressed in a mature biofilm on metallic implants. Thus, the proteomic profiles of two different strains of MRSE were compared when growing in planktonic and sessile forms. The analysis of the proteins expressed under these different culture conditions after 72 hours of culture might describe both the mechanisms behind biofilm steady state and the differences between the two tested bacterial strains. Potentially, this study, based on the characterization of the regulation of prokaryotic cells, could lead to new diagnostic biomarkers or therapeutic targets to detect latent and chronic infections mediated by low virulence pathogens such as *S. epidermidis*.

Materials and Methods

MRSE isolation and phenotypic characterization

Methicillin-resistant *Staphylococcus epidermidis* GOI1153754-03-14 analyzed in this study was isolated from an infected knee prosthesis of a patient who underwent revision surgery at the Center for Reconstructive Surgery of Osteoarticular Infections (C.R.I.O., IRCCS Galeazzi Orthopedic Institute, Milan, Italy). The isolate was subsequently characterized at the Laboratory of Clinical Chemistry and Microbiology of the IRCCS Galeazzi Orthopedic Institute (Milan, Italy).

The phenotypic characterization of the microorganism was performed by means of VITEK2 System (Biomerieux) using the card AST 632 specific for staphylococci. This evaluation defined the antimicrobial susceptibility of the strain along with the minimum inhibitory concentration (MIC) of a panel of antibiotics.

Furthermore, the capability of the MRSE GOI1153754-03-14 to produce biofilm was tested *in vitro* according to a spectrophotometric assay [12]. Briefly, a 0.5 McFarland suspension was prepared and 20 µl were inoculated in 96-well plates containing 180 µl of Tryptose Soy Broth (TSB; BioMérieux). Wells containing 200 µl of TSB were used as negative controls. After a 48-hour incubation at 37°C, wells were washed with phosphate buffered saline (PBS; Gibco) to remove floating bacteria not embedded in the biofilm. The biofilm was dried under a laminar flow hood and, subsequently, 200 µl of 5% crystal violet solution (Merck) were added into each well and incubated at room temperature (RT) for 10 minutes, then the wells were washed three times with PBS to remove any dye excess. After air-drying, the dye attached to the biofilm was solubilized using 200 µl of absolute ethanol and the optical density (OD) of each well was measured at 595 nm by using a microplate reader (Multiskan FC, Thermo Scientific). The strain was classified as a strong, moderate or weak biofilm producer [13].

MRSE genotypic characterization

The entire genome of MRSE GOI1153754-03-14 was sequenced and the sequence has been deposited at the European Nucleotide Archive (ENA) under the accession number FWCG01000000 [14]. Briefly, genomic DNA from bacterial culture was extracted using the Bacterial Genomic DNA Isolation Kit (Norgen Biotek Corp.) according to the manufacturer's guidelines, and quantified using the NanoDrop 2000 UV-Vis Spectrophotometer (Thermo Fisher Scientific Inc.). Libraries were prepared by means of ThruPLEX DNA-seq (Rubicon Genomics), then sequenced on the Illumina MiSeq platform through the MiSeq Reagent Kit v3 (600-cycles) to produce 300 bp paired-end reads (Illumina Inc.). Outputs were quality-trimmed using ERNE-Filter [15] and the sequence assembled with CLC assembly cell software (Qiagen). Finally, gene annotation was performed using RAST software [16].

Comparative genome analyses

Comparative genome analysis was first carried out by means of *BLAST* (Basic Local Alignment Search Tool, http://blast.ncbi.nlm.nih.gov). The genome of the GOI1153754-03-14 clinical isolate was inserted as a query sequence and compared to *S. epidermidis* genome sequences deposited in GeneBank, in order to explore the mechanisms underlying GOI1153754-03-14 pathogenicity.
Moreover, the genomes of *S. epidermidis* GOI1153754-03-14 and ATCC 35984 were compared against each other to identify the conserved domains shared by the two strains using a Java-based tool called Mauve (http://asap.ahabs.wisc.edu/mauve/), able to align different genomic sequences [17]. Briefly, the sequences without contigs were loaded as input and analyzed. The output was plotted in a series of colored blocks each representing a gene, making it easier to visualize the conserved regions among the genome.

Planktonic and sessile culture of MRSE GOI1153754-03-14 and ATCC 35984

GOI1153754-03-14 and ATCC 35984 MRSE were cultured both in their planktonic and sessile forms. Planktonic cultures were grown in triplicate under vigorous agitation (200 rpm) in Brain Heart Infusion broth (BHI, Biomerieux) at 37°C under aerobic conditions. After 72 hours, the bacterial suspensions were centrifuged at 3000 rpm for 10 minutes at 4°C in order to collect triplicate 50 mg bacterial pellets. The cell pellets were carefully washed six times with ice-cold PBS and, after the removal of the supernatant, the pellets were stored at -20 °C until use.
To obtain sessile culture samples, bacteria were grown on sandblasted titanium disks to mimic bacterial biofilm formation on prosthetic implants, as previously reported [2]. Briefly, sterile sandblasted titanium disks (Ø 25 mm; thickness 5 mm) (Adler Ortho, Italy; batch J04051) were incubated in six-well plates containing 5 ml of fresh BHI and approximately 1.5 x 10^8 CFU/ml of MRSE GOI1153754-03-14 or ATCC35984. Plates were then incubated at 37°C under aerobic conditions for 72 hours. At the end of the experiment, the titanium disks were washed three times with ice-cold PBS and scraped with a sterile silicone cell scraper (VWR International) on ice. The bacterial suspensions were centrifuged and washed as previously described in order to collect triplicate 50 mg bacterial pellets. All the samples were then stored at -20°C for later analysis.

Protein extraction and quantification

The bacterial pellets obtained from the planktonic and sessile cultures of MRSE GOI1153754-03-14 and ATCC 35984 were suspended at a 1:10 (w/v) ratio in rehydration buffer containing 7M urea, 2M thiourea, 2% 3-[(3-Cholamidopropyl) dimethylammonio]-1-propanesulfonate hydrate (CHAPS) supplemented with a mix of protease inhibitors and nucleases (GE healthcare), according to the manufacturer's instructions. The samples were processed using six cycles of 60 sec bead beating at 4000 rpm (MiniLys, Bertin Technologies) using 0.1 mm Zirconium Silica beads

(BioSpec USA), added in the ratio of 1:1 (w/v) to the pellet suspension. Bead beating was interspersed by 5 min cooling on ice and 5 min centrifugation at 2°C and 20000 g. After the bead beating cycles, the samples were centrifuged at 20000 g at 2°C for 30 min. Supernatants were collected and the protein concentration in the samples was determined using the Bradford assay (BioRad Protein Assay). Absorbance was measured using a spectrophotometer (Gene Quant 100, GE Healthcare) at 595 nm. The extracted proteins were stored at -80°C for later analysis.

2-DE

Proteins were separated using two-dimensional electrophoresis (2-DE). For the isoelectric focusing (IEF) step, immobilized pH gradient (IPG) polyacrilamide gel strips (GE Healthcare, 7 cm, pH 4.0-7.0) and Protean IEF Cell (Bio Rad) were utilized. Prior to IEF, 100 µg of protein sample was dissolved in a solution containing 7 M urea, 2 M thiourea, 2% w/v CHAPS, 30 mM DTT, 0.5% w/v ampholine (pH 3.5-10.0) and 1% w/v bromophenol blue. IPG strips were first actively rehydrated in the presence of the sample at 50 V and 20°C for 16 h. After the rehydration step, paper wicks soaked in milliQ water (8 µl) were placed between the cathode, the anode and the gel strip to prevent the burning of the strips caused by high voltage. The voltage was gradually increased according to the following protocol: 100 V (4 h), 250 V (2 h), 5000 V (5 h), 5000 V until the cumulative voltage reached 50 kVhand a maximum current of 50 µA per gel strip. Following IEF, each strip was chemically reduced for 15 min in 5 ml of solution containing 6 M urea, 2% w/v SDS, 50 mM Tris-HCl buffer, pH 8.8 and 30% v/v Glycerol with 1% w/v DTT added, and then alkylated in 5 ml of the same solution with 2.5% w/v of IAA added in place of DTT. IPG strips were then briefly washed in 1x running buffer (25 mM Tris-HCl, pH 8.8, 192 mM glycine, 0.1% w/v SDS), loaded onto 10% w/v polyacrylamide gels along with the protein ladder and fixed in place with 0.5% w/v low melting point agarose. The second dimension was carried out in a Mini-Protean Tetra system (Bio Rad). In the first step of electrophoresis, 8 mA per gel were applied for 15 min until the bromophenol blue front line entered the gel . In the second step, 16 mA per gel were applied until the bromophenol blue front line reached the bottom of the gel. Gels were left overnight to stain in 100 ml of Coomassie Blue G-250 solution (Sigma-Aldrich).

Image acquisition and analysis

2-DE maps were acquired using a flatbed densitometer (ImageScanner III, GE Healthcare, Uppsala). Variations in protein expression were analyzed using the Progenesis SameSpots 4.6 (Nonlinear Dynamics, UK). The module for 2-DE gel analysis was used which aligns images, removes and detects background, normalizes and matches spots.

Protein identification

Protein identification was carried out as described [18]. Briefly, analysis was performed on an Ultraflex III MALDI-TOF/TOF spectrometer (Bruker-Daltonics) in positive reflectron mode. For the external calibration, the standard peptide mixture calibration (Bruker-Daltonics: m/z: 1046.5418, 1296.6848, 1347.7354, 1619.8223, 2093.0862, 2465.1983, 3147.4710) was used. To select monoisotopic peptide masses, mass spectra were analyzed with FlexAnalysis 3.3 software (Bruker-Daltonics). After an internal calibration (known autolysis peaks of trypsin, m/z: 842.509 and 2211.104) and exclusion of contaminant ions (known matrix and human keratin peaks), the created peak lists were analyzed by MASCOT v.2.4.1 algorithm (www.matrixscience.com) against SwissProt 2017_06 database restricted to *Staphylococcus epidermidis* taxonomy (20238 sequences). For the database search, the following parameters were established: carbamidomethylation of cysteines and oxidation on methionines (set respectively among fixed and variable modifications) one missed cleavage site for trypsin and maximal tolerance established at 70 ppm. For protein identification assignment only Mascot scores higher than 56 were considered significant ($p < 0.05$). To confirm the identification obtained, MS/MS spectra were acquired by switching the instrument in LIFT mode with $4–8 \times 10^3$ laser shots using the instrument calibration file. For fragmentation, precursor ions were manually selected and the precursor mass window was automatically set. For each MS/MS spectra acquired, spectra baseline subtraction, smoothing (Savitsky–Golay) and centroiding were operated using Flex-Analysis 3.3 software. The following parameters were used for the database search: among fixed and variable modifications, carbamidomethylation of cysteines and oxidation on methionine, maximum of one missed cleavage and the mass toleranceset to 50 ppm for precursor ions and to a maximum of 0.4 Da for fragments. The taxonomy was restricted to *Staphylococcus epidermidis* (20238 sequences). The confidence interval for protein identification was set to 95% ($p < 0.05$) and only peptides with an individual ion score above the identity threshold were considered correctly identified.

Statistical analysis

Statistical analysis was performed using the Progenesis Stats module on log-normalized volumes for all spots. The progenesis stats module automatically performs a One-way ANOVA on each spot to evaluate the *p value* between different groups, p-values under 0.05 were considered statistically significant.

Multiple comparisons among groups were analyzed using two-way ANOVA (Prism 5, GraphPad) and then corrected with Tukey's post hoc test. All data are expressed as means ± standard deviation (SD). Values of $p < 0.05$ were considered statistically significant.

Results

Phenotypic and genotypic characterization of MRSE GOI1153754-03-14

Antimicrobial susceptibilities along with the MIC values of *S. epidermidis* GOI1153754-03-14 are reported in Table 1.

Table 1. Antimicrobial susceptibilities and MIC values of MRSE GOI1153754-03-14

Antibiotic	Antimicrobial susceptibility	MIC (µg/ml)
Benzylpenicillin	Resistant	≥ 0.5
Oxacillin	Resistant	≥ 4.0
Levofloxacin	Resistant	4
Rifampicin	Resistant	≥ 4.0
Gentamicin	Susceptible	≤ 0.5
Erythromycin	Susceptible	≤ 0.25
Clindamycin	Susceptible	≤ 0.12
Linezolid	Susceptible	1
Daptomycin	Susceptible	0.25
Teicoplanin	Susceptible	4
Vancomycin	Susceptible	≤ 0.5
Tetracycline	Susceptible	≤ 1
Tigecycline	Susceptible	≤ 0.12
Fusidic acid	Susceptible	≤ 0.5
Trimethoprim	Susceptible	≤ 10
Sulfamethoxazole	Susceptible	≤ 10

The study of antimicrobial susceptibilities enable the comparison of the clinical isolate with that of ATCC 35884, showing comparable MIC values especially for vancomycin susceptibility [19].

The spectrophotometric assay demonstrated the ability of the clinical isolate to form biofilm *in vitro*. Based on the obtained OD values (OD/ODc = 6.38, where ODc is the OD cut-off as three SD above the mean OD of the negative control [13]), the clinical isolate was classified as a strong biofilm producer.

Whole genome sequencing resulted in the identification 51 contigs in GOI1153754-03-14 (Average = 50,720.6 Mb) with 396X fold average coverage. In Table 2 the genome characteristics of the clinical isolate GOI1153754-03-14, compared to those of ATCC 35984 already reported in the

literature, are summarized [20].

Table 2. Comparison of genome characteristics of *S. epidermidis* GOI1153754-03-14 and ATCC 35984

	GOI1153754-03-14	**ATCC 35984**
Genome Size (bp)	2,586,753	2,616,530
C+G Content (%)	31.84	32.15
N° Genes	2,467	2,562
N° rRNA	9	19
N° tRNA	55	61
Accession Number	FWCG01000000	CP000029
Reference	[14]	[20]

Comparative genome analyses

The genome sequences of *S. epidermidis* GOI1153754-03-14 (query sequence) and ATCC 35984 (reference strain) were first compared against each other by means of BLAST software. The obtained alignment score is reported in Table 3.

Table 3. Alignment scores elaborated by BLAST algorithm.

Max score	**Total score**	**Query cover**	**E value**	**Identities**	**Ident**	**Gaps**
3.123×10^5	4.969×10^6	90%	0.0	169324/169429	99%	11/169429 (0%)

The alignment scores revealed a high homology of the genomic sequences of the two *S. epidermidis* strains, with a significant E value (E value < 0.05).

To visualize the homologous regions shared by *S. epidermidis* GOI1153754-03-14 and ATCC 35984, the genomes were analyzed by means of Mauve software and the output is reported in Figure 1.

The upper part of the output is the ATCC 35984 genomic sequence, while the lower part is GOI1153754-03-14. Blocks belonging to the clinical isolate below the center line indicate regions that align in the reverse complement (inverse) orientation. White parts represent not aligned regions or genomic areas that are not shared by the two strains.

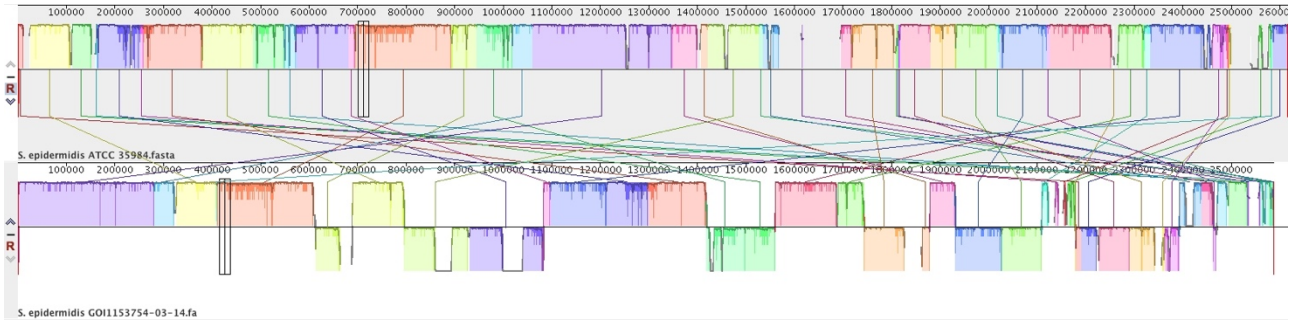

Figure 1. Mauve alignment of S. epidermidis GOI1153754-03-14 and ATCC 35984 genome.

Protein identification through 2-DE coupled with MALDI TOF/TOF MS

The proteins differently expressed among *S. epidermidis* GOI1153754-03-14 and ATCC 35984 in their planktonic and sessile forms were subsequently identified.

All the 2D maps resolved approximately 573±10 protein spots. From gel imaging analysis, a total of 7 proteins were found to be differentially expressed in planktonic and sessile bacteria in the two *S. epidermidis* strains (p<0.05) (Figure 2). In particular, 3 of the analyzed proteins were up-regulated and 4 down-regulated in biofilm forming *S. epidermidis*.

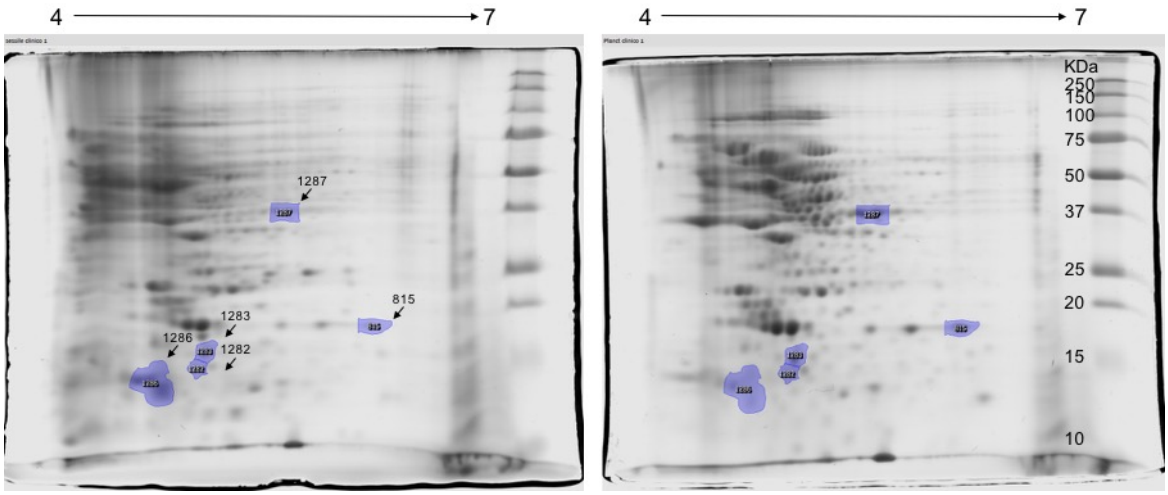

Figure 2. Two representative 2D gels showing differentially expressed proteins after Coomassie Blue staining. Numbers refer to proteins identities on the gels.

The list of the identified proteins is reported in Table 4, along with their expected molecular weights and isoelectric points, and the obtained Mascot scores; the quantification of the differentially expressed proteins according to the strain and culture conditions are presented in Figure 3.

Table 4. List of the identified proteins along with their UniProt accession numbers, expected molecular weights (kDa) and isoelectric points (pH) and Mascot scores.

Spot N°	UniProt code	Protein name	Exp-Mass (Da)	Exp. p*I*	Mascot PMF score	Mascot MS/MS score
815	Q5HNJ5	Putative universal stress protein	18469	5.44	103	120
1282	Q5HQR8	Organic hydroperoxide resistance protein-like 1	15459	4.70	66	70
1283	Q5HM88	S-ribosylhomocysteine lyase	17806	5.09	59	86
571286	Q5HP76	Nucleoside diphosphate kinase	16749	5.68	88	86
1287	Q5HRD6	Alcohol dehydrogenase	36834	5.00	92	86

Among the differentially expressed proteins, the putative universal stress protein (Y1273_STAEQ - Q5HNJ5), a cytoplasmic protein expressed by the gene SERP1273 of *S. epidermidis* ATCC 35984, was identified. Y1273_STAEQ is physiologically expressed in response to stress conditions such as starvation, temperature shock, or in response to the presence of inhibitory agents [21]. This protein was significantly downregulated in both *S. epidermidis* GOI1153754-03-14 and ATCC 35984 in sessile forms ($p<0.05$ and $p<0.001$, respectively). Interestingly, the planktonic culture of ATCC 35984 had a a significant increase in the expression of this protein compared to the clinical isolate grown under the same culture conditions ($p<0.01$).

Similarly, organic hydroperoxide resistance protein-like 1 (OHRL1_STAEQ - Q5HQR8), another cytoplasmic protein expressed by the gene SERP0480 in response to oxidative stress, was downregulated in both *S. epidermidis* strains when grown in sessile forms.

Another downregulated protein expressed by both sessile bacteria was S-ribosylhomocysteine lyase (LUXS_STAEQ - Q5HM88). This protein is secreted by bacteria in response to an increase in cell density, by a mechanism called quorum sensing (QS). Through QS, bacteria can modulate their phenotype regulating gene expression in response to stress. LuxS was particularly downregulated

in biofilm forming *S. epidermidis* ATCC 35984 when compared to its planktonic counterpart (p<0,001).

Of the three proteins which showed increased expression as a result of biofilm development, nucleoside diphosphate kinase (NDK_STAEQ - Q5HP76) was identified. This housekeeping enzyme was particularly upregulated in the sessile clinical isolate both when compared to its planktonic counterpart and when compared to sessile ATCC 35984 ($p<0.001$ and $p<0.01$, respectively). Ndk is a highly conservative bacterial protein with a crucial role in the biosynthesis of nucleoside triphosphates and in the synthesis of polysaccharides [22, 23].

Finally, among the differentially expressed proteins, we identified the alcohol dehydrogenase (ADH_STAEQ - Q5HRD6), a protein involved in different biological pathways such as glycolysis, gluconeogenesis, fatty acid and naphthalene degradation, biosynthesis of secondary metabolites in diverse environments and degradation of aromatic compounds [24]. Once again, this protein was downregulated in both *S. epidermidis* GOI1153754-03-14 and ATCC 35984 in the sessile forms (p<0.001 and p<0.05, respectively).

Unfortunately, we were not able to identify the other two proteins upregulated both in sessile *S. epidermidis* GOI1153754-03-14 and ATCC 35984 (data not shown).

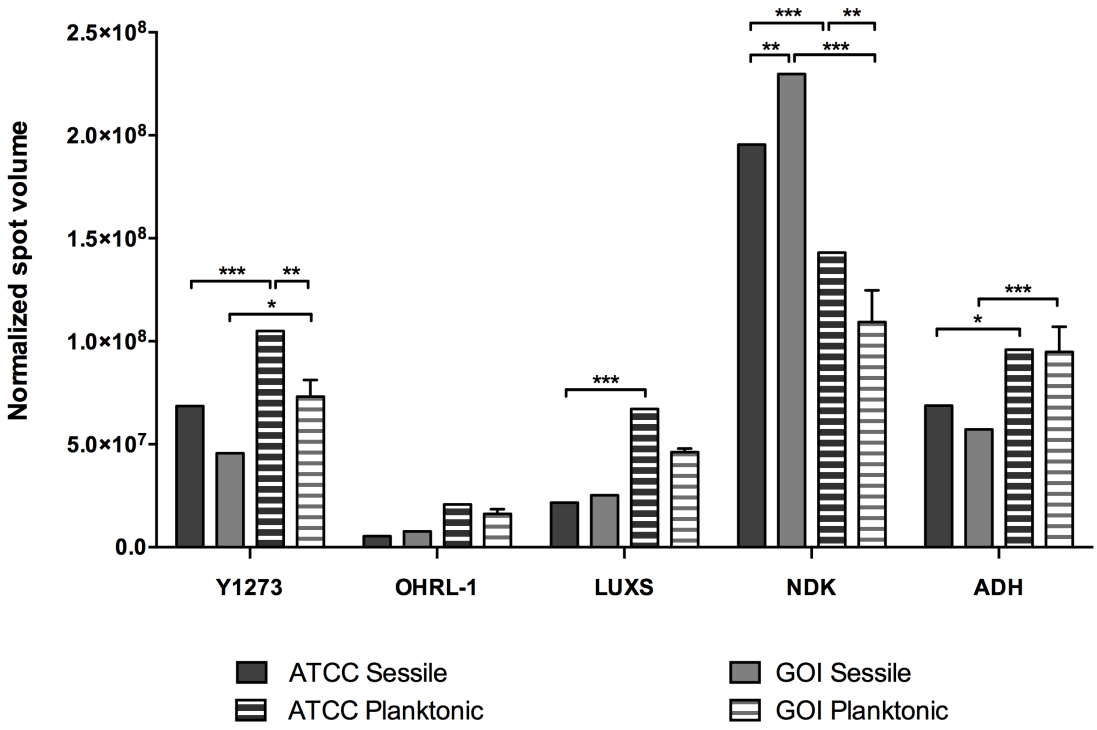

Figure 3. Quantification of the identified proteins. The histograms represent the normalized volumes of the spots determined by Progenesis SameSpots software. Data are expressed as mean ± SD. Statistical significance for p<0.05 (*), p<0.01 (**) and p<0.001 (***).

Discussion

Although staphylococcal biofilms have been extensively studied, it is a common erroneous belief that cells within the biofilm matrix are exposed to the same external conditions [25]. Biofilm is a dynamic system in constant development that permits the survival of bacteria in hostile environments [26]. The structure of mature biofilms is complex and well-organized; there are channels providing nutrients to cells that circulate through the biofilm matrix [27], and bacteria in different regions of the same matrix might exhibit different gene expression patterns according to their exposure to external agents [28].

As staphylococcal biofilms mature, it is well-known that the QS regulated expression of the *agr* dependent system leads to the release of individual cells [9]. However, biofilm can protect bacteria for long periods of time quietly without being detected by the host immune system. In this particular scenario, it is challenging to define therapeutic targets or diagnostic biomarkers to detect latent or chronic infection mediated by low virulence, biofilm forming bacteria, as *S. epidermidis*.

In the present work, mature biofilms of two different *S. epidermidis* strains were studied using a proteomic approach to evaluate the induction or repression of individual proteins, as a result of sessile or planktonic culture. The obtained data revealed that many changes in protein expression in both *S. epidermidis* strains occurred when planktonically cultured. In particular, the analysis of the proteins expressed by planktonic bacteria revealed results linked to bacterial stress, also reported elsewhere in the literature [29]. Indeed, the upregulation of the putative universal stress protein (Q5HNJ5) is a common response to stress, probably due to elevated cell density in the culture media after 72 hours incubation [29]. The universal stress protein A (uspA) superfamily is a conserved group of proteins expressed in many different species such as bacteria, fungi, Archaea and insects [21]. A high cell density in a close environment without renewed nutrient supplies inevitably provokes an alteration of physiological cell balance; harsh conditions such as nutrient deprivation, pH decrease, exposure to oxygen and nitrogen species predictably lead to global stress responses [30].

Based on these assumptions, the higher expression of Ohrl-1 (Q5HQR8) and LuxS (Q5HM88) in *S. epidermidis* when planktonically cultured can be explained in light of stress. Ohrl-1 (Q5HQR8) is a highly conserved protein identified in many different bacterial species, such as *Bacillus subtilis* [31], *Pseudomonas aeruginosa* [32], *Actinobacillus pneumoniae* [33], etc. This protein belongs to the peroxiredoxin family, considered to be the primary cellular protector against oxidative stress in all living organisms, detoxifying organic peroxides while favoring microbial survival [34]. Indeed, staphylococci evolved many oxidative defense strategies that allow them to face the near constant challenge of surviving in the presence of exogenous and endogenous oxidants [35].

As cell density increases, the QS system is activated in order to coordinate the expression of

different genes in response to cell density through small signaling molecules, called autoinducers (AIs) [36].

LuxS (Q5HM88) is involved in the synthesis of the autoinducer-2, a QS signaling pheromone expressed both by Gram positive and negative bacteria [37]. The mechanisms of LuxS activation and regulation are still unclear [38], however, its upregulation is known to be closely connected to QS stress [39, 40]. The lack of LuxS enzyme in humans made this protein an attractive target for new therapeutic agents [41], however inhibitors of LuxS enzymes actively increase the virulence of *S. epidermidis*, increasing their ability to form biofilm [36]. Indeed, in *S. epidermidis*, the LuxS system negatively affects the expression of polysaccharide intracellular adhesin (PIA) and, consequently, the synthesis of extracellular matrix [42].

Among the downregulated proteins expressed by sessile *S. epidermidis*, we also identified Adh (Q5HRD6). In the literature, there a little information concerning the role of Adh in planktonic cells, however there is some evidence of increased Adh expression in *Candida albicans* cells grown in suspension compared to biofilm forming cells [43]. Moreover, Mukherjee and colleagues reported that the inhibition of this enzyme leads to greater biofilm production *in vitro*.

In contrast to the upregulation of stress-related proteins found in planktonic bacteria, biofilm forming *S. epidermidis* demonstrated a superior resistance to various stress conditions during 72 hours of culture. This phenomenon can be easily explained by the protection that the self-produced EPS matrix confers to sessile bacteria [44]. After 72 hours of static culture on titanium disks, both *S. epidermidis* GOI1153754-03-14 and ATCC 35984 were metabolically active, which we can assume by the upregulation of the nucleoside diphosphate kinase (Ndk, Q5HP76). The main role of Ndk is the biosynthesis of nucleoside triphosphates other than ATP (CTP, UTP and GTP) (UniRule: UR000089065). Due to its housekeeping function, Ndk is a highly conserved enzyme that can be found in both eukaryote and prokaryote cells [45]. Furthermore, in addition to its phosphotransferase activity, Ndk plays an active role in bacterial virulence. As reported by Yu and colleagues [23], depending on its intracellular or extracellular expression, it can suppress a series of host defense mechanisms (e.g. phagocytosis, inflammatory response, cell death, etc.) or can have a cytotoxic effect on host cells.

Unfortunately, the two proteins that were not identified in this study were both upregulated in sessile *S. epidermidis* GOI1153754-03-14 and ATCC 35984. The inability to identify the proteins was probably due to the very low amount expressed during the experimental conditions which fell below the limit of detection of the instrument. Along with the need to identify these spots, there is also the need to verify if upregulation of the stress-related proteins in planktonic *S. epidermidis* is related to the choice of a late sample time point.

For this reason, a future study involving proteomic analysis of *S. epidermidis* GOI1153754-03-14 and ATCC 35984 performed at different time points may overcome limitation due to the cell density.

References

1. Cooper H.J. Emerging applications of proteomics in hip and knee arthroplasty. Expert Review of Proteomics, 2015 11:1, 5-8.
2. Drago L, Romanò CL, Mattina R, et al. Does dithiothreitol improve bacterial detection from infected prostheses? A pilot study. Clin Orthop Relat Res. 2012 Oct;470(10):2915-25.
3. Trampuz A, Widmer AF. Infections associated with orthopedic implants. Curr Opin Infect Dis 2006;19:349–356
4. Arciola CR, D, Ehrlich GD, Montanaro L. Biofilm-based implant infections in orthopaedics. Adv Exp Med Biol 2015 830:29-46.
5. Ziebuhr, W., Hennig S, Eckart M, et al. Nosocomial Infections by Staphylococcus epidermidis: How a Commensal Bacterium Turns into a Pathogen. International Journal of Antimicrobial Agents 2006. 28(1):14-20.
6. Lovati AB, Bottagisio M, de Vecchi E, et al. Animal Models of Implant-Related Low-Grade Infections. A Twenty-Year Review. Adv Exp Med Biol. 2016 Oct 9.
7. Fey PD, Olson ME. Current concepts in biofilm formation of Staphylococcus epidermidis. Future Microbiol. 2010 5(6): 917-933.
8. Patel, R. Biofilms and Antimicrobial Resistance. Clinical Orthopaedics and Related Research 2005. 437:41-47.
9. Otto M. Staphylococcal Biofilms. Curr Top Microbiol Immunol. 2008;322: 207–228.
10. Büttner H, Mack D, Rohde H. Structural basis of Staphylococcus epidermidis biofilm formation: mechanisms and molecular interactions. Front Cell Infect Microbiol. 2015 Feb 17;5:14.
11. Vuong C, Kocianova S, Yao Y, et al. Increased colonization of indwelling medical devices by quorum-sensing mutants of Staphylococcus epidermidis in vivo. J Infect Dis. 2004 Oct 15;190(8):1498-505.
12. Christensen GD, Simpson WA, Younger JJ, et al. Adherence coagulase-negative staphylococci to plastic tissue culture plates: a quantitative model for the adherence of staphylococci to medical devices. J Clin Microbiol 1985; 22:996–1006.
13. Stepanovic S, Vukovic D, Dakic I, et al. A modified microtiter-plate test for quantification of staphylococcal biofilm formation. Microbiol Methods 2000; 40:175–179.
14. Bottagisio M, Soggiu A, Lovati AB, et al. Draft genome sequence of Staphylococcus epidermidis clinical strain GOI1153754-03-14 isolated from an infected knee prosthesis. Genome Announcements 2017.
15. Vezzi F, Del Fabbro C, Tomescu AI, et al. rNA: a fast and accurate short reads numerical aligner. Bioinformatics 2012. 28(1):123-124.
16. Aziz RK, Bartels D, Best AA, et al. The RAST server: Rapid Annotations using Subsystems Technology. BMC Genomics 2008. 9:75.
17. Darling AE, Mau B, Perna NT. progressiveMauve: multiple genome alignment with gene gain, loss and rearrangement. PLoS One. 2010 Jun 25;5(6):e11147.
18. Piras C, Soggiu A, Greco V, et al. Mechanisms of antibiotic resistance to enrofloxacin in uropathogenic Escherichia coli in dog. J Proteomics. 2015 8;127(Pt B):365-76.

19. Curtin J, Cormican M, Fleming G, et al. Linezolid compared with eperezolid, vancomycin, and gentamicin in an in vitro model of antimicrobial lock therapy for Staphylococcus epidermidis central venous catheter-related biofilm infections. Antimicrob Agents Chemother. 2003 Oct;47(10):3145-8.
20. Gill SR, Fouts DE, Archer GL, et al. Insights on evolution of virulence and resistance from the complete genome analysis of an early methicillin-resistant Staphylococcus aureus strain and a biofilm-producing methicillin-resistant Staphylococcus epidermidis strain. J Bacteriol. 2005 Apr;187(7):2426-38.
21. Kvint K, Nachin L, Diez A, et al. The bacterial universal stress protein: function and regulation. Curr Opin Microbiol. 2003 Apr;6(2):140-5.
22. Yu H, Xiong J, Zhang R, et al. Ndk, a novel host-responsive regulator, negatively regulates bacterial virulence through quorum sensing in Pseudomonas aeruginosa. Sci Rep. 2016 Jun 27;6:28684.
23. Yu H., Rao X., Zhanga K. Nucleoside diphosphate kinase (Ndk): A pleiotropic effector manipulating bacterial virulence and adaptive responses. Microbiological Research Volume 205, December 2017, Pages 125-134.
24. Reid MF, Fewson CA. Molecular characterization of microbial alcohol dehydrogenases. Crit Rev Microbiol. 1994;20(1):13-56.
25. Coenye T. Response of sessile cells to stress: from changes in gene expression to phenotypic adaptation. Pathogens and Disease Volume 59, Issue 3 August 2010 Pages 239–252.
26. Costerton JW, Stewart PS, Greenberg EP. Bacterial biofilms: a common cause of persistent infections. Science. 1999 May 21;284(5418):1318-22.
27. Donlan RM. Biofilms: microbial life on surfaces. Emerg Infect Dis. 2002 Sep;8(9):881-90.
28. Stewart PS, Franklin MJ. Physiological heterogeneity in biofilms. 2008 Nat Rev Microbiol 6:199-210.
29. Ayarza JM, Mazzella MA, Erijman L. Expression of stress-related proteins in Sediminibacterium sp. growing under planktonic conditions. J Basic Microbiol. 2015 Sep;55(9):1134-40.
30. Foster PL. Stress-induced mutagenesis in bacteria. Crit Rev Biochem Mol Biol. 2007 Sep-Oct;42(5):373-97.
31. Fuangthong M, Atichartpongkul S, Mongkolsuk S, et al. OhrR is a repressor of ohrA, a key organic hydroperoxide resistance determinant in Bacillus subtilis. J Bacteriol. 2001 Jul;183(14):4134-41.
32. Ochsner UA, Hassett DJ, Vasil ML. Genetic and physiological characterization of ohr, encoding a protein involved in organic hydroperoxide resistance in Pseudomonas aeruginosa. J Bacteriol. 2001 Jan;183(2):773-8.
33. Shea RJ1, Mulks MH. ohr, Encoding an organic hydroperoxide reductase, is an in vivo-induced gene in Actinobacillus pleuropneumoniae. Infect Immun. 2002 Feb;70(2):794-802.
34. Cao Z, Lindsay JG. The Peroxiredoxin Family: An Unfolding Story. Subcell Biochem. 2017;83:127-147.
35. Gaupp R, Ledala N, Somerville GA. Staphylococcal response to oxidative stress. Front Cell Infect Microbiol. 2012 Mar 16;2:33.
36. Xu L, Li H, Vuong C, Vadyvaloo V, et al. Role of the luxS quorum-sensing system in biofilm formation and virulence of Staphylococcus epidermidis. Infect Immun. 2006 Jan;74(1):488-96.
37. Kırmusaoğlu S. Staphylococcal Biofilms: Pathogenicity, Mechanism and Regulation of Biofilm Formation by Quorum-Sensing System and Antibiotic Resistance Mechanisms of Biofilm-Embedded

Microorganisms. Immunology and Microbiology » "Microbial Biofilms - Importance and Applications", book edited by Dharumadurai Dhanasekaran and Nooruddin Thajuddin, ISBN 978-953-51-2436-8, Print ISBN 978-953-51-2435-1,

38. Trappetti C, Potter AJ, Paton AW, et al. LuxS mediates iron-dependent biofilm formation, competence, and fratricide in Streptococcus pneumoniae. Infect Immun. 2011 Nov;79(11):4550-8.
39. Arciola CR, Campoccia D, Speziale P, et al. Biofilm formation in Staphylococcus implant infections. A review of molecular mechanisms and implications for biofilm-resistant materials. Biomaterials. 2012 Sep;33(26):5967-82.
40. Li M, Villaruz AE, Vadyvaloo V, et al. AI-2-dependent gene regulation in Staphylococcus epidermidis. BMC Microbiol. 2008 Jan 8;8:4. doi: 10.1186/1471-2180-8-4.
41. Alfaro JF, Zhang T, Wynn DP, et al. Synthesis of LuxS inhibitors targeting bacterial cell-cell communication. Org Lett. 2004 Sep 2;6(18):3043-6.
42. Limoli DH, Jones CJ, Wozniak DJ. Bacterial Extracellular Polysaccharides in Biofilm Formation and Function. Microbiol Spectr. 2015 Jun;3(3).
43. Mukherjee PK, Mohamed S, Chandra J, et al. Alcohol dehydrogenase restricts the ability of the pathogen Candida albicans to form a biofilm on catheter surfaces through an ethanol-based mechanism. Infect Immun. 2006 Jul;74(7):3804-16.
44. Fux CA, Costerton JW, Stewart PS et al. Survival strategies of infectious biofilms. Trends Microbiol 2005 13: 34–40
45. Ray NB, Mathews CK. Nucleoside diphosphokinase: a functional link between intermediary metabolism and nucleic acid synthesis. Curr. Top. Cell. Regul., 33 (1992), pp. 343-357

General Discussion and Conclusions

Non-union fractures, as a severe failure of bone healing, are among the most difficult and challenging orthopedic complications. Non-unions represent a clinical burden, as well as a socio-economic encumbrance that decreases the quality of patients' lives and requires surgical treatment and long recovery times which increases the burden on the National Health Service. Depending on the type of surgery and depending on the health status and age of the patients, orthopedic complications can be severe; it has been estimated that fracture healing, for example, is delayed in 600,000 patients per year in the United States alone, and approximately 100,000 of the fractures result in non-unions [1]. The percentage of fractures leading to non-union is between 5 and 10% and generally occurs in long bones like tibia, femur, humerus, radius, and ulna. The triggering events leading to non-union development might be linked to old age, poor compliance with rehabilitation, smoking, alcoholism, diabetes, and immunodeficiency. Moreover, orthopedic complications might result in non-union development due to inadequate fracture treatments, like poor mechanical stability or, again, due to the administration of pharmacological agents such as steroids, ciprofloxacin, chemotherapy drugs, etc., or due to excessive movement of the patients [2]. Non-union might also be the result of severe trauma characterized by open fracture with significant bone loss, soft tissue damage and contamination, which can increase by a factor of 19 the rate of septic non-union development [3].

Furthermore, in the presence of orthopedic devices used in the case of osteosynthesis (e.g. prosthesis, wire, plate screw, etc.), the incidence of infection increases because the surface of these implants offers the perfect substrate for bacterial adhesion and growth [4]. Loss of life or limb due to infection is very rare, but still occasionally occurs. Therefore, to keep the risk as low as possible, patients undergoing orthopedic surgery are treated with antibiotics as prophylaxis. Despite prophylaxis, there is a 1-4% chance of developing a deep infection extending to the bone, surrounding soft tissues, and to the implanted medical device [5, 6]. In these cases, revision surgery is required to remove both the infected tissues and implants in order to eradicate the infection [7, 8].

Hence, there is the real need to minimize the risk of implant-related infections, emphasizing prophylaxis measures while discouraging the impairment of bone healing. Consequently, the design, development and use of preclinical models are necessary steps to investigate the pathogenesis of septic non-unions as major consequence of infection of the fracture site.

With this aim, in the first phase of the project, we developed three preclinical models of infected non-unions able to resemble the clinical features of nosocomial implant-associated infection caused by a low virulence pathogen (Chapter 1). The development of these models provides a standardized tool to study preventive and therapeutic strategies in the case of subclinical, sub-acute and chronic onset of septic non-unions.

Indeed, despite the large number of animal models of infected fractures described in the literature, there are several limitations in comparing them due to the use of different bacterial strains, concentrations and fracture stabilization methods [9]. Indeed, these studies are mainly focused on the analysis of bone repair through the assessment of critical size defects in long bones, in the presence of virulent bacteria (e.g., *S. aureus*, *Escherichia coli*, *Pseudomonas aeruginosa*, etc.) [10-14]. No models of *S. epidermidis*-mediated septic non-unions have been described so far. This variety of conditions encouraged us to focus our efforts on the development of more reproducible preclinical models to assess the role of *S. epidermidis* in the impairment of bone healing to provide relevant information to be translated to clinics [15].

There are many characteristics that distinguish a reliable animal model of septic non-union; first of all, the stabilization of the fracture. Indeed, the lack of stability of the fracture will result in the failure of bone healing even in the absence of bacteria. Therefore, in our models of septic non-unions, we used plates and screws as the fixation method to standardize the stability of fractures in order to impede uncontrolled movement that may detrimentally affect the healing process. The aforementioned method provides reproducible mechanical conditions, while minimizing the interference of the implant with surrounding soft tissues and allowing the biological response to fractures [16]. Conversely, intramedullary nails provide little stability and poorly defined biomechanical conditions for the fracture site, resulting in a less reproducible model [17].

Another important characteristic of a reliable animal model of septic non-union concerns the features of the fracture gap. In order to create reproducible fracture gaps, we performed an osteotomy with a circular saw, since it has been demonstrated that bone healing in this case is comparable to that of normal fractures [18]. Thus, the reproducibility of this model and the comparability of the results are expected to be high.

Moreover, to understand the role of bacteria in non-union development, it is important to avoid the generation of critical size bone defects. A critical size defect is defined as a bone defect that will not heal completely over the natural lifetime of an animal [19]. Hence, there is the need to develop non-unions through the establishment of an infection, rather than through a critical size bone defect.

Once the stabilization and the fracture methods were assessed, the other crucial decision was the choice of the bacterial species and strain involved in the development of this model. According to data reported by the National Health Care Safety Network, coagulase-negative staphylococci (CoNS) are the most frequent cause of implant- or surgery-associated nosocomial infections in the United State of America, and among them, the most frequently isolated CoNS is *Staphylococcus epidermidis* [20, 21]. Indeed, *S. epidermidis* has recently emerged as a common cause of nosocomial infections associated with medical devices (e.g., catheters, pacemakers, metal implants, etc.). Interestingly, *S. epidermidis* was rarely pathogenic before the advent of modern medicine and before the massive use of indwelling devices, but now it is recognized as an important human pathogen [22]. This is mainly due to its presence on healthy human skin as a commensal bacterium:

the skin of healthy people is normally colonized by 10-24 *S. epidermidis* strains at any time, notably increasing the risk of contamination during surgery [23].

S. epidermidis is commonly classified as low virulence pathogen compared to *S. aureus* since it does not encode many pathogenicity islands. Its major virulent propriety is the ability to form biofilm on implants enabling bacteria to live in a protected environment, without being affected by the host immune system. *S. epidermidis* contaminations often result in low-grade infections in which patients complain about persistent pain and/or functional impairment, with mixed positive and negative markers of infection and inflammation [9, 24].

To recreate a setting as closer as possible to clinics, a clinical methicillin-resistant *S. epidermidis* isolate (MRSE) was employed due to its ability to contaminate implants. In this regard, the most challenging aspect in designing an animal model with clinical isolates is to determine the bacterial concentration able to induce the infection with respect to the virulence of the inoculated pathogen [9]. In the first experimental phase of this project, we were able to establish three clinically different tools to study prophylactic and therapeutic strategies. In particular, we were able to demonstrate that the use of a low *S. epidermidis* concentration (10^3 CFU/inoculum) established a subclinical onset characterized by an inconsistent grade of non-union development without any signs or symptoms of infection. Animals in this group were characterized by a high variability in the development of the septic non-union because sometimes the host immune response was able to spontaneously eradicate the infection (33% of the animals). However, this model can be an important tool to analyze the signs of subclinical events in terms of pathogenesis and host response. Conversely, the injection of a high amount of *S. epidermidis* (10^8 CFU/inoculum) systematically resulted in the impairment of fracture healing caused by rapid biofilm formation on the implant surface. All the animals in this group showed signs of a chronic condition in which biofilm played a crucial part in camouflaging bacteria from the host immune system. This model of chronic non-union can be used to investigate methods to detect or disrupt mature biofilm *in vivo*.

The reduction of the bacterial load to 10^5 CFU/inoculum resulted in a sub-acute host response characterized by the presence of free cocci in the fracture site. The signs of osteomyelitis were severe, with vascular and bone damage, that affected the stability of the fracture, impairing the healing process. Sub-acute events can be reasonably controlled by preventive antimicrobial treatment, since bacteria are poorly embedded in a weak and immature extracellular matrix.

The achievements obtained in the first part of the project made it possible to evaluate different non-union preventive strategies (Chapter 2). Clinically, systemic pharmacological treatments are routinely used to prevent implant-related infections; despite this, localized strategies have several advantages including being able to deliver antibacterial agents to the injured site thus requiring lower drug dosages, and reducing systemic side effects [25]. When dealing with fracture stabilization, the local application of antibacterial coatings may be a promising approach to prevent the establishment of infections. However, the development of new antibacterial coatings for this

purpose appears extremely challenging [26]. The coating itself should not interfere with the implant osseointegration, while actively preventing bacterial adhesion during its half-life [27]. Moreover, when enriched with antibiotics, the half-life of the coating should be brief enough to prevent both biofilm formation and the development of antibiotic resistance [26]. In our experimental setting, we exploited the biodegradability and osteoinductive features of a new hydrogel enriched with vancomycin, used as a coating, to test its antimicrobial properties. In particular, we compared its use to the systemic injection of vancomycin, as the gold standard in the treatment of septic non-unions characterized by the presence of methicillin-resistant bacteria. Both the systemic injection and the local delivery of vancomycin by means of the hydrogel resulted in a good response in terms of bone healing and absence of osteomyelitis, suggesting the synergistic use of these two treatments as an effective strategy to prevent the establishment of septic non-unions [28]. Along with this possible strategy, this study aimed also at testing the feasibility of the bone marrow mesenchymal stem cells BMSCs cell therapy for this purpose.

In the last few years, cell-based therapy has achieved impressive results in the restoration of tissue function, as well as in the treatment of non-unions [29-31]. BMSCs has been used as an accessible source of progenitor cells able to differentiate in mesenchymal tissue and as a safe source, due to the lack of major histocompatibility complex II (MHC II) which permits the allogeneic transplant of these cells [32]. This important characteristic made it possible to study the role of allogeneic BMSCs in bone defect and non-union fracture in a clinical trial (ClinicalTrials.gov #NCT02307435). Furthermore, BMSCs immunomodulatory and antimicrobial features have been recently demonstrated [33-36]. Thus, we applied our rat model of sub-acute septic non-union to study the immunomodulatory effects of allogeneic BMSCs by measuring the systemic level of inflammatory cytokines and their role in the prevention of infection and bone healing. The detection of a set of mediators correlated with the septic non-union inflammatory process may promote a better understanding of the physiopathology of bone healing while offering new diagnostic biomarkers. Unfortunately, there were some limitations in our study. The intravenous injection of BMSCs caused the death of 50% of the animals due to the “pulmonary first-pass theory”, as supported by the histopathological analyses. This outcome was unpredicted, since the amount of injected BMSCs was concordant with the dose used in other preclinical and clinical studies presented in the literature [37, 38, ClinicalTrials.gov #NCT02307435] and it may be related to cell adhesion or to the activation of the coagulation pathway [38, 39]. A possible approach to reduce the risk of pulmonary embolism could be the use of vasodilators or anticoagulants in conjunction with the systemic injection of BMSCs, or again, the use of a syringe pump to slowly perfuse the solution containing the cells. However, further manipulation of BMSCs might negatively influence cell viability and function once transplanted *in vivo* [40].

Due to this drawback, data obtained by the systemic use of BMSCs are not able to support definitive conclusions and should be considered as a preliminary study, given the reduced sample size of the

group. However, it is necessary to identify an effective, time-convenient and safe administration route for BMSC transplantation, taking into consideration the risks related to the use of BMSCs in regenerative medicine (e.g., dimensions, proliferation capability, differentiation status, etc.). More importantly, it is fundamental to state in scientific publications the occurrence of animal death following a treatment in order to be aware of the risks connected with the proposed procedure.

Another limitation of the study is linked to the analysis of the serum cytokine, which is strictly correlated to the patients' health and infection status. Indeed, stress condition and the experimental time points of blood withdraws and analyses may have a crucial part in the detection of cytokine levels, eventually introducing biases in their analysis [41]. Hence, there is the need to identify new and stable markers of infections in order to target bacterial biofilm determinants, intensifying molecular research focused on biofilm-mediated infections.

The aim of the last part of my Ph.D. project was to define future diagnostic biomarkers to detect latent implant-related infections and new therapeutic targets, using a comparative proteomic study to analyze mature staphylococcal biofilms.

The investigation of the interaction between host and microorganisms is certainly difficult due to the enormous number of variables implicated. Therefore, the need to thoroughly understand the mechanisms related to biofilm-mediated infections and their pathogenesis encouraged the scientific community to pour over the causes of bone healing impairment, starting from the main cause: biofilm producing bacteria.

Through the comparison of genomes of various types of bacteria, it is possible to identify the key factors responsible for different bacterial virulence, as well as factors regulating biofilm production [22]. The success of *S. epidermidis* as a pathogen relies on its ability to adhere to foreign body surfaces and to form biofilm, causing sub-acute and chronic infections [42]. The advent of the post-genomic era rapidly advanced the understanding of microorganisms' biology. Through proteomic analyses, it is now possible to assay the expression of target genes and evaluate their modulation in accordance with different growing conditions. Sorting individual proteins from heterogeneous samples can be performed by an initial separation according to their isoelectric point followed by a second-dimension separation based on their molecular weight. The resulting two-dimensional map of proteins provides a wide-ranging view of proteins expressed under certain conditions, showing variations in the level of expression, and showing either the presence of isoforms or post-translational modifications. However, protein identification requires the availability of genomic information in public databases, such as functional annotation of sequenced genes. For this reason, in order to appropriately identify changes in the proteomic profile of the clinical isolates, the whole genome of *S. epidermidis* GOI1153754-03-14 used in our rat model of septic non-union, was sequenced through next generation sequences analysis (Chapter 3). The deposition of its genomic sequence in the ENA public database not only is important for the proteomic analysis of the specimen, but also will enable a deeper insight into the mechanisms of orthopedic infections.

Profiling the gene expression pattern of biofilm producing bacteria thorough omics science is important to decipher the genetic basis of biofilm formation. Moreover, the protection conferred by biofilm permits bacteria to quietly survive within the host for long periods of time without being detected by the immune system. In this particular scenario, defining therapeutic targets or diagnostic biomarkers is mandatory to detect latent or chronic infections mediated by low virulence, biofilm forming bacteria, such as *S. epidermidis* [43].

With the aim to define markers expressed by a mature staphylococcal biofilm on metallic implants, the proteome of *S. epidermidis* GOI1153754-03-14 was compared to that of *S. epidermidis* ATCC 35984 to evaluate the induction or repression of individual proteins as the result of sessile or planktonic cultures (Chapter 4). The analysis of the proteins expressed under these different culture conditions after 72 hours of growth can provide information regarding both the mechanisms behind biofilm steady state and the differences of the two tested bacterial strains. To recreate a mature biofilm *in vitro*, *S. epidermidis* was cultured on sandblasted titanium disks for 72 hours, according to an experimental time point set in a previous study [44]. Indeed, Drago and colleagues [44] demonstrated through confocal microscopic analysis that bacteria are able to establish a mature biofilm on titanium disks after 72 hours of culture. However, data obtained in our study revealed that many changes in protein expression in both *S. epidermidis* strains occurred when planktonically cultured. In particular, the analysis of the proteins expressed by planktonic bacteria after 72 hours revealed some unexpected results linked to bacterial stress. A high cell density in a close environment without renewed nutrients inevitably results in an alteration of the physiological cell balance; harsh conditions such as nutrient deprivation, pH decrease, exposure to oxygen and nitrogen species predictably lead to global stress responses [45]. The chosen experimental time point represents a limit of this study, but also an important clue for future analyses. Indeed, in order to compare the features of mature biofilm, there is a need to study gene expression of bacteria at different experimental time points. For this reason, proteomic analysis of *S. epidermidis* GOI1153754-03-14 and ATCC35984 at different time points may overcome these limitations due to cell density while allowing the comparison of their proteomes at the same experimental time points.

The study of regulatory mechanisms of biofilm-mediated infections may encourage the development of innovative therapeutic strategies to discourage bacterial colonization of medical devices at the molecular level. However, the presence of biofilm makes the diagnosis of infections and the subsequent selection of the apposite treatment particularly challenging [44, 46]. Biofilms may slow the metabolism of bacteria, while prolonging their survival inside the infected host, leading to chronic infections and favoring also the development of antibiotic resistances [47].

Although many efforts have been made to improve the sensitivity of tests for the diagnosis of implant-related infections, a microbiological gold standard has not yet been established. Consequently, guidelines have been discussed and proposed at national and international meetings

[48-50]. The technological progression of the field might be achieved through the standardization of the protocols in the scientific community. Hence, to promote the advancement of knowledge of the human proteome, in 2010, the Human Proteome Organization (HUPO) and the Human Proteome Project (HPP) were founded [51]. Through the alliance of independent groups of scientists whose research is focused on specific diseases or molecular processes, it will be possible to provide standardized methods and resources for mass spectrometry and to facilitate accessibility of these resources to the broader life science research and clinical communities. In the near future, the standardization of protocols along with the study of many different biofilm-forming bacterial species might make it possible to identify chronic infections thereby defining the antibiotic susceptibility profile of the bacteria involved and subsequently the best therapeutic strategy by the analysis of sera of patients.

References

1. Miranda MD, Moon MS. Treatment strategy for nonunions and malunions. Surgical treatment of orthopedic trauma. 2007. 1:77-100.
2. Imam MA, Holton J, Ernstbrunner L, et al. A systematic review of the clinical applications and complications of bone marrow aspirate concentrate in management of bone defects and nonunions. Int Orthop. 2017. Aug 13.
3. Mills L, Tsang J, Hopper G, et al. The multifactorial aetiology of fracture nonunion and the importance of searching for latent infection. Bone Joint Res. 2016 5(10):512-519.
4. Ribeiro M, Monteiro FJ, Ferraz MP. Infection of orthopedic implants with emphasis on bacterial adhesion process and techniques used in studying bacterial-material interactions. Biomatter. 2012 2(4):176-94.
5. Boxma H, Broekhuizen T, Patka P, et al. Randomised controlled trial of single-dose antibiotic prophylaxis in surgical treatment of closed fractures: the Dutch Trauma Trial. Lancet. 1996. 27;347(9009):1133-1137.
6. Trampuz A, Widmer AF. Infections associated with orthopedic implants. Curr Opin Infect Dis. 2006. 19:349–356.
7. Pelser P. Management of septic non-unions. SA Orthopaedic Journal. 2009. 8.2: 29-34
8. Bhatia C, Tiwari AK, Sharma SB, et al. Role of antibiotic cement coated nailing in infected nonunion of tibia. Malays Orthop J. 2017. 11(1):6-11.
9. Lovati AB, Bottagisio M, de Vecchi E, et al. Animal Models of Implant-Related Low-Grade Infections. A Twenty-Year Review. Adv Exp Med Biol. 2017;971:29-50.
10. Alt V, Lips KS, Henkenbehrens C, et al. A new animal model for implant-related infected non-unions after intramedullary fixation of the tibia in rats with fluorescent in situ hybridization of bacteria in bone infection. Bone 2011;48:1146–1153.
11. Chen X, Tsukayama DT, Kidder LS, et al. Characterization of a chronic infection in an internally-stabilized segmental defect in the rat femur. J Orthop Res 2005;23:816–823.
12. Chen X, Schmidt AH, Tsukayama DT, et al. Recombinant human osteogenic protein-1 induces bone formation in a chronically infected, internally stabilized segmental defect in the rat femur. J Bone Joint Surg [Am] 2006;88A:1510–1523.
13. Chen X, Schmidt AH, Mahjouri S, et al. Union of a chronically infected internally stabilized segmental defect in the rat femur after debridement and application of rhBMP-2 and systemic antibiotic. J Orthop Trauma 2007;21:693–700.
14. Sanchez CJ Jr, Prieto EM, Krueger CA, et al. Effects of local delivery of D-amino acids from biofilm-dispersive scaffolds on infection in contaminated rat segmental defects. Biomaterials 2013;34:7533–7543.
15. Lovati AB, Romanò CL, Bottagisio M, et al. Modeling Staphylococcus epidermidis-Induced Non-Unions: Subclinical and Clinical Evidence in Rats. PLoS One. 2016 21;11(1):e0147447.
16. Histing T, Garcia P, Matthys R, et al. An internal locking plate to study intramembranous bone healing in a mouse femur fracture model. J Orthop Res. 2010 28(3):397-402.

17. Kaspar K, Matziolis G, Strube P, et al. A new animal model for bone atrophic nonunion: fixation by external fixator. J Orthop Res. 2008 26(12):1649-55.
18. Dumont C, Kauer F, Bohr S, et al. Long-term effects of saw osteotomy versus random fracturing on bone healing and remodeling in a sheep tibia model. J Orthop Res 2009;27:680-6.
19. Spicer PP1, Kretlow JD, Young S, et al. Evaluation of bone regeneration using the rat critical size calvarial defect. Nat Protoc. 2012 7(10):1918-29.
20. Hidron AI, Edwards JR, Patel J, et al. NHSN annual update: antimicrobial-resistant pathogens associated with healthcare-associated infections: annual summary of data reported to the National Healthcare Safety Network at the Centers for Disease Control and Prevention, 2006–2007. Infect Control Hosp Epidemiol. 2008;29:996–1011.
21. Drago L, De Vecchi E. Microbiological Diagnosis of Implant-Related Infections: Scientific Evidence and Cost/Benefit Analysis of Routine Antibiofilm Processing. Adv Exp Med Biol. 2017;971:51-67.
22. Massey RC, Horsburgh MJ, Lina G, Höök M, Recker M. The evolution and maintenance of virulence in Staphylococcus aureus: a role for host-to-host transmission? Nat Rev Microbiol. 2006;4(12):953-8.
23. Fey PD, Olson ME. Current concepts in biofilm formation of Staphylococcus epidermidis. Future Microbiol. 2010. 5(6):917-933.
24. Romanò CL, Romanò D, Morelli I, et al. The Concept of Biofilm-Related Implant Malfunction and "Low-Grade Infection". Adv Exp Med Biol. 2017;971:1-13.
25. Goodman SB, Yao Z, Keeney M, et al. The future of biologic coatings for orthopaedic implants. Biomaterials. 2013 Apr;34(13):3174-83.
26. Romanò CL, Malizos K, Capuano N, et al. Does an Antibiotic-Loaded Hydrogel Coating Reduce Early Post-Surgical Infection After Joint Arthroplasty? J Bone Jt Infect. 2016 19;1:34-41.
27. El-Husseiny M, Patel S, Macfarlane RJ, et al. Biodegradable antibiotic delivery systems. Jour of Bone and Joint Surg. 2011. 93(2):151-157.
28. Lovati AB, Drago L, Bottagisio M, et al. Systemic and Local Administration of Antimicrobial and Cell Therapies to Prevent Methicillin-Resistant Staphylococcus epidermidis-Induced Femoral Nonunions in a Rat Model. Mediators Inflamm. 2016;2016:9595706.
29. Quarto R, Mastrogiacomo M, Cancedda R, et al. Repair of large bone defects with the use of autologous bone marrow stromal cells. The New England Journal of Medicine. 2001. 344(5):385–386.
30. Hernigou P, Mathieu G, Poignard A, et al. Percutaneous autologous bone-marrow grafting for nonunions. J Bone Joint Surg Am. 2006. 88(1):322–327.
31. Tseng SS, Lee MA, Reddi AH. Nonunions and the potential of stem cells in fracture-healing. J Bone Joint Surg Am. 2008. 90(1):92–98.
32. Ryan JM, Barry FP, Murphy JM, et al. Mesenchymal stem cells avoid allogeneic rejection. J Inflam. 2005. 2:8.
33. Frank MH, Sayegh MH. Immunomodulatory functions of mesenchymal stem cells. Lancet. 2004. 363(9419):1411-1412.
34. Aggarwal S, Pittenger MF. Human mesenchymal stem cells modulate allogeneic immune cell response. Blood. 2005. 105:1815-1822.

35. Fibbe WE, Nauta AJ, Roelofs H. Modulation of immune iesponses by mesenchymal stem cells. Ann N Y Acad Sci. 2007. 1106:272–278.
36. Johnson V, Webb T, Dow S. Activated mesenchymal stem cells amplify antibiotic activity against chronic Staphylococcus aureus infection. J Immunol. 2013. 190(1):180.11.
37. Freyman T, Polin G, Osman H, et al. A quantitative, randomized study evaluating three methods of mesenchymal stem cell delivery following myocardial infarction. European Heart Journal. 2006;27(9):1114–1122.
38. Kean TJ, Lin P, Caplan AI, et al. MSCs: delivery routes and engraftment, cell-targeting strategies, and immune modulation. Stem Cells International. 2013;2013:13.
39. Barbash I. M, Chouraqui P, Baron J, et al. Systemic delivery of bone marrow-derived mesenchymal stem cells to the infarcted myocardium: feasibility, cell migration, and body distribution. Circulation. 2003;108(7):863–868.
40. Herberts CA, Kwa MS, Hermsen HP. Risk factors in the development of stem cell therapy. J Transl Med. 2011 22;9:29.
41. Zhou X, Fragala MS, McElhaney JE, et al. Conceptual and methodological issues relevant to cytokine and inflammatory marker measurements in clinical research. Curr Opin Clin Nutr Metab Care. 2010;13(5):541-7.
42. Vuong C, Otto M. Staphylococcus epidermidis infections. Microbes Infect. 2002 Apr;4(4):481-9.
43. Yao Y, Sturdevant DE, Otto M. Genomewide analysis of gene expression in Staphylococcus epidermidis biofilms: insights into the pathophysiology of S. epidermidis biofilms and the role of phenol-soluble modulins in formation of biofilms. J Infect Dis. 2005. 15;191(2):289-298.
44. Drago L, Signori V, De Vecchi E, et al. Use of dithiothreitol to improve the diagnosis of prosthetic joint infections. 2013. J Orthop Res 31:1694.
45. Foster PL. Stress-induced mutagenesis in bacteria. Crit Rev Biochem Mol Biol. 2007 Sep-Oct;42(5):373-97.
46. Romano` CL, Toscano M, Romano` D, et al. Antibiofilm agents and implant-related infections in orthopaedics: where are we? 2013. J Chemother 25(2):67–80
47. Calori GM, Colombo M, Navone P, et al. Comparative evaluation of MicroDTTect device and flocked swabs in the diagnosis of prosthetic and orthopaedic infections. Injury. 2016 Oct;47 Suppl 4:S17-S21.
48. Caola I, Drago L. Percorso diagnostico: infezioni delle protesi articolari e dei mezzi di osteosintesi. 2013. http://www.amcli.it/wp-content/uploads/ 2015/10/ PercorsodiagnosticoprotesiarticolariAMCLI2013.pdf.
49. Zmistowski B, Della Valle C, Bauer TW et al. Diagnosis of periprosthetic joint infection. J Arthroplasty 2014a;29:77–83.
50. Zmistowski B, Della Valle C, Bauer TW et al. Diagnosis of periprosthetic joint infection. J Orthop Res 2014b;32(Suppl 1):S98–S107.
51. Van Eyk JE, Corrales FJ, Aebersold R, et al. Highlights of the Biology and Disease-driven Human Proteome Project, 2015-2016. J Proteome Res. 2016 4;15(11):3979-3987.

Appendix

Scientific publications

First year:

- **Bottagisio M**., A.B. Lovati, S. Lopa, and M. Moretti. 2015. Osteogenic Differentiation of Human and Ovine Bone Marrow Stromal Cells in response to β-Glycerophosphate and Monosodium Phosphate. Cellular Reprogramming 17(4):235-242.

Second year:

- Lovati A.B., C.L. Romanò, **M. Bottagisio**, L. Monti, E. De Vecchi, S. Previdi, R. Accetta and L. Drago. 2016. Modeling Staphylococcus epidermidis-Induced Non-Unions: Subclinical and Clinical Evidence in Rats. PLoS One 21;11(1):e0147447. 28

- Lovati A.B.§, **M. Bottagisio§** and M. Moretti. 2016. Decellularized and Engineered Tendons as Biological Substitutes: A Critical Review. Stem Cells International 2016:7276150.

- Lovati A.B, S. Lopa, C. Recordati, G. Talò, C. Turrisi, **M. Bottagisio**, M. Losa, E. Scanziani and M. Moretti. 2016. In Vivo Bone Formation Within Engineered Hydroxyapatite Scaffolds in a Sheep Model. Calcified Tissue International 99(2):209-223.

- **Bottagisio M.**, A.F. Pellegata, F. Boschetti, M. Ferroni, M. Moretti and A.B. Lovati. 2016. A new strategy for the decellularisation of large equine tendons as biocompatible tendon substitutes. European Cells & Materials 8;32:58-73.

- Lovati A.B., L. Drago, **M. Bottagisio**, M. Bongio, M. Ferrario, S. Perego, V. Sansoni, E. De Vecchi and C.L. Romanò. 2016. Systemic and Local Administration of Antimicrobial and Cell Therapies to Prevent Methicillin-Resistant Staphylococcus epidermidis-Induced Femoral Nonunions in a Rat Model. Mediators of Inflammation 2016:9595706.

- De Vecchi E., **M. Bottagisio**, M. Bortolin, M. Toscano, A.B Lovati and L. Drago. 2016. Improving the Bacterial Recovery by Using Dithiothreitol with Aerobic and Anaerobic Broth in Biofilm-Related Prosthetic and Joint Infections. Advances in Experimental Medicine and Biology. DOI 10.1007/5584_2016_51 [Epub ahead of print].

- Perucca Orfei C., A B. Lovati, M. Viganò, D. Stanco, **M. Bottagisio**, A. Di Giancamillo, S. Setti, and L. de Girolamo. 2016. Dose-related and Time-dependent Development of Collagenase-induced Tendinopathy. PLoS One 22;11(8):e0161590.

Third year:

- Lovati A.B.§, **M. Bottagisio§**, E. de Vecchi, E. Gallazzi and L. Drago. 2016. Animal models of implant-related low-grade infections. A twenty-year review. Advances in Experimental Medicine and Biology 971:29-50. doi: 10.1007/5584_2016_157.

- **Bottagisio M.**, A. B. Lovati. 2017. A review on animal models and treatments for the reconstruction of Achilles and flexor tendons. Journal Material Science: Materials in Medicine 28(3):45. doi: 10.1007/s10856-017-5858-y.

- Pellegata A.F.§, **M. Bottagisio§**, F. Boschetti, M. Ferroni, M. Bortolin, L. Drago and A.B. Lovati. 2016. Terminal sterilization of equine-derived decellularized tendons for clinical use. Materials Science & Engineering C 75 (2017) 43–49.

- **Bottagisio M.§,** Lopa, S.§, V. Granata, G. Talò, C. Bazzocchi and A. B. Lovati. 2016. Different combinations of growth factors for the tenogenic differentiation of bone marrow mesenchymal stem cells in monolayer culture and in fibrin-based three-dimensional constructs. Differentiation 16;95:44-53. doi: 10.1016/j.diff.2017.03.001.

- **Bottagisio M.**, A. Soggiu, A. B. Lovati, M. Toscano, C. Piras, C. L. Romanò, L. Bonizzi, P. Roncada, and L. Drago. Draft Genome Sequence of Staphylococcus epidermidis Clinical Strain GOI1153754-03-14 Isolated from an Infected Knee Prosthesis. Genome Announc. 18;5(20). pii: e00378-17. doi: 10.1128/genomeA.00378-17.

- Berzero G.F., A. Pozzi§, **M. Bottagisio§** and A.B. Lovati. 2016. Pyrocarbon Adaptive Proximal Scaphoid Implant (APSI) in treatment of scaphoid nonunion: an over ten-year retrospective study. J Orthop Trauma Res [Under Review].

- Lovati A. B., **M. Bottagisio**, S. Maraldi, M. B. Violatto, M. Bortolin, E. De Vecchi, P. Bigini, L. Drago and C.L. Romanò. In vivo effects of Vitamin E and silver coated titanium implants in reducing osteomyelitis in prosthetic infections. Clinical Orthopaedics and Related Research [Under Review].

- D'Arrigo D.§, **M. Bottagisio§**, S. Lopa, M. Moretti, and A.B. Lovati. Tissue engineering approaches to develop decellularized tendon matrices functionalized with progenitor cells cultured under undifferentiated and tenogenic conditions. AIMS Bioengineering. [Under Review]

§ equally contributed

Abstract

- **Bottagisio M.**, L. Drago, C. L. Romanò and A. B. Lovati. 2015. Animal models of dose-related methicillin-resistant Staphylococcus epidermidis infected non-union after osteosynthesis. European Cells & Materials 30(2):44.eCM XVI Conference: Bone and Implant Infection, 24-26 June 2015, Davos, Switzerland. Poster presentation.

- Cozzi M.C., **M. Bottagisio**, E. Frigo, M. G. Strillacci, F. Schiavini, R.T. Prinsen and A. Bagnato. 2015. Molecular Tests for Horse Coat Color Determination. ASPA Animal Production for Feeding the Planet, 9-12 June 2015, Milan, Italy. Poster presentation.

- **Bottagisio M**., L. Drago, C. L. Romanò, L. Bonizzi and A. B. Lovati. 2016. Animal models of dose-related methicillin-resistant Staphylococcus epidermidis infected non-union after osteosynthesis. Veterinary and Animal Science (VAS) Days 2016, 15-17 July 2015, Milan, Italy. Oral presentation.

- **Bottagisio M.**, L. Drago, C. L. Romanò, L. Bonizzi and A. B. Lovati. 2016. Evaluation of Antibiotic and Cell-based Therapy in Preventing S. epidermidis-induced Nonunion in Rats. oral presentation. International Journal of Health, Animal Science and Food Safety DOI: http://dx.doi.org/10.13130/2283-3927/7061. Veterinary and Animal Science (VAS) Days 2016, 8-10 June 2016, Milan, Italy. Oral presentation.

- **Bottagisio M.**, A. F. Pellegata, F. Boschetti, M. Moretti and A. B. Lovati. 2016. Tissue Engineering Approaches to Optimize the Decellularization of Equine Tendons as Biological Grafts for the Replacement of Damaged Tissues. European Cells &Materials 31(1): 76. TERMIS-EU 2016, 28 June – 1 July 2016, Uppsala, Sweden. Poster presentation.

- Lovati A.B., L. Drago, **M. Bottagisio**, M. Bongio, S. Perego, V. Sansoni, E. De Vecchi and C. L. Romanò. Antibiotic and Cell-based Therapy to Prevent the Development of Methicillin- resistant Staphylococcus epidermidis- induced Nonunion in Rats, poster presentation. EBJIS 2016, 1-3 September 2016, Oxford, United Kingdom. Poster presentation.

- Ferroni M., A. F. Pellegata, **M. Bottagisio**, M. Moretti, A. B. Lovati and F. Boschetti. 2016. Tendon tissue engineering: decellularization protocol for equine-derived tendon matrix. ESB-ITA 2016, 8-9 September 2016, Palermo, Italy. Poster presentation.

- **Bottagisio M.**, A. Soggiu, A.B. Lovati, M. Toscano, C. Piras, C.L. Romanò, L. Bonizzi, P. Roncada and L. Drago. Phenotypic and genomic identification of Staphylococcus epidermidis GOI1153754-03-14 isolated from an infected orthopedic prosthesis. International Journal of Health, Animal Science and Food Safety. Veterinary and Animal Science (VAS) Days 2017, 6-8 June 2017, Milan, Italy.

- Perucca Orfei C., A. B. Lovati, M. Viganò, **M. Bottagisio**, S. Setti, A. Di Giancamillo and L. de Girolamo. Utilizzo di campi elettromagnetici pulsati (PEMF) per il trattamento della tendinopatia achillea: studio sperimentale in modello animale. SIOT 2017, 20-23 October 2017, Palermo, Italy. Oral presentation.